

AperTO - Archivio Istituzionale Open Access dell'Università di Torino

Conditions of ore formation at the Gorno MVT deposits (Lombardy, Italy): insights from fluid inclusions

This is the author's manuscript

Original Citation:

Availability:

This version is available <http://hdl.handle.net/2318/1798620> since 2021-08-30T16:52:28Z

Publisher:

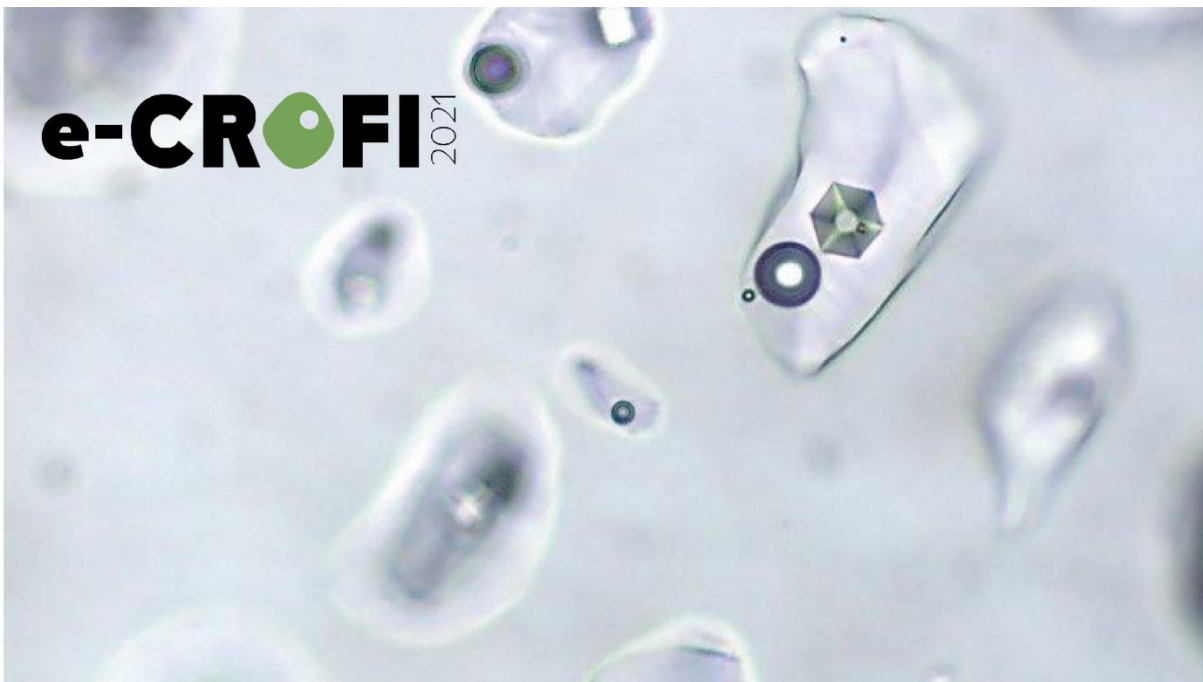
Enik Bali

Terms of use:

Open Access

Anyone can freely access the full text of works made available as "Open Access". Works made available under a Creative Commons license can be used according to the terms and conditions of said license. Use of all other works requires consent of the right holder (author or publisher) if not exempted from copyright protection by the applicable law.

(Article begins on next page)



European current research on fluid and melt inclusions

June 28th to July 2nd 2021

Abstract Book



The international congress e-CROFI 2021 (Current Research on Fluid Inclusions) was held online from June 28th to July 2nd, 2021. It is the 26th edition of the biennial international conference dedicated to the investigation of fluids and magmas at all scales through the study of fluid and melt inclusions.

This conference was organised by GeoRessources and CRPG (Université de Lorraine – CNRS) in partnership with the University of Iceland, the Università Degli Studi di Torino, and the Eötvös Loránd University of Budapest.

Cover photo: (c) Guillaume Barré GeoResources Lab, Université de Lorraine – CNRS – CREGU, Nancy, France, In "Inclusion", ASGA édition, Nancy, France 2017

Edited by: Enikő Bali,
University of Iceland



UNIVERSITY OF ICELAND
INSTITUTE OF EARTH SCIENCES



norden

Nordic Volcanological Center

Scientific Committee:

David Banks, Professor,
University of Leeds, United
Kingdom

Robert J. Bodnar, Professor,
Blacksburg University –
VirginiaTech, USA

Larryn W. Diamond, Professor,
Institute of Geological Sciences,
University of Bern, Switzerland

Maria Luce Frezzotti, Professor,
Dipartimento Scienze
dell'Ambiente e della Terra,
Università di Milano-Bicocca, Italy

Alfons Van den Kerkhof, Doctor,
Geologisches Zentrum der
Universität Göttingen, Germany

Volker Lüders, Doctor, German
Research Centre for Geosciences,
Potsdam, Germany

Jacques Pironon, Senior
Research Fellow at the CNRS,
Université de Lorraine, Nancy,
France

Csaba Szabó, Professor,
Department of Petrology and
Geochemistry, Eötvös Loránd
University, Budapest, Hungary

Benedetto De Vivo, Professor,
Università Telematica Pegaso,
Napoli, Italy

Alexander Sobolev, Professor,
Institut des Sciences de la Terre
(ISTerre), Université Grenoble
Alpes – CNRS, France

Steering Committee:

László Előd Aradi, Eötvös Loránd
University, Hungary

Enikő Bali, University of Iceland,
Iceland

Luca Barale, CNR – Institute of
Geosciences and Earth Resources,
Torino, Italy

Márta Berkesi, Eötvös Loránd
University, Hungary

Barbara Brenachot, Université
de Lorraine – GeoRessources,
France

Marie-Camille Caumon,
Université de Lorraine –
GeoRessources, France

Véronique Ernest, Université de
Lorraine – GeoRessources, France

François Faure, Université de
Lorraine – CRPG, France

Simona Ferrando, Università
degli Studi di Torino, Italy

Marcello Natalicchio, Università
degli Studi di Torino, Italy

Jacques Pironon, CNRS –
GeoRessources, France

Antonin Richard, Université de
Lorraine – GeoRessources, France

Csaba Szabó, Eötvös Loránd
University, Hungary

Alexandre Tarantola, Université
de Lorraine – GeoRessources,
France

MONDAY 28 th June		TUESDAY 29 th June		WEDNESDAY 30 th June		THURSDAY 1 st July		FRIDAY 2 nd July		
02:00	e-CROFI OPENING CEREMONY	FROM MAGMA GENESIS TO ERUPTIONS	FROM DIAGENESIS TO UHP METAMORPHISM	FROM DIAGENESIS TO UHP METAMORPHISM	FROM DIAGENESIS TO UHP METAMORPHISM		NEW FRONTIERS	FROM MAGMA GENESIS TO ERUPTIONS	FROM DIAGENESIS TO UHP METAMORPHISM	
	NEW FRONTIERS	02:00 Hanley Jacob	02:00 Fail Andras	02:00 Rana Shruti	02:00	02:00	Aradi Laszlo	Cao Yi	Abidi Riadh	
02:15	McFall Katie	02:30 Ouattara Zie	02:30 Elias Bahman Alexy	02:15 Michels Raymond			Richard Antonin	Li Rongxi	Barale Luca	
02:45	Auxerre Marion	02:45 Shapley Sarah	02:45 Balitsky Vladimir	02:30 Sprantiz Tamás			Lopez-Elorza Maialen	Daya Priyal	Matfini Natalia	
03:00	Lange Thomas	03:00 PACROFI 2022 in Edmonton	03:00 Shaparenko Elena	02:45 Matfais Andreea			Bakker Ronald	Gomez Garcia Gabriel	Marques de Sá Carlos	
				03:00 ECHROFI 2023 in Reykjavik				Soleyman Majid	Trilla Jordi	
03:15	Break	03:15 Break	03:15 Break	03:15 Break			Shishkina Tatiana	Yensepyeyev Taltat		
FROM MAGMA GENESIS TO ERUPTIONS		FROM DIAGENESIS TO UHP METAMORPHISM	FROM MAGMA GENESIS TO ERUPTIONS	NEW FRONTIERS	04:00	AWARD CEREMONY AND e-CROFI CLOSURE				
03:20	Morotó Emanuel	03:20 Balitskaya Elizaveta	03:20 Astudillo Manosalva Daniel	03:20 Wang Wenjing						
03:35	Tapia-Rodriguez Fabian	03:35 Sosa Graciela	03:35 Caracciolo Alberto	03:35 Marc Laureline						
03:50	Grishina Svetlana	03:50 Terekhova Anna	03:50 Hernández Prat Loreto	03:50 Wilske Cornelia						
04:05	Nizamedinov Ildar	04:05 Lüders Volker	04:05 Break	04:05 Deicha Cyril						
04:20	Break	04:20 Break		04:20 Break						
FROM DIAGENESIS TO UHP METAMORPHISM		NEW FRONTIERS	NEW FRONTIERS	FROM MAGMA GENESIS TO ERUPTIONS						
04:25	Smith-Schmitz Sarah	04:25 Van den Kerhof Altons	04:10 Saadallah Khouloud	04:25 Stoltnow Maite						
04:40	Giorno Michele	04:40 Fan Junjia	04:25 Remigü Samantha	04:40 Sosnicka Marta						
04:55	Hanligi Nurullah	04:55 Kontak Daniel	04:40 Le Van-Hoan	04:55 Introduction to poster session						
			04:55 Bakker Ronald							

e-CROFI2021

e-CROFI 2021

***NEW FRONTIERS IN FLUID AND MELT
INCLUSION RESEARCH***

e-CROFI 2021

High temperature (>800°C) brines present in Northern Bushveld magmatic sulfide Cu-Ni-PGE deposits (*keynote*)

McFall K.^{1*}, McDonald I.¹, Yudovskaya M.², Kinnaird J.², Hanley J.³, Kerr M.³, Tattitch B.⁴

¹ School of Earth and Environmental Science, Cardiff University, UK; ² University of Witwatersrand, South Africa; ³ Department of Geology, Saint Mary's University, Canada; ⁴ School of Earth Sciences, University of Bristol, UK.

*mcfallk@cardiff.ac.uk

Keywords: fluid inclusion, new frontiers, ore deposits

The role of volatiles in the development of layered intrusion-hosted magmatic sulfide deposits is still poorly understood. We present petrological and fluid inclusion evidence that an aqueous brine phase was present during the formation of the Aurora, Waterberg PTM and Troctolite Unit mineralisation from the northern Bushveld Complex where magmatic sulfide deposits are hosted both in leucocratic rocks of the Main and Upper Zones. This brine phase was present while the system was at least partially molten and we present direct evidence of brine – sulfide melt interaction.

Fluid inclusions were identified in cumulate magmatic silicates (feldspar, olivine, and pyroxene) in all deposits. These comprise brine and vapour inclusions which do not crosscut crystal boundaries and terminate against peritectic reaction rims. Optical microscopy and confocal Raman spectroscopy show that the brine inclusions contain multiple daughter minerals (including halite and carbonates), 10-15% vapour and 15-25% liquid water; whereas vapour inclusions contain CH₄ and N₂. Microthermometry shows that brine inclusions homogenise to liquid by vapour disappearance between 819 – 1000°C in the Aurora deposit (n=281), between 877 – 994°C in Waterberg (n=256), and between 860 – 942°C in the Troctolite Unit (n=428). Halite dissolves between 521 – 697°C, giving salinities of 61-87 wt.% NaCl equivalent (Bakker, 2018).

At the estimated trapping temperatures of these brines (895 – 1028°C, corrected for an assumed trapping pressure of 150 MPa) sulfides would be partially molten.

Examples of co-eval interaction and entrapment of brine and Cu-rich sulfide melt are observed in all deposits, implying this was a common factor during their development. The PGE in the Aurora project and the T zone at Waterberg are hosted in platinum group minerals (PGM) that are spatially removed from magmatic sulfides and hosted in late silicates such as quartz, suggesting PGE remobilisation by hydrothermal processes. The petrological similarity between inclusions in all Main Zone deposits suggests the high temperature fluids had a similar origin, likely from late magmatic degassing or possibly from assimilated dolomite country rock.

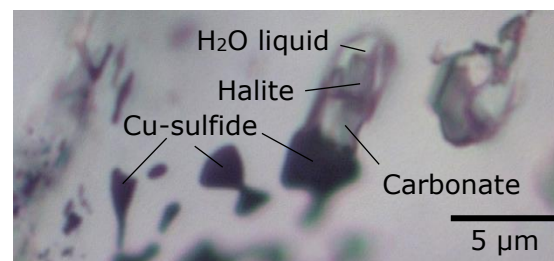


Fig. 1: Photomicrograph of brine – Cu-sulfide inclusions in pyroxene from the Waterberg PTM Ni-Cu-PGE deposit, South Africa.

Preliminary petrological studies of Platreef samples have shown similar brine inclusions present in Critical Zone mineralisation in the Northern Limb. The results of this study have important implications for northern Bushveld Ni-Cu-PGE deposits, and layered intrusion-hosted deposits more generally.

References:

Bakker R.J., (2018): *Comput Geol*, Vol 115, pp 122-133.

Experimental investigation of melt inclusion formation during olivine growth in chondritic liquid

Auxerre M.^{1*}, Faure F.¹, Lequin D.¹

¹ Centre de Recherche Pétrographiques et Géochimiques, France

*marion.auxerre@univ-lorraine.fr

Keywords: Experiments, Melt Inclusion

Melt inclusions and embayments hosted within olivine crystals are classically observed in chondrules, principal constituent of chondrites (primitives' meteorites). Melts inclusions and embayments potentially mark thermal conditions of chondrule's crystallization. We performed dynamic crystallization experiments to determine temperature range and cooling rates that allow reproducing these melt inclusions or embayments. Superliquidus experiments ($+\Delta T$), i.e. experiment that begin above the liquidus temperature, and slow cooling ($< 10\text{ }^{\circ}\text{C/h}$) allow reproducing both olivine morphology and macroscopic defects like melt inclusions and embayments. We showed that at least two generations of embayments are produced during this simple slow cooling history.

The first is linked to nucleation step, which occurs when liquid supersaturation is high. To eliminate this supersaturation, viable nuclei grow rapidly and develop a skeletal/dendritic shape. These initially skeletal crystals evolve toward polyhedral morphology (Lofgren, 1989). Long embayments result of this shape evolution (Fig.1a). These embayments tend to segment in small pools of liquid to decrease interfacial energy. The real melt inclusions formed with shrinkage bubble are not connected with external liquid.

The second episode of inclusion formation is due to an increase of supersaturation during crystallization. Indeed polyhedral crystals, controlled by interface processes, do not grow fast enough to decrease liquid super-saturation. In reaction to this, crystals develop again a fast morphology growth. Textural ripening of dendritic overgrowth will close embayments leading to a new generation of melt inclusions (Fig.1b).

In conclusion these results show that the type of embayment/inclusion can be an indicator to understand the steps of olivine crystallization according to thermal conditions (Fig.1c).

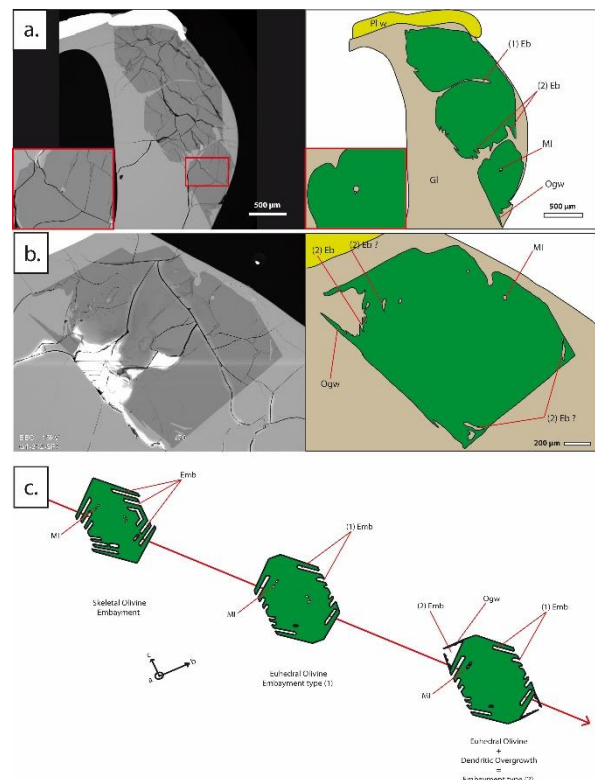


Fig.1: (a.) and (b.) SEM images of experimental charge and their interpretative sketch, (a.) Fo#18 with $+\Delta T = 8^{\circ}\text{C}$, (b.) Fo#19 with $+\Delta T = 75^{\circ}\text{C}$; (c.) Step of different embayment formation during cooling of liquid after superheating; MI: melt inclusion; (1) Eb: first type of embayment; (2) Eb: second type of embayment; Ogw: Overgrowth of olivine.

References:

Lofgren, (1989) *Geochim. & Cosmochim. Ada*, 50, 1715-1726

Dislocation driven amphibole formation at fluid inclusion-clinopyroxene boundary, Perşani Mountains Volcanic Field (Transylvania, Romania)

Lange T. P.^{1,2*}, Pálos Z.³, Berkesi M.^{1,2}, Molnár G.^{2,4,6}, Pósfai M.⁵, Pekker P.⁵, Szabó C.^{1,6}, Kovács I. J.^{2,6}

¹Lithosphere Fluid Research Lab, Institute of Geography and Earth Sciences, Eötvös Loránd University, Budapest, Hungary; ²MTA Pannon Lithoscope Lendület Group; ³Mineral Resources and Geofluids Group, Department of Earth Sciences, University of Geneva, Switzerland; ⁴Alba Regia Technical Faculty, Institute of Geoinformatics, Óbuda University, Székesfehérvár, Hungary; ⁵Nanolab, University of Pannonia, Veszprém, Hungary; ⁶Institute of Earth Physics and Space Science, Sopron, Hungary.

*thompiman@student.elte.hu

Keywords: amphibole, new frontiers, fluid inclusion

In the upper mantle beneath the Perşani Mountains Volcanic Field (Transylvania, Romania) evidence for an interaction between fluid inclusion and host clinopyroxene forming amphibole lamella was revealed. Studied fluid inclusions are CO₂-rich, isometric, secondary with minor H₂O, H₂S and N₂. Solid phases found in fluid inclusions are dolomite and anatase. Fluid inclusions occur in intimate link with amphibole lamellae. We propose composition gradient of CO₂/H₂O increasing with distance from the fluid-solid boundary into the centre of the fluid inclusion. H₂O enrichment at the boundary should have enhanced amphibole formation. As the studied rock is slightly deformed, a dislocation-induced precipitation mechanism is considered. A newly formed, 'wet' amphibole-clinopyroxene phase boundary enhances fluid loss, supporting amphibole growth. Diffusion in the [001] direction is the fastest, owing to misfit-dislocation channels found at the clinopyroxene-amphibole boundary (Fig.1). A misfit-dislocation migration through translation and rotation of the surrounding structures, accompanied by octahedral chain-breaking and re-bonding is modelled and supported by STEM observations. Misfit-dislocation channels can store escaped fluid components that will interact with clinopyroxene during the misfit dislocation migration (i.e., amphibole formation). Preliminary calculations of misfit-dislocation channel cross sections

suggest the possibility of the diffusion of 'non-wetting' fluid components (e.g., CO₂) from the fluid inclusion that, when the amphibole lamellae reach the host mineral boundary, escape to the open grain boundary system. Our results provide a better understanding of nanoscale mantle CO₂ degassing.

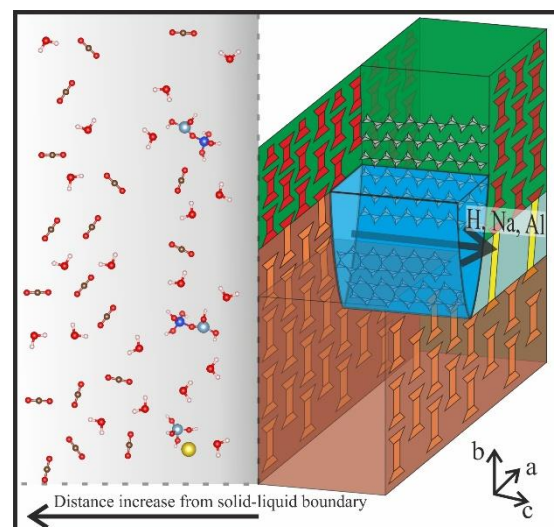


Fig. 1: Schematic figure of the solid - fluid boundary and the misfit dislocation channel (blue) found at the clinopyroxene (green) - amphibole (brown) boundary. CO₂/(H₂O + dissolved molecules) molecular ratio increases with distance from the boundary. Mobile elements migrate through the misfit-dislocation channel and interact with the pyroble (yellow) found next to the misfit dislocation during dislocation migration.

Volatile organic compounds in barite-hosted 3.5 billion-year-old fluid inclusions (Pilbara, Australia)

van den Kerkhof A. ^{1*}, Mißbach H. ², Duda J.-P. ³, Lüders V. ⁴, Pack A. ¹, Reitner J. ¹, Thiel V. ¹

¹Geoscience Center (GZG), University of Göttingen, Germany; ² Geobiology, University of Cologne, Germany; ³ Sedimentology & Organic Geochemistry, University of Tübingen, Germany ⁴ GFZ German Research Centre for Geosciences, Potsdam, Germany

*akerkho@gwdg.de

Keywords: fluid inclusion, hydrothermalism, surface

Primary fluid inclusions in c. 3.5-billion-year-old black-grey barite (Dresser Fm, Pilbara Craton, W-Australia) contain gases and organic molecules. The barites are interbedded within sulfidic stromatolites. We combined fluid inclusion petrography, microthermometry, Raman spectrometry, GC-MS, and stable isotope analysis to explore the full range of volatiles (Mißbach *et al.* 2021).

The barites contain primary (1) aqueous carbonic-sulfuric inclusions with water vol. frags of 0.1-0.99, and (2) non-aqueous carbonic-sulfuric fluid inclusions. At room temperature, they typically exhibit a double meniscus, indicating the presence of water + another (CO₂-H₂S-rich) liquid + vapour. In comparison, non-aqueous fluid inclusions usually contain a CO₂-H₂S-rich liquid and a vapour phase. Both types of fluid inclusions typically contain solid daughter phases. Aqueous inclusions usually contain strontianite (SrCO₃) and sulfur as daughter crystals (Fig. 1). Varieties with pure CO₂ in the vapour phase may additionally include anatase (TiO₂), pyrite, and possibly also halite (NaCl). In non-aqueous inclusions, typical daughter phases are sulfur, kerogen and sometimes halite.

The main gas components in both fluid inclusion types are CO₂ and H₂S, accompanied by minor amounts of CH₄, N₂, and COS (carbonyl sulfide). Aqueous fluid inclusions contain less H₂S than non-aqueous fluid inclusions (0–24 mol% and 21–36 mol%, resp.). Th ranges from 100 to 195 °C, with a maximum between 110 and 150°C. Most fluid inclusions decrepitate at temperatures >230 °C.

Both aqueous and non-aqueous fluids represent heterogeneous trapping.

GC-MS analysis yielded high amounts of CO₂, H₂S, and H₂O, thus confirming results from Raman analysis. Furthermore, COS, CS₂, SO₂, together with numerous organic molecules containing oxygen (aldehydes, ketones, acetic acid, oxolane) and sulfur (thiophene, thiols, organic polysulfanes) were detected, accompanied by minor amounts of aromatic hydrocarbons.

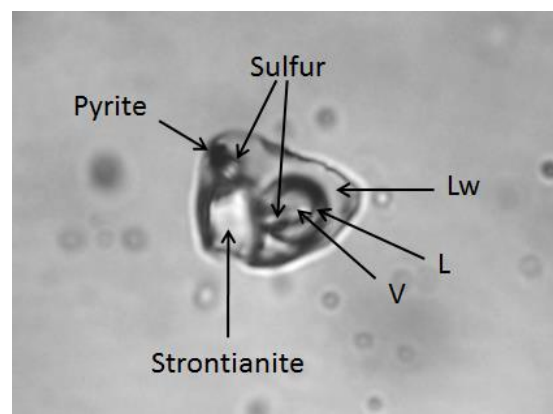


Fig. 1: Aqueous carbonic-sulfuric fluid inclusion. Gas composition: CO₂(84) H₂S(16).

The fluids in black barites revealed lower $\delta^{13}\text{C}$ compared to the grey variety (i.e., mean 10.3 and -6.3 ‰, resp.) reflecting the addition of a biomass-derived carbon to the fluids.

Our findings demonstrate that early Archaean hydrothermal fluids contained essential primordial ingredients that provided fertile substrates for earliest life on our planet.

Reference:

Mißbach H., Duda J.-P., van den Kerkhof A.M., Lüders V., Pack A., Reitner J. Thiel V. (2021): *Nature Comm.*, 12, pp 1-11.

The significance of applying external pressure during liquid-vapour homogenization experiments for fluid inclusions hosted in soft minerals

Fan J.^{1*}, Chou I.², Li J.³, Pironon J.⁴, Lu X.¹, Elias Bahnan A.⁴, Deng J.³

¹ Research Institute of Petroleum Exploration and development, RIPED, Beijing 100083, China.; ² Institute of Deep-sea Science and Engineering, Chinese Academy of Sciences, Sanya, Hainan 572000, China.; ³ Institute of Mineral Resources, Chinese Academy of Geological Sciences, Beijing 100037; ⁴ Université de Lorraine, CNRS, GeoRessources lab, 54000 Nancy, France.

* fanjunjia@petrochina.com.cn

Keywords: Fluid inclusion, experiments, diagenesis

Trapping pressure-temperature (P - T) conditions of fluids in fluid inclusions (FI) in an oil and/or gas reservoir can be derived from the measured homogenization temperatures (T_h) of liquid (L) and vapour (V) phases in the FI, provided that no stretching of the FIs occurs during heating. This becomes particularly important for FIs hosted in soft minerals (e.g. calcite, fluorite) which frequently undergo stretching during T_h measurements. To overcome this limitation, the method described by Schmidt et al. (1998) was employed, such that doubly polished FI-containing chip(s) was/were loaded in the sample chamber of a hydrothermal diamond-anvil cell (HDAC), together with certain amount of H_2O , such that FIs were under elevated external P during T_h measurements to avoid stretching (Figs. 1a and 1b).

Two-phase (L+V) FIs found as clusters within growth zones in fluorite in the dolomite reservoirs of the Dengying formation in the Anyue gas field, Sichuan basin, China were studied. The major component in the L and V phases is H_2O and CH_4 , respectively (Fig. 1). Raman spectroscopic analyses show that the major component of the single-phase FIs shown in Fig. 1c is CH_4 with minor CO_2 . When measured under the conventional Linkam THMSG600 heating-cooling stage, the T_h s of the two FI assemblages (FIA) in fluorite were 205-215°C (Fig. 1c) and 225-260°C (Fig. 1d). However, the T_h s measured in the HDAC for the two petrographically identical FIAs hosted in a twin sample were 199-202°C at an

external confining P s of 43.9-136.6 MPa and 220-230°C under 69.9- 129.2 MPa, respectively. T_h s have thus dropped by 20-45°C for identical FIAs when studied under the HDAC.

Our results show that, FIs in soft minerals tend to be stretched during T_h measurements, unless external confining P is applied, and that only a threshold external P is needed to prevent stretching or decrepitation. However, more work is needed to quantify this threshold P as a function of mineral type and FI properties.

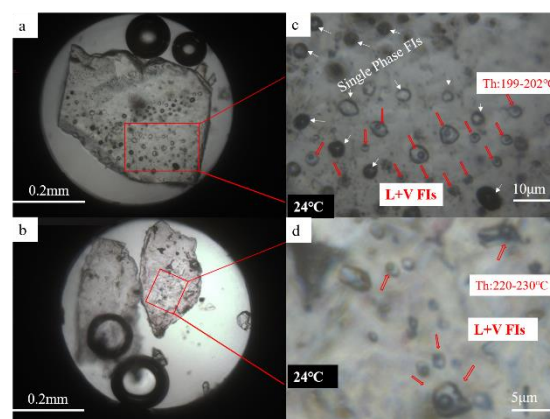


Fig. 1: (a) & (b): FIs in fluorite chip(s) from the Anyue gas field, Sichuan, China, loaded with water in the sample chamber of the HDAC. (c) FIs in a FIA (shown in a) having the similar L/V ratio together with single phase (V) FIs. (d) FIs of the FIA shown in b.

Reference:

Schmidt, C., Chou, I. et al. (1998). "Microthermometric analysis of synthetic fluid inclusions in the hydrothermal diamond-anvil cell." *American Mineralogist* 83(9-10): 995-1007.

Recognition and potential implications of carbonic (CO₂-CH₄) fluid inclusions in the five-element Ag-rich veins of Cobalt (Canada)

Kontak D. J.^{1*}, Rush L. V.¹, Sherlock R. L.¹, Santaguida F.², White, S. E.³

¹ Harquail School of Earth Sciences, Laurentian University Sudbury, ON, Canada; ² First Cobalt Corp., Toronto, ON, Canada; ³ Department of Geology, St. Mary's University, Halifax, NS, Canada.

*dkontak@laurentian.ca

Keywords: ore deposits, fluid inclusions, hydrothermalism

Cobalt (Ontario, Canada) is famed as a past producing Ag-rich district (≈ 500 Moz production) and part of the five-element (Co-Ni-Ag-As \pm Bi, U) deposit type. These ca. 2220 Ma veins are hosted in Archean basic and felsic volcanic and interflow graphitic sedimentary rocks that locally host massive sulfide lenses (Py-Po-Cpy-Sph-Gal), the 2220 Ma Nipissing diabase, and Paleoproterozoic clastic sedimentary rocks. The high-tenor sulfarsenide (Co-Ni-As) - native Ag veins are characterized by dendritic textures, and narrow (<3-5 cm) alteration haloes with propylitic-type assemblages. Previous fluid inclusion (FI) studies noted both highly saline (25-35 wt. %) Na-Ca fluids and lower salinity (<10 wt. %) Na-type fluids, questionable evidence for fluid unmixing, and a temperature of fluid entrapment of ca. 300-350°C (reviewed in Marshall, 2008).

As part of a regional lithogeochemical and mineralogical/paragenetic study of the Cobalt district (Rush, 2021), FI were also examined to assess potential regional trends. This work revealed the following FI types, each of which define FIAs present as P, PS, S and I types: 1) L_{H2O}-V_{H2O}-Halite(H); 2) L_{H2O}-V_{H2O}-H-solids; 3) L_{H2O}-V_{H2O} with 20% V_{H2O}; 4) L_{H2O}-V_{H2O} with 40% V_{H2O}; and 5) V rich \pm L_{H2O} rim (<5-10%). In addition, we note abundant decrepitated FI and the presence of melt inclusions that include native Bi and Ag plus other unidentified phases. These FI types occur through the paragenesis in pre-ore, CL-zoned comb quartz and post-ore CL-zoned carbonates of the Co-Ni-Ag veins, in addition to quartz and sphalerite in synchronous base-metal (Zn-Cu-Pb) sulfide veins. Notably, type 5 V-rich FI, not reported in earlier FI studies, are the

most abundant FI type in samples used in this study.

Initial microthermometric data for the base-metal veins indicate: 1) type 1 FIA have Th(H) of 168-280°C, Th(Tot) of 190-295°C and T_{eutectic} that are similar to the L-V-H FI in the Ag-rich veins noted previously; and 2) type 5 V-rich FIA includes two sub-types of mixed CO₂-CH₄ fluids based on their Th data: i) CH₂-rich with Th (to liquid) of -120 to -106°C; and ii) CO₂-rich with T_{mCO2} of -62.3 to -64.4°C and Th(CO₂) of -17.8 to +7.8°C.

Our new observations support the earlier suggestions that graphitic and sulfide-rich Archean interflow sedimentary rocks may be relevant to the Cobalt deposit model. We further suggest these carbonic fluids: 1) were in part sourced from the interflow sedimentary rocks due to a transient high geotherm related to the the Nipissing dike swarm; 2) were in part sourced from the graphitic sedimentary rocks; 3) mixed heterogeneously with a regional saline Ca-rich basinal-type fluid; 4) may have played a role in the hydrofracturing of the host rocks and subsequent dilation of the Co-Ni-Ag veins; and 5) facilitated transport of sulfarsenide melts sourced in the metal-rich basement rocks into the dilations via a floatation model, as suggested for IOA deposits (Knipping et al., 2015).

References:

- Knipping, J. and 8 others (2015): *Geology*, Vol 453, pp. 591-594.
- Marshall, D. (2008): *Geosci Canada*, Vol 35, pp. 137-145
- Rush, L. (2021): *Unpubl MSc thesis, Laurentian University, Sudbury, ON, Canada.*

Thermodynamic behaviour of sulfur and nitrogen systems at high pressure and temperature: an experimental Raman approach

Saadallah K.^{1*}, Caumon M.-C.¹, Sterpenich J.¹, Randi A.¹, Lachet V.², Creton B.²,

¹ Université de Lorraine, CNRS, GeoRessources Laboratory, BP 70239, F-54506 Vandœuvre-lès-Nancy, France, ² IFP Energies nouvelles, 1 et 4 avenue de Bois-Préau, 92852 Rueil-Malmaison, France

* khouloud.saadallah@univ-lorraine.fr

Keywords: energy storage, experimental, thermodynamic calculations

Phase diagrams, solubility data and other thermodynamic properties are necessary to describe, understand, and predict the evolution of most terrestrial systems including fluid inclusions entrapped at upper mantle conditions. Fluids are indeed ever-present in all Earth envelopes: geosphere, hydrosphere, and atmosphere. SO₂ is known for having a high reactivity as an acid and oxidizing agent when solubilized in water (Amshoff et al., 2018). Thus, the knowledge of the solubilities and rates of solubilization of this gas in the aqueous phase and the co-solubility of water in the gas phase is of primary interest. However, despite significant advances in both experiments and modeling, thermodynamic data concerning SO₂-water-salt systems are still scarce or even unavailable. This thesis proposes to acquire new thermodynamic data on H₂O/SO₂/salt systems at high pressures (up to 600 bar) and high temperatures (up to 200 °C). The experimental and analytical protocol which is carried out within the framework of this thesis combines Raman spectrometry (RS), fused silica capillaries and Monte-Carlo molecular simulations. A silica capillary tube is sealed at one end before being connected to a secure gas loading line located in a securitized fume cupboard. The tube is then filled with pure SO₂ or with a binary system containing an aqueous phase (water or brine). Gas is captured by cold trap by immersing the capillary in liquid nitrogen. Capillary tubes are then sealed at the other end to obtain a Fused Silica Capillary Capsule or connected to a pressurization device (Stevanovic et al., 2014). RS were also obtained as a function of temperature by setting the capillary on a heating-cooling stage

(Linkam CAP500). The Raman spectra of SO₂ are recorded individually and in the presence of water at different pressures and temperatures. The evolution of the different spectral parameters (peak position, peak area, peak intensity, etc. Fig. 1) is studied at different pressures and temperatures. Therefore, the components and speciation can be estimated, as Raman is able to identify the molecular aspects of the sample based on its characteristic spectrum. RS is a semi-quantitative approach which explains the need for data calibration using Monte-Carlo simulation. The latter has been proven as a theoretical complementary approach to experimental measurements.

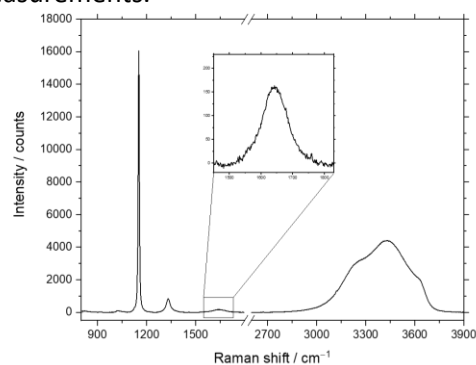


Fig. 1: Raman spectra of dissolved SO₂ in an aqueous solution at 50°C

References:

- P. Amshoff et al. (2018): *Journal of Greenhouse Gas Control*, 79, 173–180
 S. Stevanovic et al. (2014): *Energy Procedia*, 63, 3775-3781

In-situ determination of the $^{13}\text{C}/^{12}\text{C}$ isotope ratio in CO_2 fluid inclusions by Raman micro-spectroscopy

Remigi S.^{1*}, Frezzotti M. L.¹, Bodnar R. J.², Sandoval-Velasquez A. L.³, Rizzo A. L.⁴, Aiuppa, A.³

¹ Department of Earth and Environmental Sciences, University of Milano - Bicocca, Piazza della Scienza 4, 20126, Milano, Italy; ² Department of Geosciences, Virginia Tech, 926 West Campus Drive, Blacksburg (VA), 24061, USA.; ³ Department of Earth and Sea Sciences, University of Palermo, Via Archirafi 36, 90123, Palermo, Italy; ⁴ National Institute of Geophysics and Volcanology, Via Ugo La Malfa I-153, 90146, Palermo, Italy.

*s.remigi@campus.unimib.it

Keywords: fluid inclusions, mantle

We applied Raman micro-spectroscopy to determine the $^{13}\text{C}/^{12}\text{C}$ isotope ratio in single CO_2 fluid inclusions (FI). We measured the area ratios of $^{13}\text{CO}_2$ and $^{12}\text{CO}_2$ ν_1 bands, which are proportional to the $^{13}\text{C}_{\text{CO}_2}$ and $^{12}\text{C}_{\text{CO}_2}$ concentrations. Selected CO_2 inclusions ($d=0.73\text{-}1.07\text{ g/cm}^3$) are present as small clusters or trails in Ol, Opx, and Cpx of peridotites from the Lake Tana region (Injibara, Ethiopia) and El Hierro (Canary Islands, Spain) ($P\text{-}T$: 1.3-2 GPa at 900-1150°C; Frezzotti et al., 2010; Oglialoro et al., 2017). FI show negative-crystal to rounded shapes, are 5 - 21 μm in size and are located at a depth from 5 to 20 μm (Fig. 1).

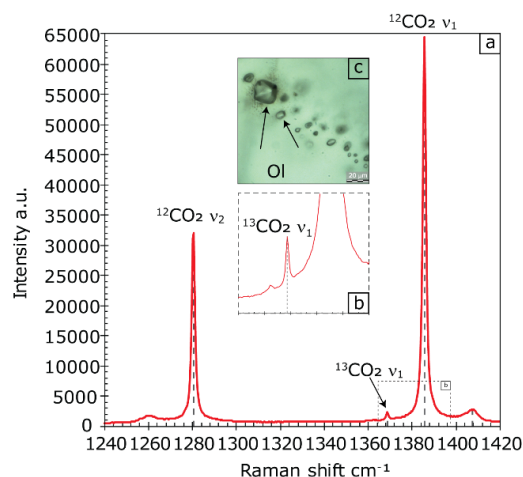


Fig. 1: a) Raman spectrum of a CO_2 FI; b) $^{13}\text{CO}_2 \nu_1$; c) CO_2 FI photomicrograph.

In 42 FI, 2 sets of 3 Raman spectra (i.e., 84 sets of 3 spectra each) have been acquired by high-resolution analyses with variable acquisition times. Of these sets,

23 were eliminated from further consideration because of band shape modifications due to random noise. In 61 averaged sets of three spectra, the calculated $\delta^{13}\text{C}_{\text{CO}_2}$ are $-6.73 \pm 1.04\text{‰}$ for FI in Ol and $-7.34 \pm 0.81\text{‰}$ for FI in Opx from Lake Tana peridotites, and $2.40 \pm 2.42\text{‰}$, $0.92 \pm 6.45\text{‰}$, and $-1.87 \pm 0.39\text{‰}$ for FI in Ol, Opx, and Cpx from El Hierro. 95% of the calculated $\delta^{13}\text{C}_{\text{CO}_2}$ values show errors of $\approx \pm 2\text{‰}$, while 5% show higher error $\leq \approx \pm 6.75\text{‰}$. The C_{CO_2} isotopic composition of FI from the Lake Tana region peridotites fall within the mantle range (Mattey et al., 1984), while the $\delta^{13}\text{C}_{\text{CO}_2}$ of FI from El Hierro peridotites is considerably heavier. In these rocks, the $\delta^{13}\text{C}_{\text{CO}_2}$ has been further analyzed by isotope ratio mass spectrometry, after in-vacuo bulk extraction of CO_2 from 0.1-2.0g of single mineral phases. $\delta^{13}\text{C}_{\text{CO}_2}$ are $0.38\text{‰} \pm 0.58\text{‰}$ in Ol, $-1.75 \pm 0.58\text{‰}$ in Opx, and -1.94‰ in Cpx, confirming the accuracy of Raman analyses. Present results suggest that Raman micro-spectroscopy is a promising technique to analyze the $^{13}\text{C}/^{12}\text{C}$ isotope ratio at the scale of single FI.

References:

- Frezzotti M. L. et al. (2010): *Geochim. Cosmochim. Acta.*, 74, 3023-3039
 Mattey et al. (1984): *Geochim. Cosmochim. Acta.*, 53, 2377-2386
 Oglialoro E. et al. (2017): *Bull. Volcanol.*, 79, 1-17

FRAnCIs calculation program with universal Raman calibration data for the determination of PVX properties of CO₂-CH₄-N₂ and CH₄-H₂O-NaCl systems and their uncertainties

Le V-H.^{1*}, Caumon M-C.¹, Tarantola A.¹

¹ Université de Lorraine, CNRS, GeoRessources Laboratory, BP 70239, F-54506 Vandoeuvre-lès-Nancy, France

*van-hoan.l@univ-lorraine.fr

Keywords: fluid Inclusions, thermodynamic

Many experimental calibration data linking the variation of Raman spectral parameters (i.e., peak position, peak area/intensity ratio...) with the PVX properties of pure gases or mixtures of CO₂-CH₄-N₂ or CH₄-H₂O-NaCl systems have been published in literature by different laboratories. However, the measured spectral parameters were demonstrated to be instrument dependent (Lu et al., 2007; Lamadrid et al., 2017; Remigi et al., 2021).

The noticeable discrepancy between these existing calibration data can lead to a significant difference of the estimated pressure or density, depending on which densimeter or barometer is used. Consequently, each laboratory has to establish their own calibration to ensure the highest accuracy of the quantitative measurement of fluid inclusions.

In this work, the inter-laboratory applicability of the calibration data based on CH₄ peak position at ~ 2917 cm⁻¹ (ν_1) and CO₂ Fermi diad splitting (Δ) which are published in literature over more than 30 years are examined in order to provide the unified calibration data (Fig. 1).

78 universal regression calibration equations based on the relative variation of ν_1 or Δ , and the peak area ratio of CH₄/H₂O, that are applicable for any Raman apparatus within any laboratory, are provided and integrated into a calculation program, named FRAnCIs. The FRAnCIs (acronym for Fluids: Raman Analysis of the Composition of Inclusions) program with user-friendly interface facilitates the application of these calibration data as well as to estimate the uncertainty of the measurements.

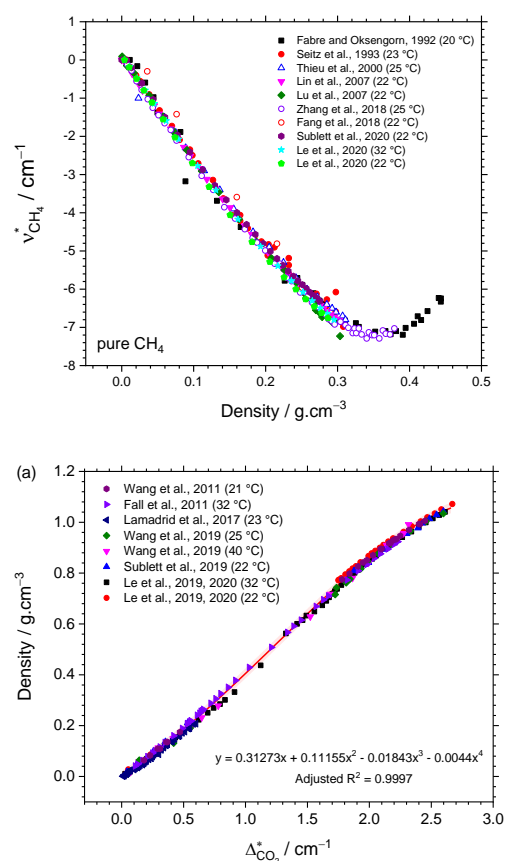


Fig. 1: Relative variation as a function of density of ν_1 within pure CH₄ (top) and of Δ (bottom) within pure CO₂. (Universal data of gas mixtures are not shown here)

References:

- Lu, W., Chou, I.-M., Burruss, R.C., Song, Y., 2007. *Geochim. Cosmochim. Acta.* 71, 3969–3978.
- Lamadrid, H.M., Moore, L.R., Moncada, D., Rimstidt, J.D., Burruss, R.C., Bodnar, R.J., 2017. *Chem. Geol.* 450, 210–222.
- Remigi, S., Mancini, T., Ferrando, S., Frezzotti, M.L., 2021. *Appl. Spectrosc.*

The perfection of Raman spectroscopic gas densimeters

Bakker R. J.

*Resource Mineralogy, Department of Applied Geosciences and Geophysics,
MontanUniversity Leoben, Austria*

bakker@unileoben.ac.at

Keywords: theory, experiments, new frontiers

Raman spectroscopy of gases can be used to determine density, because the energy of fundamental vibrational modes is affected by intermolecular distances. The key problem is the estimation of exact peak positions of Raman bands of gases, because the variability is mostly less than the pixel resolution of Raman spectrometers. Peak positions can only be accurately determined if Raman band shapes are well-defined and spectrometers are correctly calibrated. Both factors have been poorly addressed in literature, which is directly evidenced by the well-known inconsistency of all experimental data, and abundant and not uniform calibration procedures. Raman band shapes were reproduced with best-fit probability distribution functions (*PDF*), and multiple analyses of the same band resulted in the calculation of averages and standard deviations of peak position. This is also known as "reproducibility" and is mistaken for "uncertainty" in measurements. There are abundant disadvantages of this numerical data processing, that can be summarized by: 1. different types of *PDF* may result in a large variety of shape properties; 2. the least-squares fitting method is highly biased, dependent on the number of pixels involved in the fitting procedure and the intensity of the background noise (baseline); 3. a *PDF* does not give any information about the uncertainty.

The present study proves that different Raman spectrometers provide similar empirical relationships between gas density and Raman band wavenumber (peak position), as expected for quantitative analyses of fundamental material properties. The method of analysis and optical and mechanical properties of the machinery that is used

for detection of the dispersion have to be scrutinized to confirm this statement.

A new method to determine peak positions of Raman bands and atomic emission lines in a discontinuous spectrum without mathematical manipulations is tested in this study: modified scanning multichannel technique. Raman spectrometers are equipped with a Sinus Arm Drive to relocate the gratings (rotation) to be able to detect different wavelength ranges at the same pixel array of the detector. Relocation can be performed over a distance that is only a fraction of the pixel size which allows the estimation of peak positions with precisions smaller than the pixel resolution, and to determine the uncertainty in this estimation.

Numerous factors turned out to be crucial for the correct estimation of peak position. A well-defined wavelength of the laser is a prerequisite for accurate determination of Raman shifts. He-Ne laser wavelength can be reproduced with an uncertainty of ± 3 pm, but the Nd-YAG laser has a variable wavelength dependent on laboratory conditions (± 300 pm) and must be estimated before each measurement session. Calibration must be performed with simultaneously recorded atomic emission lines within a single spectral window. Peak positions are affected by the relative position within a spectral window, and by relocation of the gratings (irregularities of the Sinus Arm Drive).

The best estimates of wavenumber uncertainty of the Fermi diad (CO_2) is ca. $\pm 0.26 \text{ cm}^{-1}$, the Raman band of CH_4 has an uncertainty of ca. $\pm 0.12 \text{ cm}^{-1}$.

A new method for P - V - T - x reconstruction of gas-rich geofluids: high precision Raman calibration models and its application on fluid inclusions in accretionary prism (Shimanto, Japan)

Wang W.¹, Lu W.^{1*}

¹ College of Marine Science and Technology, China University of Geosciences, 430074 Wuhan, China

* wjlu@cug.edu.cn

Keywords: fluid inclusion, experiments

Composition-density properties and isochoric evolution path of fluid inclusions are vital and irreplaceable in P - V - T - x reconstruction in geofluid research (Roedder and Bodnar, 1980). In microthermometry method, restricted and inaccuracy measurement of homogenization temperature and volume filling degree of vapor phase could bring obvious error in composition-density determination in gas-rich fluid inclusion analysis (Bakker and Diamond, 2006). Previous Raman analytical procedures also have deficiency and indispensable uncertainties in composition-density calculation of gas-rich systems (Wang et al., 2019). In the present study, a new method for P - V - T - x reconstruction of gas-rich geofluids was built. Based on high pressure optical cell instrument system, Raman spectra of $\text{H}_2\text{O}(\text{g})$ in gas-rich systems were collected precisely at the P - T range of 10 MPa-120 MPa, 100 – 300 °C, i.e. 0.0091-0.894 of X (H_2O) molar fraction, and quantitative calibration models for composition-density calculation of CO_2 -rich and CH_4 -rich systems were constructed.

This Raman quantitative modeling calculates the bulk density and composition of CO_2 -rich and CH_4 -rich fluid inclusions, as well as their P - T isochoric paths. Compared with previous approaches, tens of times higher accuracy were revealed in composition-density calculation by our Raman calibration models. In addition, by Raman spectroscopic analysis and the application on CO_2 -rich fluid inclusions collected from Muroto Cape, Shimanto belt, SW Japan,

we determined composition-density properties of the CO_2 -rich inclusions and P - V - T - x characteristics of the geofluids were reconstructed successfully. Furthermore, we also demonstrated the relationship between genesis and migration patterns of the CO_2 -rich geofluid and asthenospheric upwelling event during Philippine Sea Plate subduction process in the middle Miocene (Fig 1).

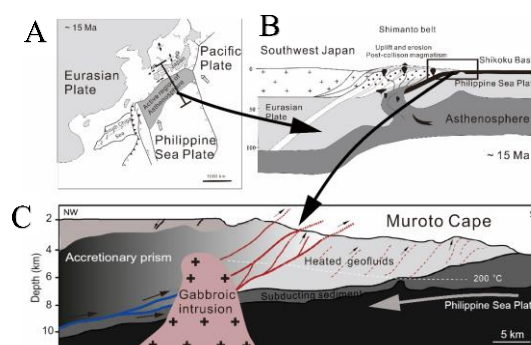


Fig. 1: (A) Hypothetical geodynamic reconstruction of the collision event between Philippine Sea Plate and Eurasian Plate at 15 Ma. (B) Asthenospheric upwelling mechanism in subduction process. (C) Migration model of the CO_2 -rich geofluid under the effect of magmatism in the middle Miocene

References:

- Roedder, E. and Bodnar, R.J. (1980) *ANNU REV EARTH PL SC*, Vol 8, pp 263-301.
- Bakker R. J. and Diamond L. W. (2006) *AM MINERAL* Vol 91, pp 635-657.
- Wang W., Caumon M.-C., Tarantola A., Pironon J., Lu W. and Huang Y. (2019) *CHEM GEOL* Vol 528, 119281.

Evidence of the role of water molecules as habit modifier and their impacts in the formation of fluid inclusions of an organic salt

Marc L.^{1,2*}, Schneider J-M.², Sanselme M.¹, Coquerel G.¹

¹ SMS EA3233 Université de Rouen Normandie Place Emile Blondel F-76821 Mont Saint Aignan CEDEX FRANCE ² SEQENS'Lab 2-8 rue de Rouen 78440 Porcheville FRANCE

*laureline.marc@univ-rouen.fr

Keywords: Habit modifier, fluid inclusions, organic compounds

Ibuprofen is a widely used anti-inflammatory drug. Actually, it is a 50-50 mixture of two enantiomers with different pharmaceutical effects versus dose. The separation of this two components R and S can be performed by using a chiral resolution amine: the S- α -benzylamine in ethanol. In order to limit the consumption of resolving agent a part of it is substituted by soda.

In order to separate the two salts a selective crystallization is used. The less soluble salt –containing the desired drug– crystallizes as very fine needles. This is not convenient for the: filtration, storage and flow-ability of the solid particles. In view to resolve those issues, we tried different pharmaceutically acceptable additives which could act as habit modifiers. Water appeared to be the simplest and safest habit modifier, transforming the very fine needles into platelets (Figure 1). Nevertheless, this elegant solution creates another problem since large fluid inclusions in crystals are frequent. The presence of NaOH increased the occurrence of fluid inclusions. The crystal structure of this salt leads to understand the change in morphological indexes of the different faces when adding water in the mother liquor.

The observed inclusions correspond to a too fast crystal growth rate as soon as the crystals exceed a threshold in size. They also produce a symmetrical pattern already observed in other compounds (Cooper et al., 2020). Nevertheless, these vacuoles filled by the saturated mother liquor with a bubble of gas at RT are not repetitive along the main axis of the single crystals, as what have been observed with ammonium perchlorate for instance (Bobo et al., 2015, 2016).

The effect of gas dissolved in the mother liquor has been investigated. CO₂ deserved a special attention since its solubility is much greater than the other gas and literature shows several examples of its importance in the formation of fluid inclusions (Waldschmidt et al. (2015).

In order to avoid the formation of these fluid inclusions: crystal growth in soda free solution at lower supersaturation in a vigorously stirred and degassed mother liquor proved to be promising at laboratory scale.



Figure 1: Encircled in red the symmetrical fluid inclusions obtained in a mixture: ethanol–Water (80-20%) and a supersaturation: $\beta = 1.8$ at 20°C; seeding at 40°C.

References:

- ¹Cooper J. et al.; (2020) *Cryst. Growth Des.* 20, 7120–7128
- Bobo, E. et al. (2016): *CrystEngComm* 18, 5287–5295
- Bobo, E. et al. (2015): *Chemical Engineering & Technology*, 38, (6), 1011-1016
- Waldschmidt et al. *Cryst. Growth Des.*, 2011, 11 (6), 2463-2470

First experimental results of noble gases from fluid inclusions with the vacuum crushing system at CSIRO's noble gas facility

Wilske C. ^{1,2*}, Suckow A. ², Deslandes A. ², Crane P. ², Gerber C. ², Spooner N. ¹, Mallants D. ²

¹ The University of Adelaide, School of Physical Sciences, North Terrace, The Braggs, Adelaide SA 5000, Australia; ² CSIRO Land and Water, Gate 5, Waite Rd., Urrbrae, SA 5064, Australia

*cornelia.wilske@adelaide.edu.au

Keywords: fluid inclusions, experiments, noble gases

Noble gases provide a unique tool to investigate geological processes from macro to micro scales. In geologic formations with very slow to no advective groundwater flow (e.g. aquitards and shales), noble gases (NG), especially helium, are excellent tracers quantifying diffusion-dominated transport. In “dry” formations of extremely low porosity and permeability, such as igneous rocks, noble gases within fluid inclusions are studied to assess the chronology of ancient fluid migration in the rock matrix and of mineralisation processes.

Australia's National Science Agency the CSIRO operates the Environmental Tracer Laboratory (ETL) at Waite Campus, South Australia (Fig. 1). The ETL has developed a new high vacuum crushing system to extract fluid inclusions from minerals and to measure their noble gas concentrations and isotopic composition. It operates one of only a few High-Resolution Noble Gas Mass Spectrometers in Australia (Helix MC Plus, Thermo Instruments). The preparation system allows purifying the noble gas fractions and measuring, in fully automated mode, rare isotope ratios like $^{136}\text{Xe}/^{132}\text{Xe}$, $^{21}\text{Ne}/^{20}\text{Ne}$ and $^3\text{He}/^4\text{He}$ in groundwater and pore fluids. In fluid inclusions, these noble gas isotopes are the only means to evaluate how long pore fluids were isolated from the water cycle and to quantify primordial and radiogenic components. We present technical details of the high vacuum crusher and the first experimental outcomes based on quartz samples.



Fig. 1: Experimental set up: A - Automated NG machine at CSIRO, B - Assembly of one crusher container, C - WC sample plates filled with 1mm quartz grains, D - Pre-vacuum system for crusher container, E -Crusher container connected to NG line including press

In the beginning:

The movie that triggered interest for inclusions .

Deicha C. ^{1*} , Deicha I. ²

¹ member of COFRHIGEO Paris; European Physical Society section Liechtenstein, POB 705, CH-9490-Vaduz-FL, Switzerland, ² Member of Comité national français de Géographie.

* cd@nwf.li

Keywords: Fluid Inclusions, experiments, fluid-phase equilibria

The historical background of the research on fluid inclusions was discussed during the opening session (Poty, 2017) of the ECROFI Meeting in Nancy four years ago and a call for contributions was made to save the achievements of french pioneers from oblivion.

In the meantime interesting publications appeared as well scientific as for general public and even new materials were discovered in private archives.

In particular we like to present a short video-clip about the beginnings of fluid inclusion research in France. The first french inclusionnists were filmed whilst working in the Laboratory of Applied Geology in Paris and upon their arrival at the Geological Congress of 1952 in Algiers (Deicha and Taugourdeau, 1952). The microscopical observations of moving CO₂ bubbles, which were recorded in Paris, represented a little sensation among the scientists of that times (3). The operation of the first crushing stage is visible in the video, commented by the original voice of Georges Deicha (1917-2011).

There is also a recent biography (4), with plenty of bibliographical references, and interesting arguments confirming the originality of the european scientific achievements in Paris and Nancy.

It is also worth to notice that this school of inclusionnists was probably among the first to address also to general public, for instance in collaborating with well known gemmologists as E. Gübelin or E. Bettetini, uncovering the inside of precious gemstones.

Microcinematography was very useful for such outreach policy, and the book we are preparing (5) intends to continue this

tradition of high level science popularization.

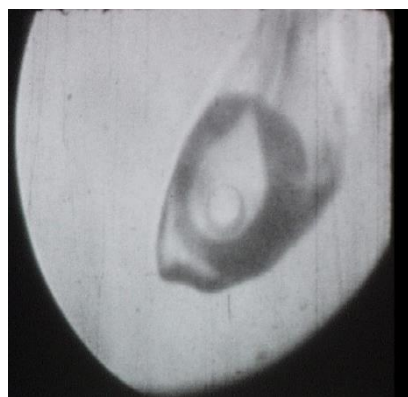


Fig 1: "This CO₂ bubble is growing or disappearing: (phase equilibrium vs. temperature)". This movie was the sensation of the International Geological Congress of 1952 and the trigger for the later interest for fluid inclusions

References :

Poty B. 2017 "Fluid inclusions science during the last hundred years. Considerations of a veteran". In Programme of the Biennial Meeting p. 22 Georesources Nancy 2017

- Deicha G., Taugourdeau Ph., (1952): "Etude microcinématographique des inclusions fluides " Soc. géol.Fr., C.R.somm. N° 11; p. 213-219

- (3) Video from microcinematographic material from 1952 in <https://www.youtube.com/watch?v=PFrwF8TNa7o>

-(4) Deicha S. "A l'occasion du centième anniversaire de la naissance de G. et B. Deicha" (2017) in <https://docplayer.fr/133184697-Vers-la-contemplation-des-phenomenes.html>

(5) Deicha C. "Call for contributions" 2017 handout in <https://deicha.li/application/files/6415/0425/1560/2017DeichaECROFI.pdf>

Posters

Challenges and perspectives in 3D Raman imaging of multiphase inclusions: examples from the Cabo Ortegal Complex

Aradi L. E.^{1*}, Spránitz T.¹, Guzmics T.¹, Berkesi M.¹

¹ *Lithosphere Fluid Research Lab, Eötvös Loránd University, Budapest, Hungary*

**aradi.laszloelod@ttk.elte.hu*

Keywords: fluid inclusion, melt inclusion, new frontiers

Fluids and melts play a crucial role in most deep geological processes from ore formation, through subduction, magmatism and metamorphism. Therefore, characterizing the fluids and melts, commonly found as inclusions of minerals, help to better understand these geological processes. The major goal of this study is to determine the compositions of primary fluid/melt inclusions, which could have been trapped as homogeneous fluid phase, as they cannot be homogenized by microthermometry. 3D Raman imaging can be a non-destructive, yet versatile tool to achieve this goal. However, the advantages and the limitations of this technique should be investigated thoroughly.

Vapor-bearing multiphase fluid inclusions (MPI) were selected from the Cabo Ortegal Complex (NW Spain), which are derived from subduction zone conditions, to present their 3D reconstruction via hyperspectral imaging using Raman microspectroscopy (Fig. 1). MPI in this study are generally showing complexity in their compositions of constituent solids (silicates, carbonates) and a vapor phase at room temperature (Fig. 1). Thus, their 3D reconstruction is crucial when trying to describe the original trapped fluid.

Raman 3D imaging on the inclusions, combined with FIB-SEM analyses, allowed to carry out mass balance calculations by considering the volume percentages and the composition of each phase. In addition, uncertainty of volume percentages of solid phases obtained from Raman 3D imaging can be independently compared to complementary FIB-SEM data, optimizing our methodology.

We demonstrate how different parameters during both data acquisition

(e.g. confocal hole, step size) and evaluation (e.g. data reduction and manipulation, modelling parameters) can be used in different host minerals under varying conditions, in order to be able to provide a relatively fast and cheap alternative to FIB-SEM sectioning. The 3D Raman image (Fig. 1) also gives the opportunity to observe the phases within the MPI by arbitrary sections in the XYZ space, without destroying the samples, unlike during FIB-SEM sectioning.

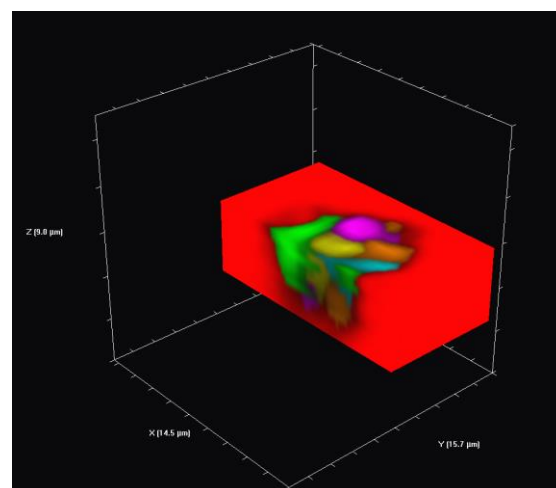


Fig. 1: 3D Raman image of MPI in garnet (red) from the Cabo Ortegal Complex. The phases are vapor CO₂ (green), magnesite (yellow), pyrophyllite (teal), quartz (purple) and corundum (orange).

The results of our study could yield valuable contributions to the chemistry and nature of the studied MPI. The presented methodology can also be applied in different geological environments, where Raman 3D imaging of fluid and/or melt inclusions is necessary.

This research was supported by the NRDIO_FK research fund nr. 132418 and by the TKP2020-IKA-05, financed by the Hungarian Ministry of Human Capacities.

How much fluid is released from fluid inclusions during cataclasis?

Richard A.^{1*}

¹ *Université de Lorraine, CNRS, CREGU, GeoRessources Lab, F-54500 Vandœuvre-lès-Nancy, France*

**antonin.richard@univ-lorraine.fr*

Keywords: fluid inclusion, theory, hydrothermalism

When minerals are subjected to brittle deformation, some of their fluid inclusions may break and fluids may be released in fractures.

Fluid inclusion breakage and leaching has been suspected to contribute significantly to some groundwater chemistry (e.g. Nordstrom D. *et al.*, 1998). However its significance for hydrothermal systems remains poorly understood.

Cataclasis (i.e. rock comminution during brittle deformation) is a common phenomenon in fault zones and therefore is intimately linked with fluid flow in the upper crust and hydrothermal systems.

While the modification of the composition of hydrothermal fluids by mineral leaching during cataclasis has been subjected to some experimental studies (e.g. Burisch M. *et al.*, 2016), little is known about the significance of fluid inclusion leaching.

One of the main limitations is the difficulty to estimate the volume of fluid per mass unit trapped as fluid inclusions in minerals, based only on optical determination of fluid inclusion size and abundance.

In order to circumvent this limitation, I use a compilation of published fluid inclusion leachate compositions obtained from "crush-leach" analyses (e.g. Banks D. A. *et al.*, 2000), coupled with average fluid inclusion salinity in the corresponding samples.

The main working hypothesis is that hand crushing and grinding of minerals in an agate pestle and mortar and leaching of mineral powder at room temperature by doubly distilled water in a laboratory is a good analogue to natural cataclasis and fluid inclusion leaching by hydrothermal fluids in fault-related hydrothermal systems.

The database allows to provide first order estimates of the volume of fluid per mass unit of cataclasite potentially released from fluid inclusions during cataclasis.

The calculated volumes are compared to usual fluid-rock ratios of hydrothermal systems in upper crustal fault zones in order to determine the conditions in which fluid inclusion breakage and leaching contributes significantly to the fluid budget.

Furthermore, in such cases, the chemical composition of the fluid inclusion leachates produced from "crush-leach" analyses can be used to determine how fluid inclusion breakage and leaching will affected the bulk salinity and the detailed composition of the hydrothermal fluids.

References:

- Banks D. A., Giuliani G., Yardley B. W. D. (2000): Miner. Deposita Vol 35, pp 699-713.*
- Burisch M., Marks M. A. W., Nowak M. (2016): Chem. Geol., Vol 433, pp 24-35.*
- Nordstrom D. K., Lindblom S., Donahoe R. J. et al. (2010): Geochim. Cosmochim. Ac., Vol 53, pp 1741-1755.*

Are two-phase fluid inclusions really common in stalagmites?

Lopez-Elorza M.^{1,2*}, Muñoz-García M. B.¹, González-Acebrón L.¹, Martín-Chivelet J.^{1,2}

¹ Dpto. Geodinámica, Estratigrafía y Paleontología, Facultad de Ciencias Geológicas, Universidad Complutense de Madrid, 28040 Madrid; ² Instituto de Geociencias IGEO (CISC-UCM), C/ Severo Ochoa 7, 28040 Madrid. Spain

*maialelo@ucm.es

Keywords: primary fluid inclusions, paleoclimatology, speleothems

The entrapment of two-phase fluid inclusions is common in vadose environments (Goldstein, 1986). Probably for this reason, two-phase fluid inclusions have been also regarded as a common feature in speleothems, without further discussion. However, Krüger et al. (2011) indicated that the preparation of petrographic sections could cause changes in fluid inclusions of speleothem calcite, including late water leaking, and suggested that most fluid inclusions trapped in stalagmites calcite could originally have been all-water inclusions, as the growth surface of the stalagmites is usually covered by a persistent film of water. To check this hypothesis, we analysed 75 petrographic sections (5 wide x 8 cm long) of calcite stalagmites from varied cave and karst systems. The study allowed to recognize primary fluid inclusions showing a variety of morphologies and characteristics (Lopez-Elorza, 2019). Remarkably, the majority of these inclusions were all-water, and only some were all-air or two-phase fluid inclusions. These later were mainly found in three specific scenarios:

1. *Interbranch two-phase fluid inclusions associated to dendritic fabric.* These were probably trapped under conditions of variable water discharge, and high supersaturation, leading to high growth rates and incorporation of both water and air.

2. *Two-phase, intra- and intercrystalline fluid inclusions, associated to condensed intervals* (i.e., characterised by very low growth rates), consisting of alternating thin layers of micrite and columnar calcite. These fluid inclusions are interpreted to result from partial dryness of the stalagmite surface when the

dripping is poor and very slow. Under these circumstances, the water film on the stalagmite surface could be very thin or intermittent, and water and gas may be trapped simultaneously. Also, the presence of air could be related to microbial activity that is commonly related to micrite fabrics (Frisia, 2015).

3. *Two-phase fluid inclusions in columnar fabrics.* Stable drips can generate a permanent film of water on the stalagmites surface and induce the development of columnar fabrics. These circumstances favoured the entrapment of only water, both as intra- or intercrystalline fluid inclusions. However, water degassing could lead to two-phase inclusions. Entrapment of CO₂ derived from degassing seems to be more effective in fluid inclusions with narrow morphologies and apertures, which prevent gas bubbles to scape and favour to be rapidly sealed by crystal growth.

Contribution to CGL2013-43257-R and CGL2017-83287-R projects (AEI, Spain).

References:

- Frisia, S. (2015): *Int. J. Speleol.*, Vol. 44, pp. 1-16.
- Goldstein, R. H. (1986): *Geology*, Vol. 14, pp. 792-795.
- Krüger, Y., Marti, D., Staub, R. H. et al. (2011): *Chem. Geol.*, Vol. 289, pp. 39-47.
- Lopez-Elorza, M. (2019): *PhD Dissertation*. UCM, Madrid. Pp. 225.

Trapping of heterogeneous fluids

Bakker R. J.

*Resource Mineralogy, Department of Applied Geosciences and Geophysics,
Montanuniversität Leoben, Austria*

bakker@unileoben.ac.at

Keywords: theory, thermodynamic calculations, experiments

In theory, the formation of a fluid inclusion assemblage from a multi-phase state (i.e. heterogeneous entrapment) is a common process at natural geological conditions. The immiscibility of multi-component fluids may occur at high temperatures and pressures and is not restricted to diagenetic conditions. Specific fluid systems are even immiscible at Greenschist-, Am

phibolite-, Blueschist-, and Granulite-facies metamorphic conditions. The identification of a heterogeneous fluid inclusion assemblage in natural rock is a major challenge in fluid inclusion research, and it is expected to be a common phenomenon. There is only little experimental knowledge about the formation of heterogeneous fluid inclusion assemblages. The synthesis of these assemblages has been used in only a few experimental studies to investigate the boundary conditions of fluid immiscibility fields. These studies included the analyses of only a few fluid inclusions (between 1 and 10 per experiment), but do not reveal the variability of the assemblage or systematics on the distribution or deviations of distinct fluid inclusion types. One inclusion is not representative for specific experiments that usually result in a variety of fluid properties.

Fluid inclusions are synthesized at approximately 600 °C and 80 MPa, from a 30 mass% NaCl aqueous solution (SR-020) and a 10 mass% NaCl aqueous solution (SR-019). For both experiments, the conditions are within the two-fluid phase field, and both should result in the formation of similar liquid-rich inclusions and similar vapour-rich inclusions, but in different proportions. Due to the unmixing at experimental conditions, two fluids are present in the capsules, i.e. a liquid-like fluid relatively enriched in NaCl

(40.42 to 41.40 mass%) and a vapour-like fluid relatively depleted in NaCl (2.41 to 2.71 mass%). The measured dissolution and homogenization temperatures are not consistent with values calculated with the thermodynamic model (Fig. 1).

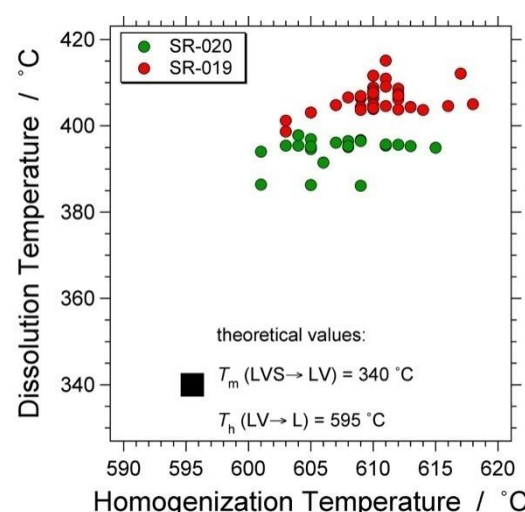


Fig. 1. Microthermometric results of liquid-rich fluid inclusions from SR-019 and SR-020. The expected values are illustrated by the black box.

These preliminary results of experiments in the H₂O-NaCl fluid system have illustrated that predicted fluid properties do not correspond to the observed assemblage. Therefore, the processes that are involved during heterogeneous entrapment need to be investigated in greater detail by systematic analyses of entire fluid inclusion assemblages to be able to predict fluid entrapment in natural systems, and to be able to deduce natural trapping conditions from the observed assemblages.

FROM MAGMA GENESIS TO ERUPTIONS
INCLUDING HYDROTHERMAL ACTIVITY

e-CROFI 2021

Incursion of Maritimes Basin brines into active epithermal gold systems, Cobequid and Antigonish Highlands, Nova Scotia, Canada (keynote)

Hanley J. J.^{1*}, Neyedley K.^{1,2}, Sharpe R.³, Fayek M.³

¹ Department of Geology, Saint Mary's University, Canada; ² Nova Scotia Dept. of Energy and Mines, Canada; ³ Department of Geological Sciences, University of Manitoba, Canada

*jacob.hanley@smu.ca

Keywords: fluid inclusions, ore deposits, volcanism

Low sulfidation epithermal gold systems are hosted in Late Devonian to Early Carboniferous bimodal volcanics (Cobequid Highlands) and Ordovician metasediments (Antigonish Highlands) in Nova Scotia, Canada. Mineralized quartz-carbonate vein textures are typical of rapid boiling ("flashing"; e.g., lattice-bladed calcite, and colloform-banded, plumose-textured, and mossy quartz). Primary and secondary fluid inclusions (L_{aqueous}+V at room T) comprise two types: *Type A* inclusions (Fig. 1) occur in early, zoned, euhedral quartz and lattice-bladed calcite. Fluid inclusion assemblages (FIAs) also show evidence of episodic boiling or "flashing". Homogenization temperatures (T_h) and salinity values are between ~120 and 290°C and 0 to ~10 wt% NaCl equiv. (variations up to 70°C and ~4 wt% NaCl equiv. within FIA). *Type B* (Fig. 1) inclusions occur in massive calcite infilling vugs in earlier quartz and calcite. Salinity values are between ~19 and 32 wt% CaCl₂ eq. and LA-ICPMS confirms abundant divalent cations (Ca-Mg-rich). T_h data ranges are narrow for individual FIA, but range overall from ~70°C to 280°C, with most type B FIA showing an inverse correlation between salinity and T_h .

End-member type A fluid likely represents a magmatic-hydrothermal (epithermal) fluid that was transiently boiling and mixed with a cooler, much higher salinity end-member type B fluid, a marine evaporate brine (Fig. 1). Support for bittern incursion is provided by *in-situ* stable O and S isotope analyses of epithermal vein minerals (quartz, calcite, barite, and pyrite) from the study areas by SIMS. These analyses show: (i) ³⁴S-enriched ($\delta^{34}\text{S}_{\text{VCDT}} = 19.4\text{--}20.8\text{‰}$) barite at the core of epithermal veins containing boiling Type A FIA; (ii) pyrite

grains with late overgrowths showing very high $\delta^{34}\text{S}_{\text{VCDT}}$ values (24.8–26.4‰); (iii) a major decrease in $\delta^{18}\text{O}_{\text{VSMOW}}$ from early growth zones in vein quartz to late growth zones in vein quartz and carbonate vug infilling, corresponding to a shift in calculated fluid $\delta^{18}\text{O}_{\text{VSMOW}}$ from ~10‰ to <0‰. Both (i) and (ii) are attributed to marine sulfate associated with formation of the earliest overlying Mississippian evaporites, with sulfide likely derived from high T sulfate reduction, while (iii), when combined with the fluid inclusion data, supports the introduction of a bittern. Evaporite formation in the overlying Maritimes Basin must have been already initiated during the waning stages of magmatic-hydrothermal activity in the study areas and implicates basinal brine incursion as a possible mechanism for metal precipitation.

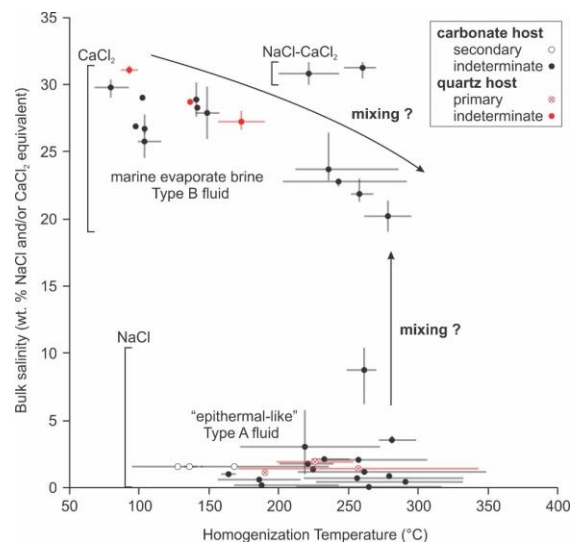


Fig. 1: Salinity- T_h plot showing data for a high salinity group (marine evaporate brine) and lower salinity group (epithermal) with possible mixing trends between the two fluids. Data points are average for individual FIA with bars representing total range for each FIA.

Composition of orthomagmatic fluids related to carbonatites

Mororó E. A. A.^{1*}, Berkesi M.¹, Guzmics T.¹

¹ *Lithosphere Fluid Research Lab, Eötvös Loránd University, Budapest, Hungary.*

**mororo.emanuel@gmail.com*

Keywords: fluid inclusion, magmatism, volcanism

Fluids associated to carbonatite magmatism contribute to the formation of Na-carbonatites, e.g., Oldoinyo Lengai (OL), and highly peralkaline silicate melts occurring worldwide. However, the characterization of fluids originated from carbonatite magmatism is challenging, as their composition can easily change after separation from carbonatite-silicate parent melts. Several studies have suggested a NaCl-H₂O-CO₂ composition for carbonatite-related fluids (Walter et al. 2021). In contrast, fluid bubbles in melt inclusions containing carbonate or immiscible silicate-carbonate melts show a H₂O-poor, S-bearing, alkali carbonate + CO₂ composition (Guzmics et al. 2019). In order to better understand the composition of such fluids among the existing models, we studied fluid inclusions (FI) from the recently active OL magmatism.

The studied FI are secondary, hosted in quartz from a metamorphic xenolith found in a CWN (combeite-wollastonite-nephelinite) tuff at OL. The quartz interacted with fluid and, later, melts originated from OL magmatism, resulting in the formation of the studied FI trails. At room-T sulfate, nahcolite and natrite daughter phases coexist with liquid- and vapor-CO₂ (Fig. 1a) within the FI (n=30). Raman microspectroscopy (n=200) showed that the majority of the daughter minerals are thenardite, arcanite, nahcolite and natrite. 3D Raman imaging (n=5, Fig. 1b) was used to estimate the volume proportions of these daughter minerals and CO₂. We could determine the homogenization-T of FI to be 800-850 °C; where no difference in the Raman spectra, taken from different parts of the FI, was observed.

Our results suggest a common alkali-carbonate-sulfate-CO₂ composition (<6 H₂O wt%) for fluids exsolved from carbonatite melts.

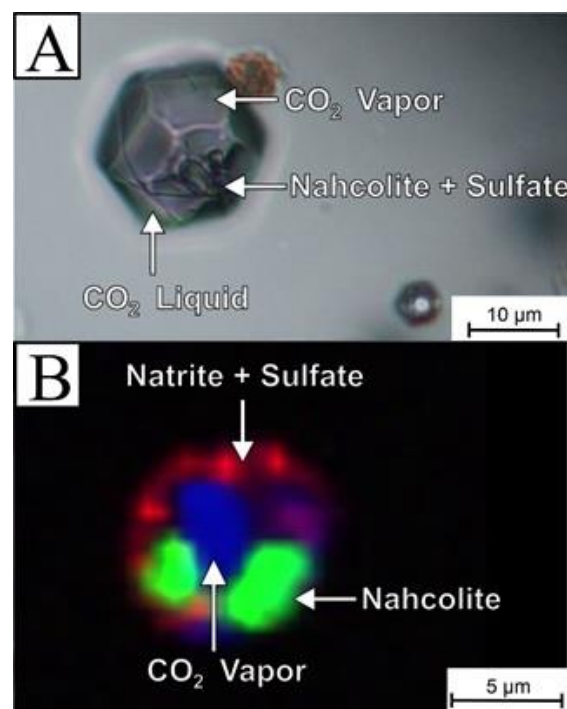


Fig. 1: Two representative quartz-hosted fluid inclusions (A and B) at room temperature. A – Photomicrograph, B – Raman image.

References:

- Walter B.F., Giebel R.J., Steele-MacInnis M. et al. (2021): *Earth-Sci. Rev.*, Vol 215, 103509.
- Guzmics T., Berkesi M., Bodnar R.J. et al. (2019): *Geology*, Vol 47, pp 527-530.

Anomalous high halogen concentration in water depleted eruptive centers from Lonquimay Volcanic Complex

Tapia-Rodríguez F.^{1*}, Cannatelli C.², Buscher J.², Fanara S.³, Morata D.⁴

¹ IMAU, Utrecht University, The Netherlands.; ² University of Alaska Anchorage, USA.; ³ Bundesgesellschaft für Endlagerung, Germany.; ⁴ Department of Geology and Andean Geothermal Centre of Excellence (CEGA), University of Chile.

*fab.tapia.rodriguez@gmail.com

Keywords Halogens, Melt Inclusions, Arc Volcanism

The last eruption of the Lonquimay Volcanic Complex (LVC), known as the Navidad eruption (December 25th, 1988), emitted anomalous high levels of F, affecting the nearby ecosystem causing mortality in cattle and sheep. LVC is in the La Araucanía region, south of Chile, above the northernmost trace of Liquiñe-Ofqui fault system (LOFS) in the Andean Southern Volcanic Zone (SVZ). LVC is made up of a main stratovolcano (Lonquimay) and minor eruptive centers and fissures located NW-SE known as Cordon Fisural Oriental (CFO) where Navidad cone is emplaced.

In this study, we focused on bubble-bearing olivine (Fo 80 to 50)-hosted melt inclusions (n=24), determining the pre-eruptive magma composition and its volatile content. We analyzed major and trace elements from two similar and contemporary lavas, one from the Lonquimay and the other from the Navidad cone, using Electron microprobe (EMPA), Secondary Ion Mass Spectrometry (SIMS), and Raman spectroscopy.

Our data show F content of 200 to 1200 ppm and Cl content of 200 to 1200 ppm in the melt. Navidad MIs have higher F (up to 1200) than Lonquimay MIs (up to 600 ppm) but similar Cl content between 200 to 1200 ppm. In addition, our data show that Navidad and Lonquimay are water-depleted magmas (0.1 to 0.25 wt.%) with a typical volcanic signature of CO₂ (520 to 1420 ppm), although Lonquimay has lower CO₂ content (up to 700 ppm).

F and Cl content in MIs are characteristic from arc volcanic setting magmas being the underlying mantle with contributions from the subducting the most likely source. REEs show that both eruptions

most likely have been fed by magmas with the same mantle source. However, MIs hosted in Navidad eruptive products are water depleted and show CO₂ contents typical of undegassed systems.

Halogenes, melt inclusions, arc volcanism.

References:

O. González-Ferrán. (1989) *Revista Geofísica*, Vol 31, pp 39–107.

This work is a contribution to the ANID-Fondap projects 15090013 & 15200001.

Carbonate-sulfate melt at the contact of chloride xenoliths in kimberlites of Udachnaya-East pipe (Siberia)

Grishina S.^{1*}, Yakovlev I.¹, Smirnov S. Z.¹

¹*Sobolev Institute of Geology and Mineralogy Siberian Branch of the Russian Academy of Sciences, Koptuyg Avenue 3, Novosibirsk 630090, Russia.*

*grishina@igm.nsc.ru

Keywords: fluid inclusion, melt inclusion, metasomatism

Alkali-rich phases were reported in kimberlites worldwide. These phases have only been identified as significant rock constituents in the Udachnaya-East kimberlites, hosted abundance of chloride xenoliths. The lack of reaction zone in the most of chloride xenoliths is likely related to the mechanical weakness of chlorides, that can be lost during xenolith transport in kimberlite. Here we present new data on the relics of the destroyed contact zone, evidenced by sulfate-carbonate melt inclusions in halite. Main components of polyphase inclusions - aphtitalite ($K_3Na(SO_4)_2$), cesanite ($Ca_2Na_3[(OH)(SO_4)_3]$), tenardite ($Na_2(SO_4)_4$) and minor -tetraphlogopite - are the same as in the small globular zonal chloride segregations (Grishina et al., 2019).

Composition variations at the rim of large (60 cm) angular chloride xenoliths are:

- ubiquitous $CaSO_4$;
- hydrous sulfates: gorgeyite ($K_2Ca_5(SO_4)_6 \cdot (H_2O)$), syngenite ($K_2Ca(SO_4)_2 \cdot (H_2O)$),
- Mg-bearing components: tychite ($Na_6Mg_2(CO_3)_4(SO_4)$), langbeinite ($K_2Mg_2(SO_4)_3$), $MgSO_4$, $MgCO_3$;
- increase in the content of $SrSO_4$, Cl and F in sulfate phases.

Daughter minerals in sulfate-rich melt inclusions in halite are very similar to those in secondary inclusions in olivin (Golovin et al., 2007). Carbonate-sulfate melts have been recently reported as a common feature of iron oxide-apatite systems associated the process of assimilation (Bain et al. 2020).

The study aims to clarify the source of the Na-S-Cl-enrichment in the Udachnaya-

East pipe, which is highly discussed. Identification of water-bearing minerals at the rims of chloride xenoliths in contrast to waterless minerals at the core (Grishina, 2018) helps to argue the succession of mineral formation in favor of late alteration rather than magmatic differentiation.

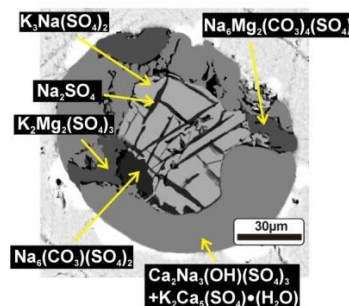


Fig. 1: SEM view of a sulfate-carbonate inclusion exposed in polished surface of halite.

References:

- Grishina, Y. Maximovich, A. A. Tomilenko, et al., *Mineral. Petrogr. Abstr. Ser.* (2019) : 10 , pp 47.
- Golovin, A.V., Sharygin, V.V., Pokhilenko, N.P., (2007). *Petrology* 15, 168–183
- Grishina S., Koděra P., Uriarte L. M, et al.(2018) *Chem. Geol.* 493, 532 pp 532–543
- Bain, W.M., Steele-MacInnis, M., Li, K. et al. (2020) *Nat. Geosci.* 13, pp 751–757.

Hydrocarbons in magmatic fluid of the Menshiy Brat volcano (Medvezhya Caldera, Iturup Island)

Nizametdinov I.^{1,2*}, Kuzmin D.², Smirnov S.², Kotov A.³, Maksimovich I.^{1,2}

¹ Novosibirsk State University, Novosibirsk, Russia; ² V.S. Sobolev Institute of Geology and Mineralogy SB RAS, Novosibirsk, Russia; ³ Tohoku University, Sendai, Japan.

*inizametdinov@igm.nsc.ru

Keywords: melt inclusions, volcanism

The presence of hydrocarbons is noted in gases of many fumarole and hydrothermal fields. For example, methane was found in gas in high-temperature fumaroles of Kudryavy volcano (Medvezhya Caldera) (Taran et al., 1995) and Gorely volcano (Kamchatka Peninsula) (Chaplygin et al., 2015). However, information obtained by the study of emitted volcanic gases can be distorted due to interactions with the atmosphere and meteoric waters.

We studied gas bubbles in melt inclusions in phenocrysts of olivine and plagioclase from basalts and pyroxenes, quartz phenocrysts from rhyolites that compose the Menshiy Brat volcano. As a result of pyrolysis-free gas chromatography-mass spectrometry analysis of gas bubbles in melt inclusions, more than 300 various compounds were found. The proportion of organic compounds is 52-92 mol. % in fluid, that includes paraffins, olefins, cyclic hydrocarbons, alcohols and other oxygenated hydrocarbons, as well as nitrogenated and sulfonated compounds, phosphorus containing compounds.

Composition of magmatic fluids (Fig. 1) of the Menshiy Brat volcano are located along the one trend near the CH₂-CO₂ line. This trend shows compositional evolution from the most reduced fluid (in olivine, plagioclase from basalts) to the most oxidized fluid (in quartz from rhyolite). Apparently, alkenes or heavy saturated hydrocarbons (C₁₅-C₁₇) could play a leading role in the earlier initial fluid, however, during further evolution, the content of CO₂ and H₂O were increased. In turn, the compositions of volcanic gases from Kudryavy volcano and Gorely volcano contain mainly water and carbon dioxide, and the methane

may be a product of the interaction of both, H₂O and CO₂ gases (Fig. 1).

The study of the gas bubbles in melt inclusions allows concluding that the composition of the magmatic fluid is more complex than the composition of volcanic gases. In this case, this is due to the large amounts of organic compounds that dominated in the magmatic fluids.

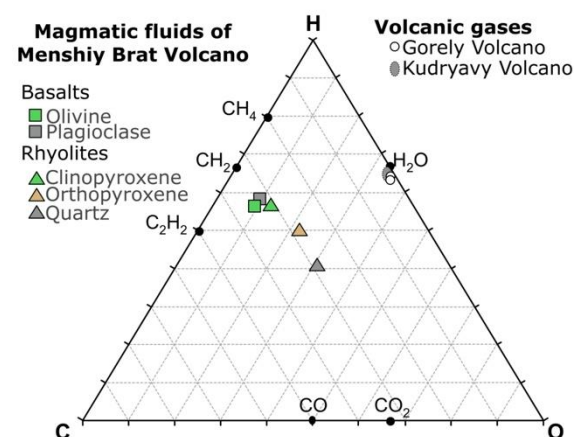


Fig. 1: Composition of magmatic fluid in phenocrysts from Menshiy Brat volcano and volcanic gases of Gorely volcano and Kudryavy volcano on the C-O-H diagram in atomic ratio.

Funding: The reported study was funded by RFBR, project number 19-35-90038.

References:

- Chaplygin I.V., Dubinina E.O., Taran Yu.A. et al. (2015): *Doklady Earth Sciences*, Vol 463(1), pp 690-694.
- Taran Yu.A., Hedenquist J.W., Korzhinsky M.A. et al. (1995): *Geochimica et Cosmochimica Acta*, Vol 59(9), pp 1749-1761.

Contribution of the fluid inclusions to the characterization of the Bonikro gold deposit, Fettekro greenstone belt, Côte d'Ivoire.

Quattara Z.^{1*}, Coulibaly Y.², Boiron M-C.³

¹Département de Géologie et Matériaux, UFR SGM, Université de Man, Côte d'Ivoire;

²Département de Géologie, Ressources Minérales et Energétiques, UFR STRM, Université Félix Houphouët-Boigny, Abidjan, Côte d'Ivoire, ³Université de Lorraine-CNRS, GeoRessources lab, Vandœuvre-lès-Nancy, France.

*ziegbana@hotmail.fr

Keywords: fluid inclusion, hydrothermalism, ore deposits

The Bonikro gold deposit belongs to the southern part of the Fettekro greenstone belt. The geology presents two main birimian units: the mafic volcanic in the East and, the westerly volcano-sedimentary. These two units are metamorphosed to the greenschist facies also are affected by the north-south Bonikro Shear Zone (BSZ) and intruded by a porphyritic granodiorite.

Gold is primarily found within the granodiorite and secondarily in the zones where this intrusive and the BSZ are also present. The mineralization is marked by a strong hydrothermal through the zones of sericitization, silicification, chloritization, albitization and of three veins: sheeted, planar and transversal.

Among these veins, the sheeted show particular characters: (i) syngenetic, (ii) a low fluid-rock ratio and (iii) scheelite-bearing veins. They appear as the veins that can help to characterize the primary gold mineralization.

Seventy-two fluids inclusions have been studied in the sheeted (34) and the planar (38) veins by microthermometry at the Université de Lorraine, Nancy in France. Ten of them have been investigated by the Raman spectroscopy method.

The deposit inclusions are mostly carbonic, aqueous, aquo-carbonic both primary and secondary fluids.

The carbonic phase is dominated by the carbonic dioxide, then nitrogen and methane. Water represents the main liquid phase. These fluids show a weak salinity.

They were able to reveal the Bonikro gold deposition conditions: the temperatures are between 350 and 400 °C then the pressure range from 200 to 450 MPa.

The hydrothermal minerals within these veins are also been investigated. The geothermometer chlorite is also consistent with these temperatures of formation.

These gold endowment conditions at Bonikro show that the deposit has some key characters similar to the others birimian known gold deposits.

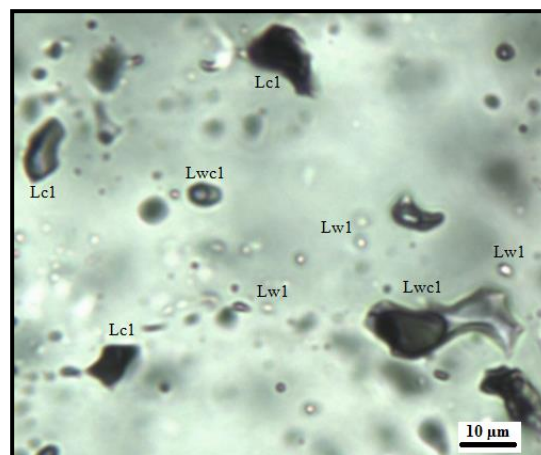


Fig. 1: Photomicrograph of fluid inclusions from the Bonikro gold deposit. W-aqueous, c-carbonic, L-Homogenization on liquid phase, 1-Primary fluid.

Fluid Inclusions and Origin of Carlin-style mineralization at the Cove Deposit, Nevada

Shapley S.^{1*}, Harlaux M.², Muntean J.²

¹University of Nevada Reno.; ² Nevada Bureau of Mines and Geology

*srshapley2@gmail.com

Keywords: fluid-inclusions, ore deposits, hydrothermalism

Carlin-style gold deposition is the leading source of gold in Nevada and the USA. Despite decades of research, there is no consensus on the source of gold or fluid. The fine-grained nature of ore assemblages (mainly Au-bearing arsenian pyrite and marcasite) as well as lack of associated quartz veins and fluid inclusions makes it difficult to determine conditions of mineralization- including the temperature, salinity, and source of the hydrothermal fluids. The Cove deposit, located in north-central Nevada, grades from deep base metal vein type (BMVT) mineralization to Carlin-style mineralization. Past research provides a strong understanding of Cove, including magmatic signatures of BMVT mineralization and minimum paleodepth estimates of ~1000m below current surface (Johnston et al., 2008; Muntean et al., 2017). The association of BMVT with Carlin-style mineralization affords a unique opportunity to investigate fluid sources of Carlin-style mineralization.

This study combines fluid inclusion (FI) petrography, microthermometry, and Raman spectrometry analysis of FIs to characterize BMVT mineralization fluids. FI petrography identified three categories of FIs: (I) primary two-phase intermediate density fluids (II) irregular secondary FIs, and (III) secondary vapor-rich and multi-phase hypersaline FI assemblages trapped in the same fracture plane. Group (I) are rounded lobate two-phase FIs with 20-40 volume % vapor bubbles. Preliminary microthermometry for group (I) indicates moderate homogenization temperatures (236-362°C avg = 330°) and low salinities (1.74-4.96 wt.% NaCl eq, avg.

3.7% wt.% NaCl eq). Clathrates were present in some assemblages. Preliminary Raman Spectrometry identified the gas phase in these FIs as avg. 0.78 mol. fraction CO₂ and .22 mol. fraction CH₄. Group (II) crosscut all other inclusions and has strong reequilibration textures. As such, no further work has been conducted. Group (III) ranges from rounded lobate to irregular in shape. Some instances of multi-phase brines are in the same fracture planes as vapor FIs in low proportions, indicating they may be trapped at phase separation, while other inclusion planes trap only brines. The hypersalinity of the brines suggest a hot source fluid. The presence of multiple fluids at similar depths at the Cove deposit may indicate telescoping of the deposit during its formation or multiple pulses of fluid emerging from depth.

Final steps for this project will evaluate the potential for BMVT fluids to evolve to Carlin-style mineralization by using laser ablation to search for enrichments of Au, As, Hg, and Tl within the BMVT fluids. Continued work on the Cove deposit will provide a better understanding of source fluids at Cove.

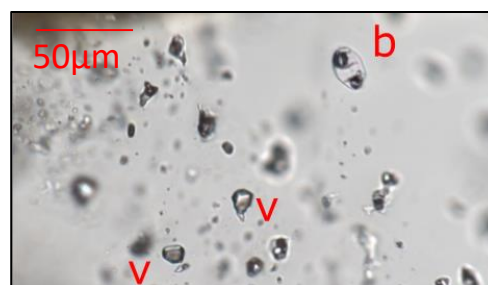


Fig. 1: Photomicrograph of vapor and multi-phase brine FIs in 1 quartz fracture plane. Sample PG1415-2609 G9. v-vapor, b-brine.

References:

Johnston, M., Thompson T., Emmons D. et al. (2008): *Econ. Geol.* Vol 103, pp 759–782.
Muntean, J., Bonner, W. Hill, T. Min. (2017): *SGA Conference Proceedings Vol 1*, pp 71–74.

Amphibole Dehydration and Crustal Contamination as Volatile Oversaturation Mechanisms in Calbuco Volcano's "silent" eruption

Astudillo Manosalva D.^{1*}, Cannatelli C.², Castruccio A.³, Schiavi F.⁴, Samaniego P.⁴, Hernández Prat L.³

¹ University of Florida, USA; ² University of Alaska, USA; ³ Universidad de Chile, Chile; ⁴ Laboratoire Magmas et Volcans, France

*Daniel.astudillo@ufl.edu

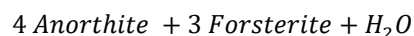
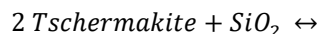
Keywords: Melt Inclusion, Magmatism, Volcanism

Calbuco Volcano, located in the Andean Southern Volcanic Zone (ASVZ, 41°S), produced two subplinian eruptions on April 22nd, 2015 with minor or absent surface deformation and scarce seismic precursors up until a few hours prior to the eruption. Several questions rise in the need to explain how one of the most active volcanoes of southern Chile could erupt without warnings on a monitored area. Melt inclusion (MI) analyses on olivine, pyroxene, plagioclase and amphibole from 2 different tephra products from the eruption, the dominant dark-coloured scoria and an amphibole-bearing white pumice indicate the chemical evolution and pre-eruptive history of the magma, including its volatiles.

Contrasting with an intermediate basaltic andesite whole rock composition, MI compositions range from basaltic andesite to dacite, representing a moderately evolved, H₂O, CO₂, SO₂ and Cl saturated magma. Crystallization is the main mechanism for the evolution of the magma, with parallel trends for the evolution of both products, with the white pumices forming from a more evolved point, with twice the concentration of Li and B as their more common counterparts. White pumices must have formed as a mixture of the original basaltic andesite melt with contamination from the chamber walls, possibly from the dehydration reaction of amphibolitic rocks as was found by Hickey-Vargas et al. (1995) for previous eruptions.

The finding of an exceptionally large, partially dissolved amphibole with a reaction rim of plagioclase olivine and pyroxene shows the origin of the abundant plagioclase and pyroxene

crystalline cumulates which often have olivine remains with ulvospinel symplectites within the pyroxenes. The following reaction explains their formation:



Olivine then reacts with the melt forming orthopyroxene with the characteristic spinel symplectite of this reaction (Ambler and Ashley, 1977). The abundance of these cumulates indicate that the pre-eruptive magma is emplaced from amphibole-bearing magma from a deeper reservoir.

Both processes would have supplied a significant addition of H₂O to an already saturated melt. Cl, F, CO₂ contents would also have been increased by the crustal component, but also by crystallization and water exsolution. Large sulphide inclusions within the large amphibole and smaller ones in plagioclase and pyroxene crystals indicate S oversaturation of the melt before and after emplacement.

The cause of the silent eruption is likely a result of substantial exsolved volatile pressure and the lack of observed deformation could be explained because a large part of the boiling would have occurred during emplacement, which could have happened decades before the eruption.

References:

- Hickey-Vargas, R., Abdollahi, M. J., Parada, M. A. et al. (1995). *Contrib. Mineral. Petrol.*, 119(4), 331-344.
- Ambler, E. P., & Ashley, P. M. (1977). *Lithos*, 10(3), 163-172.

Assessing the extent of crustal assimilation in central Iceland: oxygen isotope analyses in melt inclusions from Bárðarbunga volcano

Caracciolo A.¹, Halldórsson S. A.¹, Bali E.¹, Marshall E. W., Jeon H.², Whitehouse M. J.², Barnes J. D.³, Guðfinnsson G. H.¹, Kahl M.⁴, Hartley M. E.⁵

¹Nordic Volcanological Center, Iceland. ²Swedish Museum of Natural History, Sweden.

³Department of Geological Sciences, Texas, USA. ⁴Institut für Geowissenschaften,

Germany. ⁵Department of Earth and Environmental Sciences, Manchester, UK.

*alberto@hi.is

Keywords: melt inclusion, magmatism

Oxygen isotope ratios ($\delta^{18}\text{O}$) of Icelandic crustal rocks and neovolcanic lavas differ significantly from mantle values. $\delta^{18}\text{O}$ values have been widely used to study the role of the crust in Icelandic basalt petrogenesis, either in the form of source contamination or as crustal contamination. The Bárðarbunga volcanic system in central Iceland is envisioned as a multi-level system of crustally-seated interconnected stacked sills in which magmas are processed over a large range of depths (Caracciolo et al. 2020, 2021). With the goal of quantifying the extent of oxygen isotope exchange as melts ascend through the crust, we present trace element and $\delta^{18}\text{O}$ analyses in melt inclusions (MIs) and groundmass glasses from a well-characterised eruptive suite from Bárðarbunga volcano.

and trace element ratios (e.g. Zr/Nb), with the largest variation in $\delta^{18}\text{O}$ values and Zr/Nb observed at high MgO contents. Trace elements and $\delta^{18}\text{O}$ values are consistent with the supply of a mixture of primary melts that contain depleted (DM) and enriched (EM) mantle signatures. Low- $\delta^{18}\text{O}$, enriched mantle domains, recognised from radiogenic isotopes (e.g. Thirwall et al. 2006), have previously been identified in the Icelandic mantle. Our modelling confirms that as the melt mixtures become more evolved, their $\delta^{18}\text{O}$ values become lower as a result of exchange of oxygen with crustal rocks. Using binary mixing equations, we have determined that between 10-35% of oxygen isotope exchange with the crust is required to explain the majority of the $\delta^{18}\text{O}$ values. Finally, we show that melt equilibration pressures, estimated by applying the OPAM barometer, correlate with the extent of oxygen isotope exchange. This suggests that melts exchange more oxygen, namely become more crustally contaminated, as they move upwards through the crustal section.

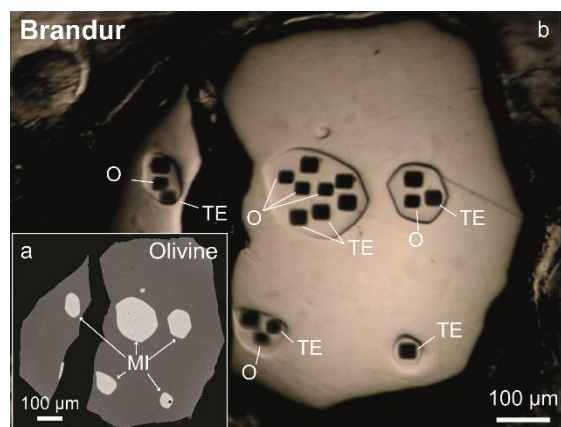


Fig. 1: BSE image of an olivine crystal containing MIs. Black rectangles indicate the SIMS craters for different analyses.

$\delta^{18}\text{O}$ values in MIs vary between +3.2‰ and +6.4‰, while groundmass glasses have $\delta^{18}\text{O}$ values between +2.6‰ and +5.5‰, on average lower than in MIs. Oxygen isotope ratios correlate with MgO

References:

Caracciolo, A., Bali, E., Guðfinnsson G.H., et al. (2020), *Lithos*, 352-353, 105234.

Caracciolo, A., Kahl, M., Bali, E., et al. (2021), *Am. Min.*, in press.

Thirwall, M.F., Gee, M.A.M., Lowry D.P., et al. (2006), *Geochim. Cosmochim. Acta* 70, 993-1019.

Late-stage rhyolitic magmatism in the Andean Central Volcanic Zone: Melt inclusion geochemical study at Cerro La Torta dome

Hernández Prat L.^{1*}, Cannatelli C.², Godoy B.¹, Astudillo D.³; Buscher J. T.², Morata D.¹

¹*Departamento de Geología y Centro de Excelencia en Geotermia de Los Andes (CEGA), Facultad de Ciencias Físicas y Matemáticas, Universidad de Chile, Chile;* ²*Department of Geological Sciences, University of Alaska, AK USA,* ³*Department of Geological Sciences, University of Florida, FL USA.*

*loreto.hernandez@ug.uchile.cl

Keywords: Melt Inclusion, Volcanism, Magmatism

Cerro La Torta is a rhyolitic low lava dome (De Astis et al. 2009) located in the El Tatio volcanic region of Chile, west of the Tocopuri Volcanic Complex. Due to its highly evolved chemical and petrological signatures, it has become an important aim of study in the central zone of the Altiplano Puna Magma Body (APMB). Through the geochemical and petrological analysis of amphibole- and plagioclase-hosted melt inclusions, using electron microprobe (EMP) and laser ablation ICP-MS (LA-ICP-MS), we reconstructed the magmatic evolution and pre-eruptive processes involved in the formation of La Torta. This lava dome was erupted from a magma source located between 4.6 y 6.9 km depth with a rhyolitic K-rich composition (74.5 wt.% silica). The crystallization of different phases occurred approximately between 949 and 723 °C and with an oxygen fugacity value close to the N-NO buffer, indicative of an oxidizing environment, and with a water content of about 4.9 wt.%. Due to the presence of small quantities of pyroxene in the samples, it is likely that the data retrieved from the analyzed melt inclusions and crystals only represent the latest stage of magma evolution, as rhyolite with these characteristics would not be able to fractionate pyroxene. We suggest the existence of a deeper and less differentiated magma as the "initial" parental magma, most likely of andesitic composition as inferred by the occurrence of andesine and Cr- and Ni-rich amphiboles. La Torta would have evolved from an andesitic to dacitic source, located deeper than 6.9 km depth and heated by the emplacement of a more primitive magmatic body, which

generated the volcanism at Tocopuri volcano and Cerros de Tocopuri around 0.8 My ago (Lucchi et al. 2009). This heating process had most likely caused the dissolution of enstatite and amphibole crystals from the mush zone into the already evolved magma, which inherited a few of these crystals and an anomalous concentration of Ni, Cr and HREE from the highly differentiated melt. Further crystallization and ascent to a more superficial area, where it has resided for quite a long time, has given the magma pre-eruptive geochemical characteristics. Finally, after destabilization due to an influx or decompression event, likely caused from the APMB emplacement, the magma erupted and formed the actual dome.

This work is a contribution to the ANID-Fondap projects 15090013 & 15200001.

References:

- De Astis, G., Lucchi, F., Tranne, C. A. et al (2009): *GeoActa*, Vol 2, pp 31-58.
- Lucchi, F., Tranne, C.A., Rossi, P.L., et al. (2009): *GeoActa*, Vol 2, pp 1-29.

Formation of deep hydrothermal vein-type Mo greisen and base metal mineralization at the Sweet Home mine, Colorado (USA)

Stoltznow M.^{1,2*}, Lüders V.², de Graaf S.³, Niedermann S.²

¹ Institute of Earth and Environmental Science, University of Potsdam, Karl-Liebknecht-Straße 24/25, D-14476 Potsdam, Germany; ² GFZ German Research Centre for Geosciences, Telegrafenberg, D-14473 Potsdam, Germany; ³ Max Planck Institute for Chemistry, Hahn-Meitner-Weg 1, D-55218 Mainz, Germany

*mstolt@gfz-potsdam.de

Keywords: ore deposits, magmatism, hydrothermalism

Deep hydrothermal Mo, W and base metal mineralization found in the Detroit City portal of the Sweet Home mine in the Alma district (Colorado Mineral Belt) was deposited in response to magmatic activity and the formation of Climax-type Mo deposits during the Oligocene.

This study presents extensive geochemical analyses of fluid inclusions in minerals from early greisen-like vein mineralization to better understand the fluid system responsible for ore formation. Quartz and fluorite, which are associated with molybdenite, huebnerite and/or pyrite mineralization, precipitated from low- to medium-salinity (1.5–11.5 wt.% equiv. NaCl), CO₂-bearing fluids at temperatures between 360 and 415°C and probably under a fluctuating pressure regime at depths of at least 3.5 km.

The formation of greisen-like and base metal mineralization at the Detroit City portal of the Sweet Home mine is related to fluids of different origin. Early magmatic fluids were the principal source for mantle-derived volatiles (CO₂, H₂S/SO₂, noble gases) and mixed with significant amounts of heated meteoric water. Fluid mixing of magmatic fluids with meteoric water is constrained by $\delta^2\text{H}$ - $\delta^{18}\text{O}$ relationships of fluid inclusion water in different minerals (Fig. 1). Whether molybdenum was derived from magmatic fluids remains unclear. Fluid inclusions in huebnerite suggest that W originated from source rocks that are enriched in organic matter rather than from magmatic fluids.

The deep hydrothermal mineralization at the Detroit City portal of the Sweet Home mine shows features similar to deep

hydrothermal vein mineralization found in Climax-type Mo deposits and their periphery, suggesting that fluid migration and the deposition of ore and gangue minerals in the Sweet Home mine was triggered by a deep-seated magmatic intrusion. The findings of this study are in good agreement with the results of previous fluid inclusion studies of the mineralization of the Sweet Home mine (Lüders et al., 2009) and from Climax-type Mo porphyry deposits in the Colorado Mineral Belt (Hall et al., 1974).

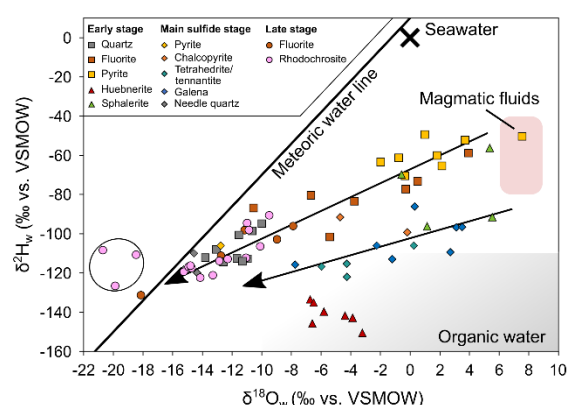


Fig. 1: Fluid inclusion hydrogen and oxygen isotope data of early-, main sulfide- and late-stage ore and gangue minerals from the Detroit City portal of the Sweet Home mine, Colorado.

References:

- Hall W.E., Friedman I., Nash J.T. (1974): *Econ Geol*, Vol 69, pp 884–901.
- Lüders V., Romer R.L., Gilg H.A. et al. (2009): *Miner Deposita*, Vol 44, pp 415–434.

Preliminary fluid inclusion study of fluorite deposits adjacent to the Tamazert alkaline igneous complex, Morocco

Sośnicka M. ^{1*}, Rddad L. ², Kraemer D. ³

¹ Friedrich Schiller University Jena, Institute of Geosciences, Burgweg 11, D-07749 Jena, Germany; ² Department of Physical Sciences, Earth and Planetary Division, Kingsborough Community College of the City University of New York, 2001 Oriental Boulevard, Brooklyn, New York, NY 11235-2398, USA; ³ Department of Physics and Earth Sciences, Jacobs University Bremen, Campus Ring 1, 28759 Bremen, Germany

*marta.sosnicka@uni-jena.de

Keywords: fluid inclusion, ore deposits, hydrothermalism

The origin of many deposits surrounding igneous cupolas remains controversial. It has been long debated whether the ore-forming fluids responsible for the deposition of ores exsolve from magmatic intrusions or result from a heat-driven mobilization of external fluids within the intruded rock successions (González-Partida et al. 2003; Lüders et al., 2008). Here, we study fluorite mineralization from the Tamazert syenite and adjacent carbonate units by means of fluid inclusions to shed a light on the ore genesis.

The Tamazert igneous complex is situated in the Central High Atlas mountain range in Morocco. It intruded Liassic carbonate sequence at depths <3km during the re-activation of Late Hercynian fault system in Eocene. The complex is composed of highly diverse rock suite including ultramafics, alkaline rocks, e.g. nepheline syenites, as well as late stage carbonatite bodies and lamprophyre sheeted dyke swarms (Bouabdli et al., 1988; Salvi et al., 2000).

The aqueous 3-phase fluid inclusions hosted in disseminated interstitial fluorite, from the peripheral part of the syenite cupola, are grouped in secondary trails and show median $T_h=199^\circ\text{C}$ and salinity: 21.2 NaCl wt.% equiv. They contain a solid phase, which was identified as shortite - $\text{Na}_2\text{Ca}_2(\text{CO}_3)_3$ by Raman spectroscopic analyses. Similar T_h and salinity values show inclusions in adjacent interstitial calcite, however they are devoid of shortite.

Carbonate-hosted fluorite ore contains 2-phase aqueous inclusions decorating

growth zones, showing median $T_h=136^\circ\text{C}$ and low salinities 1.6-8.5 wt.% NaCl equiv. Interestingly, clusters of high temperature (medians: 248°C , 314°C) 2-phase low salinity (medians: 2.4, 0.9 wt.% NaCl equiv.) fluid inclusions, locally with optically visible CO_2 phase, also occur within the same growth zones.

These results point towards a long-lived hydrothermal activity in the studied area. The high salinity aqueous inclusions containing shortite may be associated with late magmatic activity following the emplacement of carbonatites. The involvement of low salinity and low temperature fluids in the precipitation of carbonate-hosted fluorite ore casts doubt on the magmatic origin of the ore-forming fluids. This hypothesis is also supported by REY patterns for the latter fluorites, as they do not show considerable Eu anomalies. Clusters of high temperature fluid inclusions suggest multiple heat fluxes.

References:

- Bouabdli A., Dupuy C., Dostal J. (1988): *Lithos* Vol 22, pp 43-58
- González-Partida E., Carrillo-Chávez A., Grimmer J.O.W., et al. (2003): *Ore Geol Rev* Vol 23, pp 107-124
- Lüders V., Romer R.L., Gilg H.A., et al. (2008): *Miner Deposita* Vol 44: 415
- Salvi S., Fontan F., Monchoux P., et al. (2000) *Econ Geol* Vol 95, pp 559-576

Posters

The Role of Evaporative Sulfates in Iron Skarn Mineralization: A Case Study of Fluid Inclusions in Pandian Deposit, East China

Zhang Z.¹, Cao Y.^{1*}

¹ School of the Earth Sciences and Resources, China University of Geosciences, Beijing 100083, P. R. China

*e-mail: caoyi@cugb.edu.cn

Keywords: fluid inclusion, hydrothermalism, ore deposits

It is commonly thought that iron is present predominantly as ferrous iron (Fe^{2+}) in magmatic-hydrothermal systems (Crerar and Barnes 1976; Simon et al. 2013). In this case, the formation of voluminous iron oxides requires sufficient oxidation of Fe^{2+} to Fe^{3+} . However, the mechanisms by which this oxidation process takes place are not well understood. In this paper, we suggest that sulfates from the evaporitic beds have played a critically important role by oxidizing ferrous iron in the magmatic-hydrothermal fluid, leading to precipitation of massive magnetite ore.

The Pandian deposit is one of the most representative iron deposits in East China. The mineralization is dominated by massive magnetite ore along the contact zone between the early Cretaceous Pandian diorite and middle Ordovician dolomitic limestones with numerous intercalations of evaporitic beds. Cross-cutting and replacement relationships indicate four stages of hydrothermal activity during the formation of the Pandian iron skarn deposit, namely, skarn, iron oxide, sulfide and carbonate stages. We collected fluid inclusions at each stage and performed microthermometry.

The fluid inclusions in garnet and diopside in skarn stage are mainly daughter mineral-bearing multiphase fluid inclusions. These fluid inclusions formed from hot, hypersaline brines (501-550°C; 49-59 wt.% NaCl equiv.), probably of magmatic origin. There are two types of fluid inclusions in iron oxide stage, namely, daughter mineral-bearing multiphase fluid inclusions and liquid-rich two-phase fluid inclusions (Fig. 1). The liquid-rich two-phase fluid inclusions generally homogenize by disappearance

of the vapor bubble. Homogenization occurs at temperature range of 364-436°C, and the bulk salinity varies in the range of 6-13 wt.% NaCl equiv. The daughter mineral-bearing multiphase fluid inclusions homogenize by disappearance of the halite. Homogenization occurs at temperature range of 272-292°C, and the salinities varies in the range of 36-38wt.% NaCl equiv. These features indicate that the fluid inclusions in the iron oxide stage originate from two different fluids: hot, medium to low salinity fluid and Mesothermal, supersaturated brine. We suggest that the Mesothermal, supersaturated brine came from evaporitic beds and led to precipitation of massive magnetite ore.

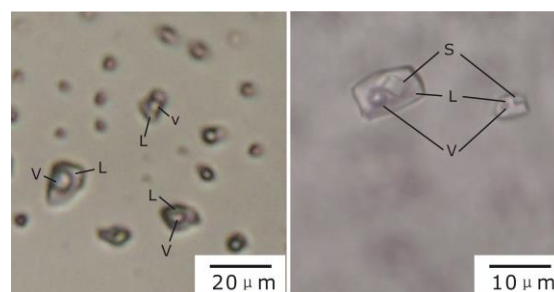


Fig. 1: Photomicrograph of liquid-rich two-phase fluid inclusions(left) and mineral-bearing multiphase fluid inclusions (right) in iron oxide stage. S-solid, L-liquid, V-vapour.

References:

- Crerar DA, Barnes HL. (1976): *Econ. Geol.*, 71:772-794
- Simon A, Bilenker L, Bell A. (2013): *Mineral. Mag.*, 77:2215

Characteristics of the fluid inclusions in the Ordovician Majiagou Formation in the central-eastern Ordos Basin, China

Rongxi L.^{*}, Xiaoli W.

School of Earth Science and Resource, Chang'an University, Xi'an 710054, China.

**rongxi99@163.com*

Keywords: gas fluid inclusion, sedimentary basin

The Ordos Basin in the North China block is the largest gas production base of China. The east-central Ordos Basin developed the Ordovician thick marine gypsum rocks bedded with dolomite gas reservoirs whose gas source rocks were proved the Upper Palaeozoic coal beds.

Core samples were collected from the Ordovician carbonate in the east-central Ordos Basin to study the fluid inclusions. The fluid inclusions mainly developed in the calcite filled in gypsum mold holes and dissolution holes, a small number of fluid inclusions developed in calcite veins. According to petrographic characteristics of fluid inclusions, the fluid inclusions can be divided into the early and late phases. The early fluid inclusions are mainly developed in sparry calcites filled in dissolution holes, which has relatively low gas-liquid ratio. The overall colors of fluid inclusions are light and transparent, and the shape is mostly stumpy and elliptical. The individual size of the fluid inclusions is generally less than 20 μm , which are mainly gas-liquid two-phase brine inclusions. The late fluid inclusions are mainly developed in the late sparry calcite filled in the gypsum mold holes. They are mainly gas-rich fluid inclusions, with relatively higher gas-liquid ratio. The overall colors of fluid inclusions are gray and black, the morphology is irregular, and the individual size is larger than 20 μm in general.

The homogenization temperature of early fluid inclusions ranged from 110 to 160 $^{\circ}\text{C}$, and the freezing temperature ranged from -13 to -10 $^{\circ}\text{C}$, where the hydrocarbon molecules was not determined based on the Laser Raman spectroscopy. The homogenization temperature of the late fluid inclusions is between 160 and 230 $^{\circ}\text{C}$, and the freezing temperature is between -8 and -3 $^{\circ}\text{C}$.

However, the Laser Raman test results show that there are abundant CH_4 and H_2S in the late fluid inclusions, which recorded very different natural gas with high content of H_2S .

This research indicated that the CH_4 with high content of H_2S in the late fluid inclusions was derived from the Ordovician potential gas source rocks rather than from the Upper Palaeozoic coal source rock as the gas reservoirs without H_2S . The H_2S in inclusions is mainly formed by thermochemical sulfate reduction of carbonate source rocks along CH_4 generation. The Ordovician marine source rocks is an important source and the dolomite rocks has more prospect for gas exploration.

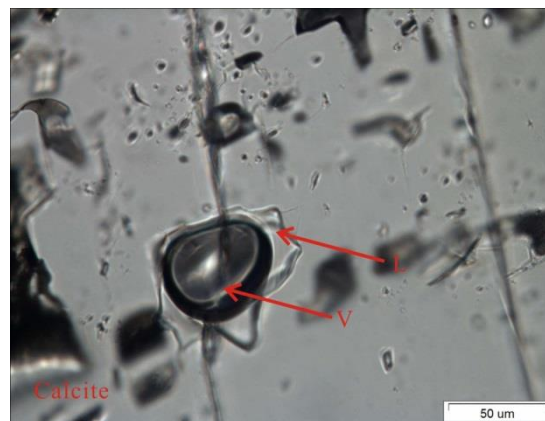


Fig. 1: Photomicrograph of fluid inclusions in Calcite from the central-eastern Ordos Basin, China. L-liquid, V-vapour.

References:

CAI Chunfang, HU Guoyi, HE Hong, et al. (2005): *Journal of Petroleum Science and Engineering*, 48 (2005), pp 209–226.

Melt inclusions from Archean VMS deposits: constraints on the pre-eruptive metal and volatile content of magmas

Daya P.^{1*}, Hanley J.¹, Neyedley K.¹, Piercey S.², Monecke T.³

¹ Saint Mary's University, Geology Department, Canada; ² Memorial University of Newfoundland, Department of Earth Sciences, Canada; ³ Colorado School of Mines, Department of Geology and Geological Engineering, United States of America

*priyal.day@smu.ca

Keywords: melt inclusion, volcanism, ore deposits

Archean VMS systems in the Abitibi Subprovince of Canada differ greatly in metal tenor and tonnage, in particular in Au endowment. In this first study of melt inclusions in such environments, primary melt inclusions in zircon hosted in pre-, syn-, and post-VMS ore felsic volcanic lithologies (flows, fragmentals) will provide compositional constraints on the initial metal and volatile chemistry of the magma before eruption, allowing a comparison of the precursor metal budgets of magmas that actively degassed, and/or were passively leached, to supply metals to the deposits. Primary methodologies in progress include (i) thin section and melt inclusion petrography (inclusion and host zircon origin, preservation, accidentally trapped phases, etc.); (ii) SEM-EDS and EMPA for determination of bulk inclusion compositions on exposed melt inclusions; and (iii) LA-ICP-MS to quantify major/trace element composition of melt inclusions (including metals) and host zircon chemistry. Magmatic zircons in VMS deposits from the Abitibi Subprovince contain silicate and phosphate mineral inclusions (50% of total inclusions), silicate melt inclusions (40%) and sulphide (melt and/or mineral) inclusions (~10%). Mineral and melt inclusions in zircon occur in primary growth zones. Mineral inclusions (1.5-60 µm) occur as needle-like to euhedral-subhedral lath-shaped crystals and are dominantly apatite with lesser occurrences of biotite and amphibole. Silicate melt inclusions (1.5-35 µm) range in shape from spherical and irregular blebs to sub-angular, elongated inclusions, are microcrystalline (recrystallized), and monomineralic to polymineralic. They are comprised

dominantly of quartz, apatite, alkali-feldspars, biotite, pyroxene, and amphibole in varying proportions. Other minerals identified include xenotime and ilmenite. Sulphide inclusions (1.5-15 µm) occur as rounded to sub-rounded spherical blebs, and are composed of chalcopyrite and/or pyrite. In some lithologies there are inclusions containing melt together with sulphide showing evidence of co-saturation. Melt inclusion compositions range from sub-alkalic rhyolite to alkalic compositions (trachytic to tephritic) notably *within single lithologies* indicating that zircons preserve melt aliquots/end-members along a variety of possible evolutionary pathways involving fractionation, contamination and/or magma mixing. Petrographic and compositional data from the melt inclusions will be combined with zircon compositional data to elucidate links between the magmatic P-T-fO₂ evolution and metal and volatile endowment, providing a means to quantitatively inform mass balance exercises concerning the magmatic contributions to VMS, and differentiate between metal-barren and -fertile volcanic districts.

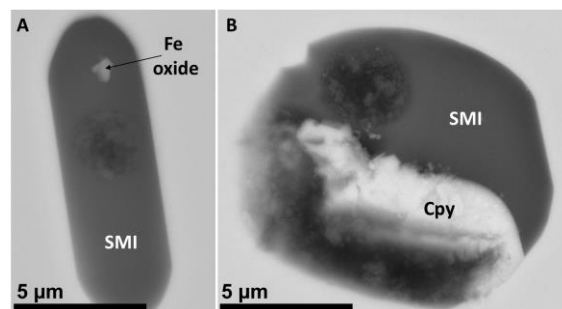


Fig. 1: BSE images of (A-B) glassy silicate melt inclusions (SMI); (B) silicate melt co-saturated with chalcopyrite.

Evaluation of magmatic processes responsible for W enrichment at the Cantung deposit, Canada: Evidence in melt inclusions

Gomez Garcia G.^{1*}, Wagner A.¹, Adlakha E.¹, Hanley J.J.¹, Lecumberri-Sanchez P.², Rasmussen K.L.³, Falck H.⁴

¹ Saint Mary's University, Department of Geology, Canada; ² University of Alberta, Department of Earth and Atmospheric Sciences; ³ University of British Columbia, Department of Earth and Ocean Sciences; ⁴ North West Territories Geological Survey.

*Gabriel.Gomez.Garcia@smu.ca

Keywords: melt inclusion, fluid inclusion, ore deposits

The Mine Stock monzogranite is a peraluminous intrusion associated with the world-class Cantung W-Cu skarn deposit, Northwest Territories, Canada. The Mine Stock, as well as associated lamprophyre and aplite dykes, are possible sources for the tungsten and causative fluids for skarn mineralization.

This study aims to investigate mechanisms for W enrichment in magmas associated with W skarn deposits by characterizing melt and fluid inclusion systematics in apatite of the Mine Stock intrusion and related rocks. Methods that include: i) EPMA of homogenized melt inclusions for determination of major element composition; ii) LA-ICP-MS for trace element compositions of melt inclusions to understand W behaviour during fractional crystallization; and iii) Microthermometry of fluid inclusions to produce isochores and determine P-T trapping conditions, and to characterize fluid salinity and composition. The data will be used to model the magmatic and hydrothermal evolution of the Mine Stock intrusion and related rocks.

Preliminary EPMA data of six homogenized melt inclusions from the Mine Stock yield a granitic composition with high SiO₂ (ave. 78.43 wt. % \pm 2.36; 1 σ), Al₂O₃ (ave. 11.80 wt. % \pm 2.54; 1 σ), CaO (ave. 4.17wt. % \pm 1.17; 1 σ), K₂O (ave. 3.30 wt. % \pm 0.88; 1 σ), Na₂O (ave. 1.68 wt. % \pm 0.45; 1 σ). Concentrations of

MgO, FeO, TiO₂, and the halogens Cl and F are low or below the detection limit. The composition of the inclusions was classified as rhyolitic using a Total Alkali vs Silica diagram (fig. 1). Mafic inclusions, such as those reported by Adlakha et al. (2018), were not observed. Current work includes the interpretation of LA-ICP-MS data of fifty unhomogenized melt inclusions of the amine Stock to model the degree of fractionation and the behaviour of W as well as other incompatible elements such as B, Cs, Nb and Bi.

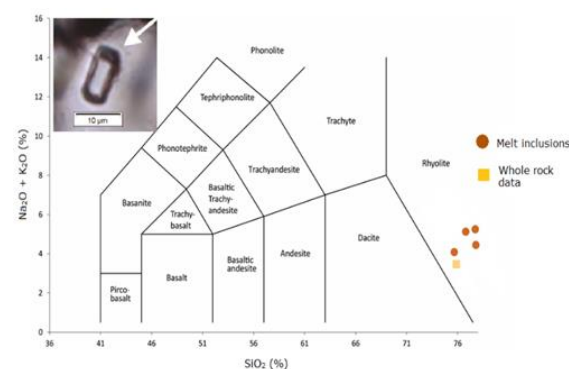


Fig. 1: Total Alkali vs Silica (TAS) diagram showing melt inclusions (dark orange) and whole rock data (light orange) of the Mine Stock. Located at the top left of the diagram is a photomicrograph of a homogenized melt inclusion.

References:

Adlakha et al. (2018). *European Journal of Mineralogy*, 30, 1095–1113.

Geology and gold mineralization in west Kasnazan gold deposit, south of Saqqez, Kurdistan, Iran

Niroomand S. ¹, Soleymani M. ^{1*}, Tajeddin H. A. ²

¹ Department of Earth Sciences, Faculty of Sciences, Tehran University, Tehran 14155-64155, Iran.; ² Department of Geology, Faculty of Basic Sciences, Tarbiat Modarres University, Tehran, Iran.

*Soleymani.majid@ut.ac.ir

Keywords: ore deposits, fluid inclusion, metamorphism

Mineral explorations along the northwest margin of Sanandaj-Sirjan Zone (SSZ) in the last two decades by the Geological Survey and Mineral Explorations of Iran (GSI) have been led to recognition of new orogenic type gold deposits. West Kasnazan gold deposit in the south of Saqqez have been explored by GSI since 2008 (Tajeddin, 2008). The deposit area is overlain by Precambrian metamorphic volcanic -sedimentary sequences and Cretaceous schist, phyllite, and marble which are cut by granitoid stocks (Hariri and Farjandi., 2003). The main host of gold mineralization is quartz syenite intrusion with mylonite-ultramylonite fabric which intrudes along shear zone within NW-SE trending, associated with hydrothermal alteration e.g., silicification, sericitization, carbonatization, and sulfidation. The mineralogy of the ore is simple and characterized by pyrite, chalcopyrite, sphalerite, galena, arsenopyrite,

magnetite, gold, and iron hydroxide. gold observed as native gold smaller than 40µm in quartz host, as well as inclusion in pyrite. Microthermometric studies of fluid inclusion suggest that mineral deposition occurred at temperatures of at least 137.4–240.5 °C from a fluid with 1.6-12.6 wt.% NaCl salinity. The comparison of the Kasnazan gold deposit with other gold deposits reflects this deposit has the most similarity with the orogenic type gold deposit.

References:

Hariri A, Farjandi F (2003) *The Saqqez Sheet map (scale1: 100,000)*. Geological Survey and Mineral Exploration of Iran, Tehran.

Tajeddin, H.A., 2008. *Exploration and introduction of the gold mineralization at the Southern Ghabaghlojeh area (SW of Saqqez, Kurdistan)*. Geological Survey and Mineral Exploration of Iran, Internal report 35p.

Bouvet Triple Junction tholeiites magma storage conditions and source heterogeneity obtained from melt inclusions and glasses

Shishkina T. A.^{1*}, Migdisova N. A.¹, Sushchevskaya N. M.¹

¹ Verndasky GEOKHI RAS, Moscow, Russia

*t.shishkina@geokhi.ru

Keywords: melt inclusion, magmatism, mantle

The Bouvet Triple Junction (BTJ) is a place in South Atlantic where three lithospheric plates (South American, African and Antarctic) meet and are separated by Mid-Atlantic (MAR), South-West Indian (SWIR) and American-Antarctic (AAR) ridges. According to previous studies BTJ oceanic tholeiites show variations in geochemical signatures, which may reflect complex geological setting and history of this region (Le Roex et al., 1983; Migdisova et al., 2017).

Compositions of naturally quenched melt inclusions in phenocrysts (olivine, plagioclase) were studied in a collection of basalts dredged from several segments of BTJ (Spiess ridge, SWIR and MAR adjacent to BTJ) together with quenched matrix glasses.

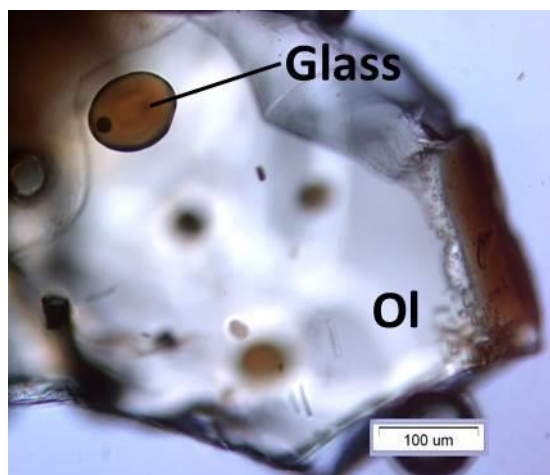


Fig. 1: Photomicrograph of melt inclusions (Glass) in olivine (Ol) from oceanic tholeiite from MAR segment of BTJ.

Magma storage conditions were determined from melt inclusion - host mineral pairs using various geothermometers and oxybarometers (e.g. Ballhaus, 1991; Danyushevsky, 2001; Shishkina et al., 2018). The temperatures of mineral - melt

equilibrium were found to be in range of about 1050–1150°C. The redox conditions estimated with different methods give quite controversial results: from QFM-0.9 to QFM+1.9 and require further investigation.

Trace elements contents and ratios (e.g. (La/Sm)_n) in melt inclusions and quenched glasses confirm the findings on the heterogeneity of magma sources in BTJ region. In general magmas from Spiess ridge and SWIR-segment of BTJ are more enriched in incompatible elements in comparison to average N-MORB. While melts from MAR-segment of BTJ are similar to typical N-MORB. The diversity of geochemical features of BTJ segments can be explained by the involvement of heterogeneous mantle sources (including recycled oceanic crust or fragments of continental lithosphere) in melting processes, influence of hotspots (Bouvet, Shona) and jumping of ridge axes during the development of BTJ region.

References:

- Ballhaus C. et al. (1991) *Contr.Min.Petr.*, Vol 107, pp 27-40.
- Danyushevsky L.V. (2001) *J.Volc.Geoth.Res.*, Vol 110, pp 265-280.
- Le Roex A.P. et al. (1983) *J.Petrol*, Vol 24(3), pp 267-318.
- Migdisova N.A. et al. (2017) *Rus.Geol Geophys*, Vol 58, pp 1289-1304.
- Shishkina T.A. et al. (2018) *Am.Min*, Vol 103, pp 369-383.

***FROM DIAGENESIS TO ULTRA HIGH
PRESSURE METAMORPHISM INCLUDING
GEODYNAMIC IMPLICATIONS AND ORE
DEPOSITS***

e-CROFI 2021

Paleofluid evolution in the Wolfcamp Formation, Permian Delaware Basin, West Texas (*keynote*)

Fall A.*, Eichhubl P., Nicot J.-P., Gale J. F. W.

Bureau of Economic Geology, Jackson School of Geosciences, The University of Texas at Austin, USA

*andras.fall@beg.utexas.edu

Keywords: sedimentary basins, diagenesis, oil & gas

The Wolfcamp Formation in the Permian Delaware Basin in West Texas is one of the best producing shale reservoirs in the United States, but oil production is often associated with high water cut, diminishing the economic value of producing wells. In this study we focus on the origin of water and cause for the high water cut in the Delaware Basin by studying the paleofluid history of the basin using structural and geochemical information collected from cemented natural fractures obtained from core in multiple wells.

Based on structural crosscutting relations, fracture cement textural observations, isotopic, fluid inclusion timing constraints, and produced water analysis the chemistry of the produced water is consistent with seawater evaporation and diagenetic water-rock interaction, while no meteoric water component is observed. Strontium isotopes are characterized by a strong radiogenic component, consistent with water-rock interaction in a siliciclastic sequence. The strontium and oxygen isotopes reflect changes in formation water chemical composition that is affected by increasing water-rock interaction. Calculated paleo-water oxygen isotopic composition based on limited fluid inclusion data is distinctly heavier than produced formation water. Fluid inclusions indicate peak pressure-corrected temperatures around 150 °C, and salinities as high as 20 wt% (Fig.1), distinctly higher than produced water salinities (30,000-100,000 ppm). Salinities later declined to produced water levels, that coincided with timing of hydrocarbon generation. In combination, these results provide evidence for two distinct stages of formation water chemical change: an early (pre-

hydrocarbon) change from Permian marine pore water to a high salinity (up to 200,000 ppm) evaporative CaCl₂ brine, followed by dilution of brines syn- and post-hydrocarbon generation to present-day salinity values. This dilution is spatially variable but does not appear to be linked to structural conduits. Isotopic and fluid inclusion observations on cements suggest some local fault-controlled influx of water of different composition without evidence for larger-scale mixing or water displacement. Carbon isotopic and paleo-pore pressure records are indicative of fracture-controlled episodic hydrocarbon leakage.

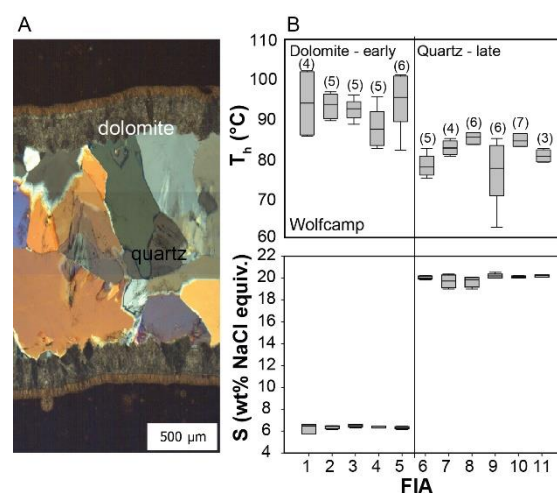


Fig. 1: Compound cement-filled opening-mode fracture (vein) in mudrock, Wolfcamp Formation, Delaware Basin, West Texas. A. The fracture is filled by early zoned dolomite, while the rest of the fracture filled by late blocky quartz cement. B. Microthermometric data of fluid inclusions in the dolomite and quartz cements, showing temperature and salinity changes during fracture formation and cementation.

Implications of fluorine-rich fluid inclusions for the genesis of the Hansonburg, New Mexico (USA) Mississippi Valley-type district

Smith-Schmitz S. E.^{1*}, Appold M. S.¹

¹ University of Missouri-Columbia Geological Sciences

*ses7f1@umsystem.edu

Keywords: fluid inclusion, ore deposits

The Hansonburg, New Mexico Ba-F-Pb district in the southwestern U.S.A. is an atypical Mississippi Valley-type (MVT) district that is highly enriched in barite and fluorite relative to typical, sulphide mineral dominant MVT districts. A long-standing hypothesis regarding the fluorite enrichment observed in Hansonburg is that the ore forming fluid was anomalously rich in F relative to typical MVT ore fluids and sedimentary brines.

This study was undertaken with the goal of testing this hypothesis by determining the F concentrations in ore-stage drusy quartz-hosted fluid inclusions. Samples of drusy quartz that paragenetically overlapped with fluorite were examined petrographically to identify primary fluid inclusion assemblages that were first analysed using microthermometry. The fluid inclusions were then thermally decrepitated generating evaporative solute mounds that were analysed using scanning electron microscope-energy dispersive X-ray spectroscopy (SEM-EDS). All of the Hansonburg evaporative solute mounds analysed contained detectable quantities of F (Fig. 1). Evaporative solute mounds generated from standard solutions with known F/Cl ratios were also analysed using SEM-EDS in order to create instrument specific calibration curves. The F/Cl ratios measured in the evaporative solute mounds were converted to fluid inclusion F concentrations using these calibration curves and the fluid inclusion salinities from microthermometry. The resultant fluid inclusion F concentrations of 320 to 2500 ppm are orders of magnitude greater than the tenth's to 10's of ppm F concentrations typical of sedimentary brines. Additionally, these high F concentrations are consistent with an ore

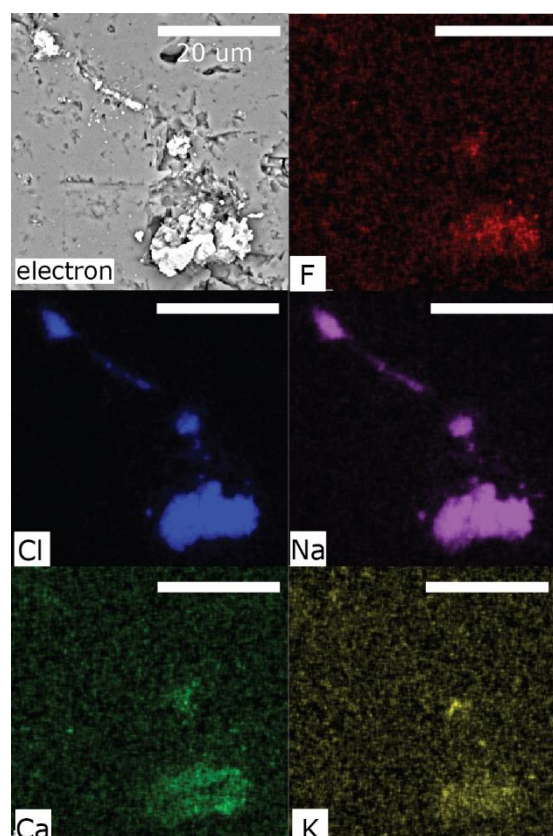


Fig. 1: BSE and false colour elemental X-ray maps of F, Cl, Na, Ca, and K from SEM-EDS analysis of evaporative solute mounds from decrepitation of quartz-hosted fluid inclusions.

fluid pH in the range of 1 to 2.4, indicating that the Hansonburg ore fluid was very acidic at the time of fluorite precipitation. This pH range is significantly lower than the pH range of 4.3 to 5.1 predicted for Hansonburg ore fluid in previous studies and the pH range of 4 to 5.5 for typical MVT deposits. The combination of high F concentrations and low pH predicted for the Hansonburg ore fluid in this study would have provided favourable conditions for the formation of the barite-fluorite rich, metal sulphide poor mineral assemblage present in the Hansonburg, New Mexico district.

Conditions of ore formation at the Gorno MVT deposits (Lombardy, Italy): insights from fluid inclusions

Giorno M.^{1*}, Barale L.², Bertok C.¹, Burisch M.^{3,4}, Frenzel M.⁴, Martire L.¹

¹ Department of Earth Sciences, Università degli Studi di Torino, Italy; ² CNR IGG – Torino, Italy; ³ Technische Universität Bergakademie Freiberg, Germany; ⁴ Helmholtz-Zentrum Dresden-Rossendorf, Germany;

*micheleandrea.giorno@unito.it

Keywords: ore deposits, hydrothermal, sedimentary basins

The strata-bound, carbonate-hosted Pb-Zn-Ag (\pm fluorite \pm barite) deposits of the Gorno mining district extend over ~ 600 km² in the Orobic Alps (Lombardy, Northern Italy). Here, the Lower Carnian stratigraphic succession experienced a complex diagenetic evolution, resulting in variable styles of alteration of host rocks and sulfide mineralization. High-grade and economically relevant sulfide ore is hosted in the 5-10 m thick basal unit of the Gorno Formation, consisting of laminated marl and siltstone beds, which are historically known as “the black shales”. Other major orebodies are hosted in the 50-100 m thick Breno Formation, which is composed of light-colored, thick-bedded peritidal limestones and in the 20-50 m thick Calcare Metallifero Bergamasco formation, composed of dark-colored, medium-bedded peritidal limestones.

The district has classically been described as an “Alpine-type” Pb-Zn deposit – its genesis still controversially debated. Hence, in this work, we aim to constrain the ore-forming conditions using fluid inclusion analyses related to samples from different localities within the district. Fluid inclusion assemblages (FIAs) were classified as primary (p; Fig. 1), pseudo-secondary (ps), secondary (s), isolated (iso) or clusters (c). Microthermometry and Micro-Raman spectroscopy were performed preferentially in the two-phase (gas-liquid) inclusions hosted by sphalerite and fluorite samples. Eutectic temperatures of fluid inclusion related to the ore-stage are around -52 °C, indicating that the ore fluid may be best described in the CaCl₂-NaCl-H₂O system. Microthermometric data suggests evolution from high salinities (up to ~ 25

eq.wt% NaCl) towards lower salinities (typically <10 eq.wt% NaCl) from primary to secondary inclusions. The homogenization temperatures do not vary significantly, range between ~ 80 and 120 °C and do not show a correlation with salinity. Additionally, Micro-Raman spectroscopy revealed the presence of methane and liquid hydrocarbons in fluid inclusions related to the ore-stage.

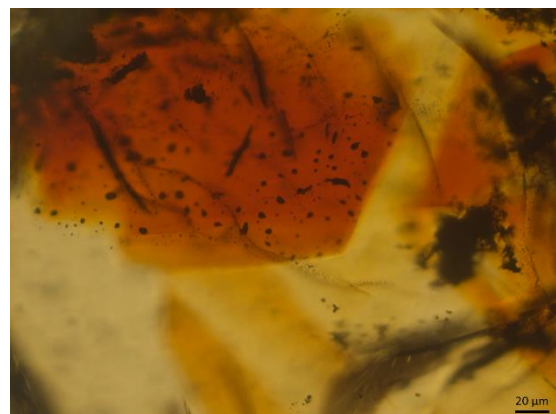


Fig. 1: Photomicrograph of hydrocarbon-bearing primary fluid inclusions in sphalerite.

Fluid inclusion systematics indicate the involvement of moderately hot, high-salinity brines in ore formation. Conversely there is no evidence for fluid mixing, which is often documented for other MVT deposit. The spatial association of sulfide bodies to organic rich shales supports a lithological control of ore deposition. Organic carbon or associated hydrocarbons are hence proposed to have acted as reactive barriers that caused reduction of the ore fluid.

Fluid inclusions and mineral chemistry of gem-quality diaspore (Milas, Turkey)

Hanilçi N.^{1*}, Van den Kerkhof A. M.², Sosa G. M.², Öztürk H.¹, Hepvidinli B.³

¹ Istanbul University-Cerrahpasa, Turkey.; ² GZG, Georg-August University of Göttingen, Germany, ³ Centerra Gold, Turkey

*nurullah@iuc.edu.tr

Keywords: fluid Inclusion, metamorphism, ore deposits

Crystals (Fig. 1a) of gem-quality diaspore (α -AlO(OH)) are found in veins and lenses from the Küçükçamlık deposit within the Milas-Yatağan Bauxite Province, Turkey. The bauxite deposit occurs along the unconformity contact between Jurassic and Triassic successions and underwent low-grade metamorphism.

LA-ICPMS analysis of diaspore crystals revealed trace elements with average concentrations in ppm (n=14) of Fe (4703), Ti (453), V (17), Cr (62), Ni (0.8) and Ga (85).

Diaspore crystals enclose two types of fluid inclusion assemblages (FIAs): (1) Primary FIAs typically show elongated or tubular shapes parallel to the crystallographic c-axis of diaspore (Fig 1b), and contain 2 or 3 phases at room temperature. Their composition is typified by the system $H_2O-NaCl-CO_2+N_2$. (2) Pseudo-secondary FIAs formed along healed intra-granular micro-fractures and contain fluids, which are re-trapped during (slight) deformation. These inclusions with $H_2O-NaCl-CO_2$ composition are always 2-phase. Total homogenization temperatures (Th_t) range between 146 and 243°C. The primary inclusions show a clear frequency maximum at 210°C, corresponding to the crystallization temperature of the diaspore. The pseudo-secondary inclusions show more frequent Th_t in the higher and lower ranges, indicating late fluid re-trapping or necking down in the 2-phase stability field. The salinity varies between 2 and 7 wt% NaCl, while the primary inclusions show a well-defined frequency maximum at 6 wt% NaCl.

Raman spectroscopy of the primary fluid inclusions (Fig. 1c) confirmed the presence of CO_2 and N_2 in the hydrothermal fluids. N_2 is

heterogeneously distributed in the primary FIAs: the regular inclusions (notably the tubular ones) contain CO_2 as the only non-aqueous compound, whereas the irregular ones typically contain 30 to 45 mol% N_2 .

The fluid inclusion compositions indicate that the diaspore crystallized from metamorphic fluids, which were generated during metamorphism of the bauxite deposit.

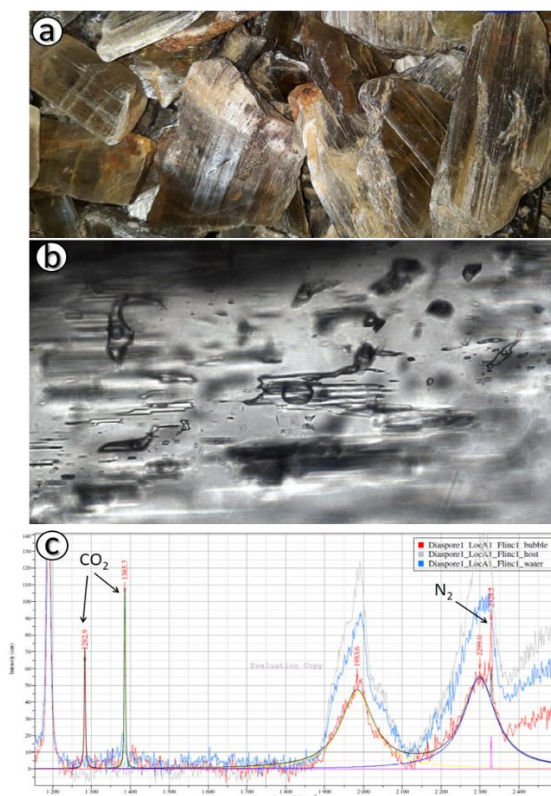


Fig. 1:(a) Gem-quality diaspore crystals, (b) Elongated primary two-phase $H_2O-NaCl-CO_2-N_2$ inclusions, and (c) CO_2-N_2 Raman spectra of fluid inclusions.

Replenishment phenomena of depleted oil and gas fields: elements of discussion using synthetic fluid inclusions

Balitskaya E.¹, Balitsky V.¹, Plotnikova I.², Pironon J.³, Barres O.³, Randi A.³, Setkova T.¹

¹ Institute of Experimental Mineralogy RAS, Russia; ² Institute of Applied Research, Tatarstan Academy Sciences, Russia; ³ Université de Lorraine, CNRS, Nancy, France

*elizaveta.balitskaya@gmail.com

Keywords: fluid inclusions, experiments, metamorphism

Experiments on the interaction of hydrothermal solutions with bituminous rocks were carried out at temperatures of 240–700 °C and pressures of 7–150 MPa, respectively. The duration of the experiments ranged from 15 to 300 days. At the same time, newly formed quartz crystals trapped water-hydrocarbon inclusions in the same experiments using previously developed methods (Balitsky V. *et al.*, 2015; Richard A. *et al.*, 2019; Teinturier S. and Pironon J., 2004).

As a result, in addition to water, liquid oil-like and gaseous (mainly methane) hydrocarbons, as well as solid bitumen, were trapped in fluid inclusions in all experiments (Fig. 1). From the experiments, it was shown that bituminous rocks, when interacting with hydrothermal solutions, are able to generate oil and gases in quantities that could be sufficient for both primary filling of oil and gas traps and re-filling of depleted fields. This creates a unified genetic model for the formation and refilling of oil and gas fields, which can be applied to Tatarstan, where several reservoir replenishments are observed after several decades of exploitation.

The data obtained confirm the ideas of many oil experts about the migration of liquid and gas hydrocarbons in the Earth's interior in the form of high-temperature homogeneous, including supercritical, fluids (Balitsky V. *et al.*, 2016, 2020). This keeps the oil from metamorphic transformation up to 500 °C. However, at 600–670 °C and pressures of 120–150 MPa, oil completely loses its stability and turns into methane and graphite. In the bowels of the earth, this should occur at depths of 25–30 km. The evolution of organic matter is not only dependent to

temperature but also to kinetic. The production of oil at high temperature requires very short times of forming or rapid migration towards „cold” reservoirs.

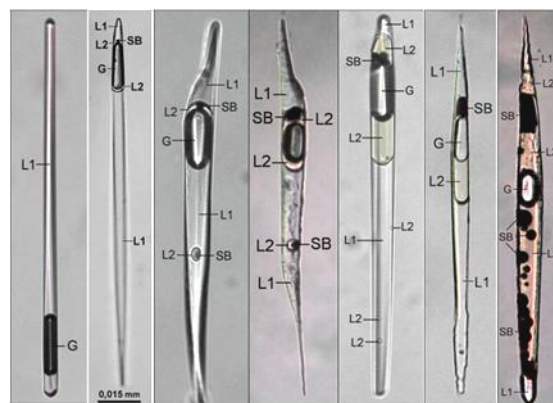


Fig. 1: Photomicrographs of water-hydrocarbon inclusions in quartz crystals grown in the temperature range 240–500° C and pressures 7–120 MPa.

The reported study was funded by RFBR and CNRS according to the research project No. 21-55-15010.

References:

- Balitsky V.S., Pentelei S.V., Pironon J. *et al.* (2016): DAN RAS, Vol 466(4), pp 454–458.
- Balitsky V.S., Setkova T.V., Balitskaya L.V., *et al.* (2020) In: Litvin Y., Safonov O. (eds) *Advances in Experimental and Genetic Mineralogy*. Springer, Cham., pp 3–34.
- Richard A., Morlot C., Créon L. *et al.* (2019) *Chemical Geology*, Vol 508, pp 3–14.
- Teinturier S., Pironon J. (2004): *Geochimica et Cosmochimica Acta*, Vol 68 (11), pp 2495–2507.

Deciphering progressive deformation on quartz veins by means of fluid inclusions and cathodoluminescence

Sosa G.^{1*}, van den Kerkhof A.¹, Oyhantçabal P.², Wemmer K.¹, Oriolo S.³

¹Georg-August-Universität Göttingen, Geoscience Center, Goldschmidtstraße 3, 37077 Göttingen, Germany; ²Departamento de Geodinámica Interna, Facultad de Ciencias, Universidad de la República, Iguá 4225, 11400 Montevideo, Uruguay; ³CONICET-Universidad de Buenos Aires. Instituto de Geociencias Básicas, Aplicadas y Ambientales de Buenos Aires (IGEBA), Intendente Güiraldes 2160, C1428EHA Buenos Aires, Argentina

*gsosa@gwdg.de

Keywords: fluid inclusion, hydrothermalism, ore deposits

Fluid inclusion and cathodoluminescence (CL) are powerful tools to reconstruct the times and rates at which progressive deformation operates. In the southernmost Late Neoproterozoic Dom Feliciano Belt, Uruguay, the pressure-temperature-deformation-fluid activity-composition-time (P-T-D-A-X-t) path of vein-type gold deposits was reconstructed (Fig. 1, Sosa et al., 2020). The quartz veins are hosted in Paleoproterozoic dolomitic marble and formed along fold hinges and sheared marble bands in an Ediacaran transpressional regime. They are associated with a post-collisional magmatism and hydrothermal fluid circulation. K-Ar muscovite dating constrained an age of 592.8 ± 8.7 Ma for the veins, being thus coeval with widespread shear zone activity in the belt.

Based on four different populations of fluid inclusions, a protracted evolution from ca. 550-500 °C and 3 kbar to 300-260 °C and 2 kbar was determined, which is supported by dynamic recrystallization conditions inferred from quartz microstructures observed under CL. The mineralizing fluid, with an estimated composition of H₂O(55)-CO₂(40)-NaCl(5) was trapped as primary fluid inclusions in non-deformed quartz (T0) showing blue CL. Alteration structures (T1-T4) are revealed by quartz showing brown and reddish CL hosting different types of fluid inclusions, and characterized by (T1) a diffusive intragranular mosaic structure related to slight ductile shearing, (T2) grain boundaries which formed as a result of dynamic recrystallization (secondary

grain growth), (T3) shear bands of fine-grained quartz without fluid inclusions, and (T4) healed micro-fractures.

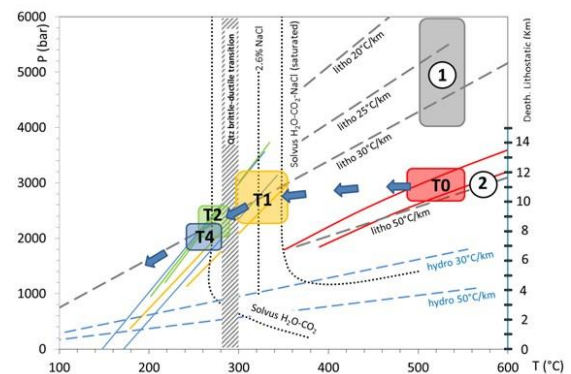


Fig. 1. Fluid evolution of the gold quartz veins. 1 = Neoproterozoic (Brasiliano) amphibolite-facies metamorphism; 2 = Post-collisional magmatic activity resulting in a higher geothermal gradient and vein mineralization. Primary aqueous-carbonic inclusions were trapped at 500-550°C / 3 kbar (T0), followed by a period of isobaric cooling. The fluid became richer in water and CaCl₂ and was retrapped in fluid inclusions along crackling structures formed during weak ductile shearing at conditions of 300-350°C / 2.5-3 kbar (T1) and 260-300°C / 2-2.5 kbar (T2). Late low-salinity NaCl-bearing fluids were trapped below ca. 250-300°C (T4). The alteration fluids were preferentially trapped around the quartz brittle-ductile transition (ca. 280-300°C).

References:

Sosa et al., 2020. *Journal of South American Earth Sciences*.
10.1016/j.jsames.2020.103079

Fluid inclusion characteristics of polymetallic Cu-Ag±Mo-Pb-Zn mineralization in the Nonacho Basin, Northwest Territories, Canada

Terekhova A.^{1*}, Hanley J.,¹ Landry K.,¹ Adlakha E.,¹ Martel E.,² Falck H.²

¹Mineral Exploration and Ore Fluids Laboratory, Department of Geology, Saint Mary's University, Nova Scotia, Canada ²Government of Northwest Territories, Canada

*anna.terekhova.m@gmail.com

Keywords: fluid inclusions, ore deposit, sedimentary basins

The Paleoproterozoic Nonacho Basin (Northwest Territories, Canada) is a major molasse basin containing a diversity of poorly characterized hydrothermal mineral deposits, including polymetallic Cu-Ag±Mo-Pb-Zn mineralization that occurs in stockworks within shear zones cross-cutting gneiss, quartzite and granitoids. Fluid inclusions occur in massive quartz veins containing bornite-chalcocite-chalcopyrite-calcite vug infillings, and sulfide-quartz breccias (Cd-rich sphalerite, galena, bornite, and chalcopyrite) associated with calc-potassic alteration.

Hot-cathode CL imaging shows three generations of quartz: (i) early magmatic or high grade metamorphic (basement host rock-related), (ii) pre-mineralization, vein-related, replacing or brecciating type (i) quartz; (iii) syn-mineralization fracture- and breccia-associated, postdating type (ii); type (iv), post-dating type (iii) and appearing in abundance near heavily mineralized areas. Three types of inclusions are associated with different quartz generations (observations at room T): Type I, early secondary aqueous-carbonic (CO₂±N₂) 2- or 3-phase (L_{aq}+L_{carb}±V_{carb}), and Type IIa secondary aqueous, 2-phase (L_{aq}+V) are hosted in type (ii) quartz. Type IIb primary aqueous, 2-phase (L_{aq}+V) are hosted in calcite filling vugs in type (iii) quartz and are coeval with sulfides. Type III, late primary aqueous, V-dominant inclusions (V_{aq}) occurring in quartz (iii) and (iv), also coeval with the mineralization. Type I fluid has the highest bulk salinity ranging from (3.83-7.54 wt% NaCl_{eq.}) with minimum T_h ranging from ~275°C to 375°C. Type II fluid is lower salinity than

type I (0.17-5.58 wt% NaCl_{eq.}), and yields lower T_h ranging from ~150 °C to ~300 °C. Inter-FIA variations in fluid density and T_h are wide, but are narrow for individual FIA, suggesting real variations in P-T conditions of the system with time. The overlap in T_h and salinity between the Type I and II (Fig. 1) suggests cooling, mixing and dilution by the introduction of meteoric water with the late, V-dominant Type III inclusions representing the end-stage of mineralization at low P conditions.

The mineralization is interpreted as intrusion-related, involving metal precipitation driven by faulting/brecciation, leading to meteoric water incursion and mixing with an aqueous-carbonic fluid. The Cu-Ag mineralization may be related to alkalic magmatism near the end of the basin formation.

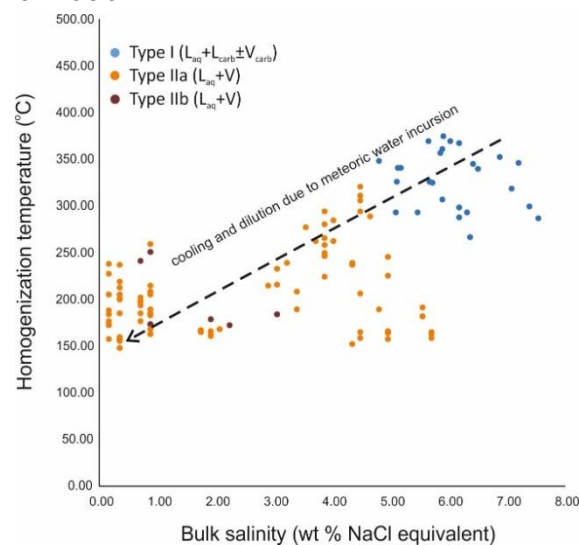


Fig. 1: T_h vs salinity plot showing data for aqueous and aqueous-carbonic fluid types, highlighting a mixing trends between the two fluids.

Formation of the Schlaining stibnite deposit in the Rednitz Window (Eastern Alps, Austria).

Lüders V.^{1*}, Sośnicka M.^{1,2}, de Graaf S.³, Banks D. A.⁴, Niedermann S.¹

¹ GFZ German Research Centre for Geosciences, Telegrafenberg, D-14473 Potsdam, Germany; ² Friedrich Schiller University Jena, Institute of Geosciences, Burgweg 11, D-07749 Jena, Germany; ³ Max Planck Institute for Chemistry, Hahn-Meitner-Weg 1, D-55218 Mainz, Germany; ⁴ School of Earth and Environment, University of Leeds, Leeds LS29JT, UK

*value@gfz-potsdam.de

Keywords: Fluid inclusion, hydrothermalism, ore deposits

The Upper and Middle Austro-Alpine units of the Eastern Alps host a variety of mostly strata-bound sub-economic polymetallic ore deposits, which belong to the so-called Sb-W-Hg formation (e.g. Höll 1978). About ten of these deposits were mined for antimony. The genesis of the Sb-rich deposits is considered to be related to Upper Ordovician to Silurian hydrothermal activity triggered by submarine volcanism (Höll 1978). The most important stibnite (with scheelite) deposits were mined in the Rabant district (Kreuzeck mountain group).

In contrast, the strata-bound, quartz-stibnite mineralization of the Schlaining mining district was deposited in Early Miocene times and differs from the Sb mineralization of the Eastern Alps by the absence of W and Hg ores. The economic stibnite (total production of about one million tons of antimony ore) was mined until the end of the 20th Century.

Comprehensive studies of fluid inclusions in quartz and stibnite (Fig. 1), including conventional and IR microthermometry, isotope ($\delta^2\text{H}$, $\delta^{18}\text{O}$, noble gases) and crush-leach analyses, show compelling evidence that two fluids of different compositions and origins were involved in the formation of quartz and stibnite mineralization: (i) a low-salinity, low- CO_2 metamorphic fluid that precipitated quartz at temperatures of about 240 °C and (ii) a stibnite-forming ore fluid that was of meteoric origin and most likely scavenged antimony and H_2S by fluid/rock interaction from sediments, metasediments and/or deep-seated

Palaeozoic stibnite deposits. Massive stibnite deposition occurred by cooling of the ore fluid to temperatures below 300°C, at a shallow depth of maximum 2000 m. Quartz precipitated at slightly lower temperatures but more or less contemporaneously with stibnite. There is no evidence that both fluids mixed at the site of ore deposition.

Fluid migration and ore deposition are likely related to high heat-flow during the exhumation of the Rednitz Window in response to Neogene extension and/or Early Miocene andesitic magmatism.

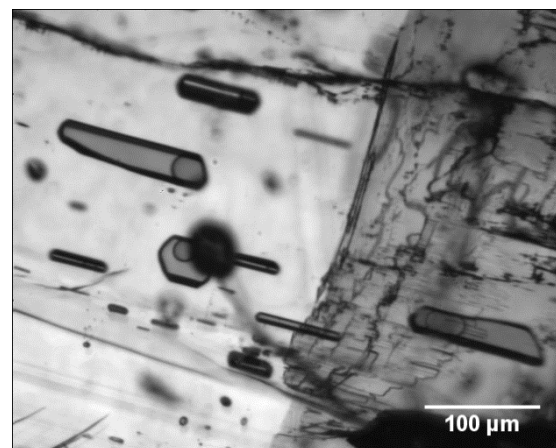


Fig. 1: IR photomicrograph of primary fluid inclusions in stibnite.

References:

Höll R (1978) *Verh. Geol. B, A Wien* 3, pp 369–387

Porosity preservation by overpressure: insights from fluid inclusions modeling

Elias Bahnan A.^{1*}, Pironon J.¹, Fan J.², Lu X.², Ma X.²

¹ Université de Lorraine, CNRS, GeoRessources lab, 54000 Nancy, France. ² Research Institute of Petroleum Exploration and development, Beijing 100083, China.

*Alexy.elias-bahnan@univ-lorraine.fr

Keywords: geodynamics, sedimentary basins, diagenesis

Understanding paleo-fluid pressures in a sedimentary basin permits the assessment of reservoir properties, the recognition of possible seal leakages, aqua-thermal expansion, and the possible maturation and cracking of hydrocarbons. Despite the wealth of technologies currently employed in the petroleum industry, fluid inclusions (FI) modeling remains the only available tool to determine fluid paleo-pressures relative to the geodynamics of the basin. To this end, 5.2 km-deep core samples from the Anyue gas field in the Sichuan Basin, SW China, were studied to understand the preservation of excellent reservoir properties even after being buried to a depth of 7km.

After constructing a paragenetic sequence, FIs were observed in fracture dolomites, fluorites, quartz and calcites. Co-genetic two-phase (L+V) and single-phase (V) inclusions were identified in quartz and fluorites. Pairs of inclusions were selected from assemblages located along growth zones inside the quartz crystals, re-affirming their co-genetic identity. These were the target of fluid PVT modeling where the double-isochore technique (Roedder and Bodnar, 1980) was applied to determine trapping P-T conditions. These increased from around 308 to 543 bars at temperatures of around 121 and 160 °C respectively (Fig.1). This trend indicates that quartz precipitated during the rifting-crustal thinning event up to the beginning of the Yanshanian flexural depression (Fig.1). When plotted against the hydrostatic pressure of the hosting reservoir, the fluid overpressure, defined as the deviation from the hydrostatic gradient, is calculated to around 90-113 bars (Fig.1). Similarly, co-genetic pairs of FIs studied from the fluorites record the

maximum trapping P-T conditions at around 225 °C and 1070 bars, corresponding to the maximum burial with an overpressure of nearly 326 bars.

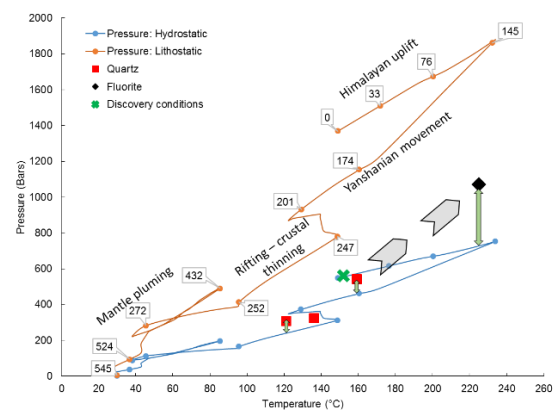


Fig. 1: Evolution of P-T conditions of the Dengying reservoir. Number tags are ages in Ma. Red and black symbols correspond to the trapping P-T conditions of FIs. Green arrows are deviations from the hydrostatic pressure gradient. Grey arrows highlight the increasing overpressure conditions in the reservoir.

Therefore, after PVT modeling of co-genetic FIs, porosity preservation by overpressure was attained before the maximum burial, which eventually prevented the collapse of porosity against the increasing overburden pressure during subsidence. Finally, the pressure drop to present-day conditions could indicate gas leakage or dysmigration to other neighbouring reservoirs.

References:

Roedder E. and Bodnar R. J. (1980) *Geologic Pressure Determinations from Fluid Inclusion Studies. Annu. Rev. Earth Planet. Sci. 8*, 263–301.

Synthetic water-hydrocarbon inclusions in quartz as a source of knowledge about the phase composition and state of deep oil

Balitsky V. S.¹, Pironon J.², Balitskaya E. D.¹, Plotnikova I. N.³, Penteley S. V.⁴, Barres O.², Randi A.²

¹ Institute of Experimental Mineralogy RAS, Russia; ² Université de Lorraine, CNRS, GeoRessources lab, Nancy, France; ³ Institute of Applied Research, Tatarstan Academy Sciences, Russia; ⁴ 9 Grande rue 5412 Deneuvre, France

*balvlad@iem.ac.ru

Keywords: fluid inclusions, experiments, metamorphism

Phase compositions and states of water and oil in deep systems have been reproduced using synthetic aqueous-hydrocarbon inclusions in quartz crystals grown by hydrothermal method in the temperature range of 240-700 °C and pressures range of 7-150 MPa. As a result, it has been shown that depending on thermobarometric parameters and volume ratios of aqueous solution, oil and gaseous hydrocarbons (HC), the following types of water-hydrocarbon fluids may exist in the earth's subsurface (Balitsky et al, 2020):

1 – Heterogeneous three-phase fluids (L1 + L2 + G) with partially dissolved liquid and gas HCs. Here and below, phases in fluid inclusions are designated as: L1 - water solution; L2 - oil; G – gaseous HCs, mainly methane and less frequently, propane, butane and steam. In addition, solid bitumen designated as SB are often present in inclusions.

2 – Heterogeneous two-phase liquid water-hydrocarbon fluids with fully dissolved hydrocarbon gases or fully and partially dissolved oil;

3 – Homogeneous liquid aqueous fluids with fully dissolved oil and gas HCs;

4 – Homogeneous liquid hydrocarbon fluids with fully dissolved aqueous (L1) and gaseous (G) phases;

5 – Homogeneous gaseous hydrocarbon fluids with fully dissolved aqueous (L1) and oil phases (L2).

The existence of these fluids and their mutual transformations due to changing the phase compositions and TP-parameters of the runs is unambiguously proved by numerous videos and

thermograms. One of these thermograms is shown in Fig. 1. The objective of this presentation will be to show several case studies thanks to the coupling of microthermometry and image acquisition data.

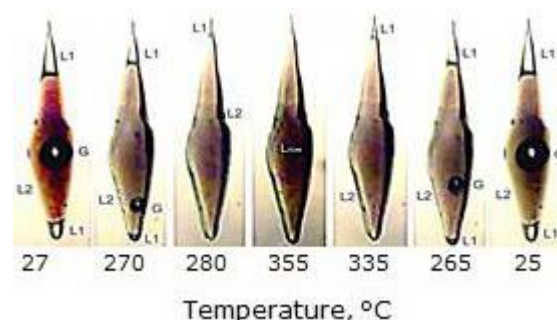


Fig. 1: Reversible changes of phase composition and state of substantially petroleum inclusion in quartz at short-term (1 - 2h) temperature increase and decrease. Volumetric phase ratios $L2 \gg L1 \approx G \gg SB$. Initial solution: 7.5 wt% Na_2CO_3 + 10 vol% oil, temperature 285/310°C, pressure 12 MPa, run duration 22 day.

The reported study was funded by RFBR and CNRS according to the research project No. 21-55-15010.

References:

Balitsky V.S., Setkova T.V., Balitskaya L.V., et al. (2020) In: Litvin Y., Safonov O. (eds) *Advances in Experimental and Genetic Mineralogy*. Springer, Cham., pp 3-34.

Hydrocarbons in fluid inclusions in minerals from gold deposits of the Yenisei Ridge (Russia)

Shaparenko E.¹, Tomilenko A.¹, Gibsher N.¹, Bul'bak T.¹, Sazonov A.², Khomenko M.¹, Petrova M.¹

¹ V.S. Sobolev Institute of Geology and Mineralogy SB RAS, Russia; ² Institute of Mining, Geology and Geotechnology of Siberian Federal University, Russia

*shaparenkoe@gmail.com

Keywords: fluid inclusion, ore deposits, hydrothermalism

The Yenisei Ridge is one of the richest Russian gold mining regions. The Olimpiadinskoe, the Blagodatnoye, the Sovetskoye, and the Eldorado deposits were studied. Gold localization is associated with quartz veins and sulfides (arsenopyrite, pyrite, and pyrrhotite). Fluids took part in the formation of gold ore deposits. Fluids represented by vapor-liquid and vapor inclusions in quartz (Fig. 1), sulfides, and native gold were studied by pyrolysis-free gas chromatography-mass spectrometry (GC-MS). When preparing samples for analysis, organic substances and acids were not used.

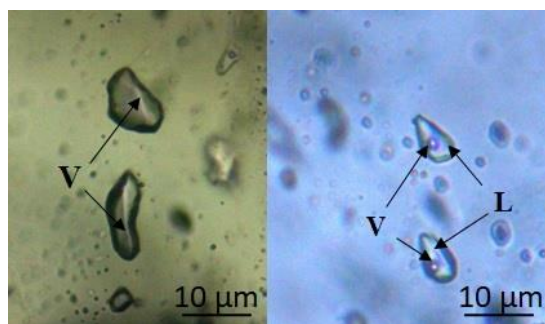


Fig. 1: Fluid inclusions in quartz from the Blagodatnoye deposit. L-liquid, V-vapour.

The data obtained show that fluids from gold, sulfides, and quartz of the studied deposits are a multicomponent mineral-forming system. Apart from water and carbon dioxide, representatives of at least 11 homologous series of organic compounds were found in the studied fluids. These are oxygen-free aliphatic and cyclic hydrocarbons (paraffins, olefins, cyclic alkanes and alkenes, arenes, polycyclic aromatic hydrocarbons - PAHs), oxygenated hydrocarbons

(alcohols, ethers and esters, furans, aldehydes, ketones, carboxylic acids), nitrogenated, sulfonated, halogenated, and organosilicon compounds. In native gold fluids, the portion of hydrocarbons in total with S-N-Cl-F-Si compounds reaches 80 rel.% (Bul'bak et al., 2020), while in sulfides and quartz – much less (10-20 rel.%). A small amount of water (0.3–13.4 rel.%) determined in fluid inclusions from native gold confirms assumptions made previously that gold was transported by “dry gas-condensate reduced fluids” (Petrovskaya, 1973). Reduced hydrocarbon fluids are able to accumulate and transfer significant amounts of gold, i.e. hydrocarbons act as ore fluid (Gize, Macdonald, 1993).

Acknowledgement

The reported study was funded by RFBR, project number 19-35-90050.

References:

- Bul'bak et al. (2020) *Russ. Geol. Geophys+* Vol 61, № 11, pp. 1260–1282.
Petrovskaya N.V. (1973) *Nauka, Moscow*. 345 p. (in Russian)
Gizé A.F., Macdonald R. (1993) *Geology*, Vol 21, pp. 129-132.

Fluid inclusion systematics in anglesite ore mineral from Uchich sulphide mineralization, Himachal Himalaya, India.

Rana S.^{1*}, Sharma R.¹

¹ *Wadia Institute of Himalayan Geology, Dehradun, Uttarakhand, India.*

**shrtrn5@gmail.com*

Keywords: fluid inclusion, ore deposit

Vein-hosted polymetallic Iron-arsenic-lead-copper (Ag-Sn-Bi-Ti) sulphide mineralisation in the Proterozoic Lesser Himalayan orogenic belt, Himachal Himalaya, India, occurs within the immediate proximity of graphitic quartz-mica-schist shear zone along the Kulu/Chail thrust (Quartzite forming the footwall and low to medium grade metamorphics constituting the hanging wall) cross cutting Manikaran Quartzite of Rampur formation, Larji Rampur window. Mineralization in quartz vein consists mainly of pyrite and arsenopyrite, with later supergene alteration of ores to anglesite and scorodite. Precious metal and accessory phases consist of silver, tin, bismuth and titanium sulphides. Replacement of galena by anglesite and arsenopyrite by scorodite indicates changes in fluid redox to low pH and oxidizing conditions as mineralization progressed. Sulphide mineralisation is coeval with the infilling fractures and dissolution cavities/vugs in the quartz.

Widely distributed monophasic, biphasic and polyphasic type of fluid inclusions in quartz indicate syn to post ore mineralization nature of the fluid. Widely varying proportion of the carbonic and aqueous phases indicate the immiscibility of fluid and liquid gas meniscus of CO₂ at room temperature and suggests the low density of the carbonic fluid. Ore mineralization is interpreted to be the result of unmixing of carbonic-aqueous fluid. Late stage aqueous inclusions are linked to the recrystallization of vein quartz, characterized by the presence of annealing texture. In order to investigate the evolution of fluid during the formation and deformation of supergene mineral, fluid inclusions in mineral anglesite are studied. Fluid inclusions in supergene anglesite are monophasic aqueous inclusions and biphasic aqueous saline

inclusions + biphasic inclusions with variable composition as H₂O+H₂S±CO₂±CH₄±N₂±SO₂. Raman spectroscopy indicates that the fluid involved in anglesite precipitation is attributed to be a complex fluid with saline water and gases like H₂S, CO₂, N₂, CH₄, and SO₂. The homogenization of the biphasic inclusions occurred, for majority of these inclusions, between 200 to 250°C. The available fluid inclusion evidences point towards a lower pressure i.e. <1 kbar at 200°C and <1.7 kbar at 300°C. The salinity estimated for the aqueous phase in anglesite is in the range of 0.7 to 17.4 equiv. wt% NaCl, specifically between 5 to 15 equiv. wt% NaCl. Typical features of fluid inclusions in anglesite point to their deformation in the internal overpressure conditions, reflecting sustained exhumation of the ore body after the anglesite formation.

Acknowledgement

The authors are grateful to the Director Wadia Institute of Himalayan Geology (WIHG) for providing facilities for this work. SR acknowledges the Senior Research Fellowship from WIHG.

Fluids evolutions from rift to post-orogenic stages: example of the Northern Pyrenees (France)

Michels R.^{1*}, Gaucher E. C.², Pironon J.¹, Elias-Bahnan A.¹, Rallakis D.¹, Barré G.^{2,3}, Calassou S.²

¹ Université de Lorraine, CNRS, GeoRessources lab, Nancy, France; ² TOTAL-CSTJF, Pau, France, ³ Université de Pau et des Pays de l'Adour, CNRS, TOTAL, LFCR, Pau, France.

*Raymond.michels@univ-lorraine.fr

Keywords: geodynamics, oil&gas, fluid inclusions

The evolution and genesis of the Aquitaine basin is closely linked to the geodynamics of the Pyrenees and the interaction between the Spanish and European plate boundaries. Recently, the geodynamic model of the Pyrenees and the south Aquitaine basin were revisited and updated to include the involvement of an Early Cretaceous rifting phase that evolved to extreme crustal thinning coupled with mantle exhumation. This event was followed by the main Pyrenean convergence leading to collision and thrusting during the late Cretaceous and the Paleogene. This revised model highlights the possible impact of hydrothermal fluids on the diagenesis of petroleum reservoirs in the southern Aquitaine Basin.

Several research programs involving many teams have been supported in the last decade by Total E&P, BRGM, CNRS and the French National Research Agency to set the Pyrenees as a reference analogue to understand the complex interplays between structural evolution, deformation, metamorphism, volcanism, hydrothermalism, fluid evolution, diagenesis and transfer over a complete Wilson cycle. Fluid inclusions, vitrinite reflection, Raman spectroscopy on graphite (Clerc et al, 2015), have been used to determine paleotemperatures. U-Pb of carbonates helped to determine absolute dating of carbonates for the first time (Motte et al., 2021). Fluid pressure have been determined in gas and oil reservoirs by the double isochore technique.

A thermal gradient from South to North is recorded over time. The highest temperatures are related to rifting and hyperextension phases of the lower

Cretaceous (350-450 °C in the Pyrenees Central Domain, up to 550 °C near mantle cores) with temperatures varying from 350 °C in the foothills (Salardon et al., 2017) to 150°C in the foreland (Renard et al., 2019).

In the foothills, intense thermal gradients are associated with fracturing of Jurassic carbonate deposits allowing fluid circulation and dolomite precipitation. A mantle contribution is suspected for the CO₂ and magnesium rich fluids observed, while high salinity is inherited from dissolution of Triassic evaporites. Jurassic petroleum source-rocks were rapidly brought to gas stage and ultimately to graphite. Interactions with sulfate rich fluids allowed intense Thermochemical Sulfate Reduction and hence H₂S formation and hydrocarbons destruction.

The study of the Pyrenees Wilson cycle thus documents the fluid formation and migration in relation to the structural evolution of the mountain range and foreland basin system. It highlights especially how earlier stages of evolution set their successive imprints in space and time and hence constitute an inheritance which strongly influences later stages of fluid geochemistry and migration.

References :

- Clerc et al. (2015): *Solid Earth*, 6, 643–668,
Motte G. et al. (2021): *Marine and Petroleum Geology*, 126, 104932.
Renard S. et al., (2019): *Chemical Geology*, 508, 30-46.
Salardon R. et al. (2017): *Marine and Petroleum Geology*, 80, 563-586.

Enrichment of N₂ in subduction fluids: a multiphase inclusion study in high-pressure rocks of the Cabo Ortegal Complex (Spain)

Spránitz T.^{1*}, Padrón-Navarta J. A.^{2,3}, Szabó Cs.¹, Berkesi M.¹

¹ Lithosphere Fluid Research Lab, Department of Petrology and Geochemistry, Eötvös University, Budapest, Hungary; ² Instituto Andaluz de Ciencias de la Tierra (IACT) (CSIC-Universidad de Granada), Av. Palmeras 4, 18100 Armilla, Granada, Spain; ³ Géosciences Montpellier, Université de Montpellier & CNRS, F-34095 Montpellier cedex 5, France.

*spratom.elte@gmail.com

Keywords: fluid inclusion, metamorphism, thermodynamic calculations

Primary fluid inclusions trapped in subducted and exhumed high-pressure (HP) metamorphic rocks, outcropping in Cabo Ortegal Complex (COC) in Spain, provide direct constraints on fluid regime of subduction-zone environment.

Our study focuses on primary multiphase inclusions (MPI) in garnet from eclogites and granulites from the COC. These inclusions occur in 3D clusters or along a growth-zone in the hosting garnet. MPI have irregular to negative crystal shape and 1-40 µm size. Detailed Raman imaging, SEM-EDS and FIB-SEM analyses confirmed that MPI have a uniform phase assemblage and nearly constant volume proportions dominated by a tight intergrowth of Fe-Mg-Ca-carbonates and phyllosilicates (pyrophyllite, chlorite and margarite) together with N₂-CH₄-CO₂ fluid among the solid phases. Thermodynamic modelling in the CaFMAS-COHN system confirmed that bulk composition of the MPI in eclogites is remarkably similar to the host garnet composition, supporting a step-daughter origin of the solid phases in the MPI. Our observations and calculations, together with mass balance constraints suggest that these MPI are products of post-entrapment reactions of a COHN fluid with the host mineral. The originally trapped fluid could have interacted with garnet after entrapment via carbonation and hydration reaction leading to the dilution (or consumption) of H₂O and CO₂ in the fluid phase. As a result, residual fluid will be highly enriched in N₂, that is, to our best knowledge has not been recognized in such detail. Pseudosection modelling revealed the appearance of the observed assemblage in the MPI, thus the

termination of the reactions below about 400°C.

This process suggests that in the shallow exhumation zone, there might be a horizon of a fluid regime with significantly elevated nitrogen content. These findings indicate that such process in the exhuming HP units may play an important role in global nitrogen cycling as well as may contribute to nitrogen supply to subsurface-surface environment during devolatilization in the forearc regions of convergent plate margins.

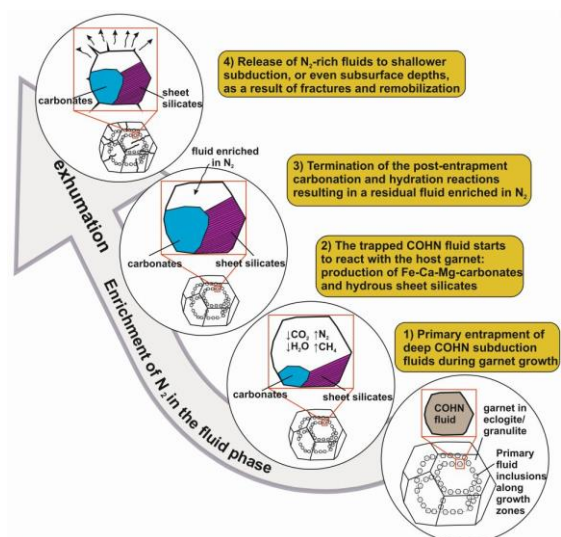


Fig. 1: A schematic flow chart showing the proposed mechanism of nitrogen enrichment during post-entrapment carbonation and hydration reactions, observed in MPI in garnet of the studied HP eclogites and granulites from the COC.

This research was supported by the NRDIO_FK research fund nr. 132418.

HP-UHP fluid inclusion post-entrapment evolution predicted by molecular and electrolytic fluid models

Maffei A.^{1*}, Ferrando S.¹, Connolly J. A. D.², Groppo C.^{1,3}, Frezzotti M. L.⁴, Castelli D.¹

¹University of Torino, Department of Earth Sciences; Via Valperga Caluso, 35, 1-10125 Torino, Italy; ²ETH Zurich, Department of Earth Sciences, Institute for Geochemistry and Petrology; Clausiusstrasse 25, CH 8092, Zurich, Switzerland; ³C.N.R. – I.G.G., Section of Torino, Via Valperga Caluso 35, 1-10125, Torino, Italy; ⁴University of Milano-Bicocca, Department of Environment and Earth Sciences; Piazza della Scienza 4, 20126 Milano, Italy.

*andrea.maffei@unito.it

Keywords: Fluid Inclusions, Metamorphism, Thermodynamic Calculations

Fluids released from a subducting plate regulate the long-term chemical cycles. So, a reliable characterisation of these fluid is of primary importance to understand metasomatic, oxidation, and melting processes affecting the overlying mantle wedge. UHP fluids are composed by solvent COHNS molecular volatiles and by solute non-volatile elements bounded to inorganic and organic species. Both direct (fluid inclusion, FI) and indirect (thermodynamic modelling, TM) approaches to study these fluids have reliability issues: the chemical fingerprint of UHP FI can be easily modified by post-trapping processes, while TM of solute-bearing fluids at UHP conditions is still in its infancy.

In this work, we evaluated the compositional data from primary (Type I) FI trapped within peak diopside from a chemically simple marble (DM675) from the UHP Brossasco-Isasca Unit of the Dora-Maira Massif (Western Alps). These tri-phase multisolid aqueous inclusions (5-25 μm in diameter) consist of $\text{H}_2\text{O}_{\text{Liq}}$ + different kinds of solids ($\text{Cc}/\text{Mg-Cc} \pm \text{Tlc} \pm \text{Dol} \pm \text{Serp} \pm \text{Tr} \pm \text{Sulp} \pm \text{Gr}$) + bubble ($\text{H}_2\text{O}_{\text{v}} \pm \text{N}_2 \pm \text{CH}_4$); Fig. 1]. Classical molecular-fluid TM allowed to model post-trapping reactions between FI and host diopside (i.e., discrimination among daughter, step-daughter, and incidentally trapped minerals). Electrolytic-fluid TM allowed modelling the chemical composition of the peak solute-bearing aqueous fluid (H_2O : 88.5 wt%; solutes: 11.34 wt%; $\text{CO}_2 + \text{H}_2\text{S} + \text{CH}_4$: 0.17 wt%) generated by progressive rock

dissolution. The comparison between the modelled fluid composition with that reconstructed from FI allows to recognise kind and extent of post-trapping chemical re-equilibration occurred within UHP FI. Applying this multidisciplinary approach, we demonstrate that the most impacting post-trapping process in UHP FI is the H_2O loss, with consequent preservation of the geochemical information in those FI lacking relevant post-trapping host-diopside chemical contamination. So, the electrolytic fluid TM is highly supportive of the classical FI study to retrieve geochemical information on deep subduction fluids.

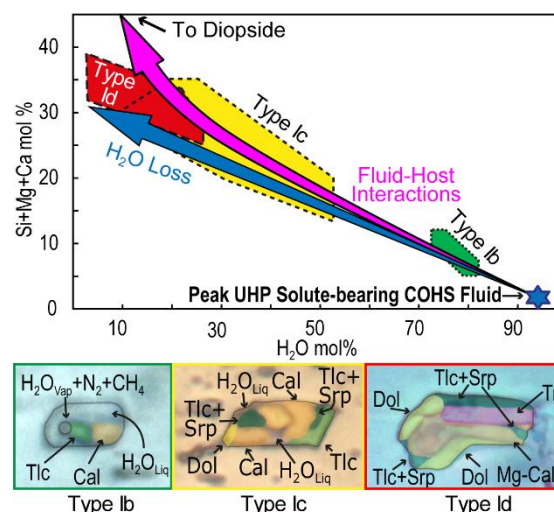


Fig. 1: FI compositions compared to the modelled peak electrolytic fluid with the most representative example of Type I FI post entrapment modification stages.

Posters

P-T-X reconstruction for ore deposits using petroleum-rich fluid inclusions in fluorite: A case study in the Bou Jaber diapir-related Ba-Pb-Zn-F deposit, Northern Tunisia

Abidi R.^{1,*}, Marignac C.², Slim-Shimi N.¹, Pironon J.², Gasquet D.³, Somarin A. K.⁴, Christophe R.⁵, Hibschi C.², Hatira N.⁶

¹ Université Tunis El Manar, Faculté des Sciences de Tunis, Département de Géologie, Campus Universitaire 2092, El Manar Tunis, Tunisia, ² Université de Lorraine, CNRS, GeoRessources lab, F-54042 Nancy, France, ³ Laboratoire EDYTEM, Université de Savoie Mont Blanc, CNRS-UMR5204, Campus scientifique, Bâtiment « Pôle Montagne », 73376, Le Bourget du Lac, France, ⁴ Department of Geology, Brandon University, Brandon, Manitoba, R7A6A9, Canada, ⁵ Université Côte d'Azur, CNRS, OCA, IRD, Géoazur, 250 rue Albert Einstein, Sophia Antipolis, 06560, Valbonne, France, ⁶ Faculté des Sciences de Bizerte, Département de Géologie, Université de Carthage, 7021 Jarzouna, Bizerte, Tunisia

*Corresponding author: abidi1riadh@yahoo.com (R. Abidi).

Keywords: Fluorite, Petroleum inclusions, PTX

The Bou Jaber ore deposit is one of the numerous diapir-related Pb-Zn-F-Ba deposits of the Dome Zone in Northern Tunisia. Its location is controlled by the regional NE-SW Tazerouine Fault. Ore minerals are hosted in the Late Aptian limestones (Serdj Formation) as open space filling and stratabound replacement bodies.

The fluorite system is characterized by the involvement of oil in the hydrothermal fluids. This oil was produced in the local environment of the deposit from the thermal maturation of the Albian Fahdene black shale source-rock at temperature range of ~140 °C–~100 °C. Two brines were involved in the fluorite hydrothermal system. The first one (L1) is a Ca-rich brine (≥ 20 wt % bulk salinity), with $\text{Na/Ca} \leq 0.18$, which is thought to have long resided in the basement, before its transfer into the Jurassic reservoir (Upper Nara Formation) and its eventual mobilization at the time of ore deposition. The second brine (L2), less saline (≤ 14 wt % bulk salinity) is more sodic, with Na/Ca up to 0.53, and represents unmodified brine originated from the nearby Triassic salt. The L1 brine was F-bearing, whereas the L2 brine was associated with oil. Fluorite deposition occurred at the estimated shallow depth of 1.7 km from cooling of the L1 brine due to the first isobaric cooling from ~160 °C

to 135 °C under sub-lithostatic conditions (36 MPa). This stage is followed by mixing with the newly incoming L2 brines (transporting oil) along a sub-isochoric decompression path (down to the hydrostatic pressure at 17 MPa) and continuously cooling from 135 °C to 125 °C. The cooling and mixing caused fluorite deposition after which a transient heat advection episode (up to 145 °C) caused late calcite deposition prior to the end of hydrothermal circulation.

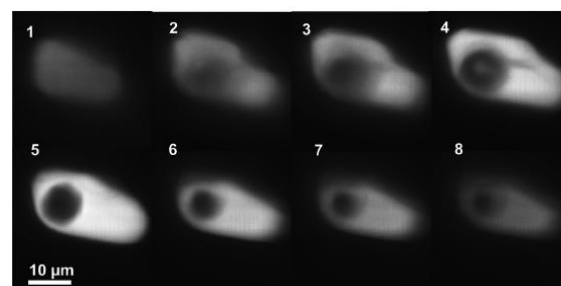


Fig. 1. Confocal Laser Scanning Microscope images through a 27 µm deep inclusion hosted in fluorite from the Bou Jaber ore deposits. Passing down through the inclusion the vapour bubble (grey) appears and disappears, and the internal shape of the inclusion changes. The diameter of the two oil bubbles may thus be measured with a great precision.

Shallow-burial hydrothermalism in Alpine Mesozoic carbonates: FI microthermometry, stable isotopes, and U/Pb geochronology

Barale L.^{1*}, Bertok C.², d'Atri A.², Ferrando S.², Incerpi N.^{2,3}, Mantovani A.², Martire L.², Piana F.¹, Bernasconi S. M.⁴, Czuppon G.⁵, Manatschal G.³, Palcsu L.⁶

¹CNR-IGG, Torino (IT); ²Earth Sciences Dept., University of Torino (IT); ³EOST-IPGS, University of Strasbourg (FR); ⁴Earth Sciences Dept., ETH Zurich (CH); ⁵IGGR, Hungarian Academy of Sciences, Budapest (HU); ⁶ICER, Hungarian Academy of Sciences, Debrecen (HU). *luca.barale@cnr.it

Keywords: fluid inclusion, hydrothermalism, sedimentary basins

Several examples of hydrothermal circulation have been recently documented in Mesozoic successions of the Western and Central Alps belonging to both the European and the Adriatic passive palaeomargins of the Alpine Tethys. We will discuss three different case studies where fault-related hydrothermal circulation developed in different geodynamic settings:

- the Middle Triassic-Berriasian Provençal succession of the Maritime Alps (Italy-France; European palaeomargin), which was intensely dolomitized in the earliest Cretaceous by hot fluids ($T \sim 200^{\circ}\text{C}$) circulating through regional strike-slip fault systems;
- the Middle Triassic-Early Jurassic Southalpine successions of N Piemonte (Italy; Adriatic palaeomargin), affected by hydrothermal circulation (dolomite and quartz precipitation in veins and breccias; $T \sim 80\text{-}120^{\circ}\text{C}$) along normal faults developed during Early Jurassic rifting phases;
- the Upper Triassic-Early Jurassic succession of the Austroalpine units of Grisons (Switzerland; Adriatic palaeomargin), affected by different phases of hydrothermal circulation (dolomitization, silicization, dolomite-quartz vein/breccia cements; $T \sim 120\text{-}150^{\circ}\text{C}$) during the latest Triassic-early Middle Jurassic evolution of the margin.

Indications on T and salinity of fluids were obtained by fluid inclusion microthermometry on hydrothermal minerals (dolomite, quartz); where the

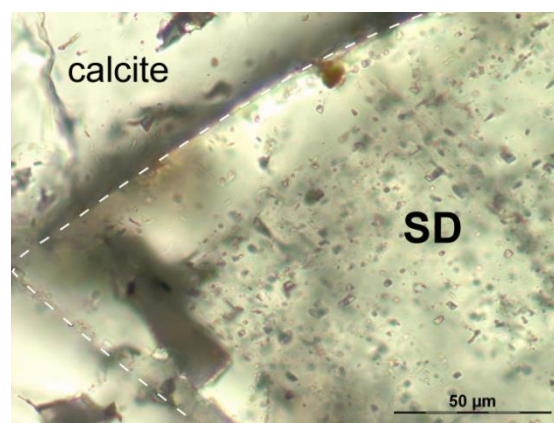


Fig. 1: Photomicrograph of primary fluid inclusions in the outer part of a saddle dolomite crystal (SD) from the Maritime Alps.

Alpine metamorphic overprint was negligible, clumped isotope thermometry on dolomite was also performed. In all three cases, stratigraphic constraints and U/Pb dolomite geochronology allowed a precise dating of hydrothermal circulation, indicating that the hot fluids circulated through the Mesozoic carbonates shortly after their deposition and thus at a very shallow depth (10's to 100's of metres). The hydrothermal systems were fed by seawater, which was heated during deep circulation reaching the crystalline basement. Strong interaction with crystalline rocks is also supported by the inferred composition of hydrothermal fluids ($\delta^{18}\text{O}$, $^{87}\text{Sr}/^{86}\text{Sr}$, $^3\text{He}/^4\text{He}$, salinity). These case studies show that sediments deposited on passive margins are commonly affected, since the early stages of their evolution, by circulation of high temperature fluids developed along deep-reaching tectonic structures and interacting with shallow buried sediments.

Entrapment and re-equilibration of fluid inclusions in hydrothermal veins related to transtensional shear zones

Maffini M. N.^{1*}, Sosa G. M.², van den Kerkhof A. M.², Coniglio, J. E.¹, Demartis M.¹, Wemmer, K.²

¹ Instituto de Ciencias de la Tierra, Biodiversidad y Ambiente (ICBIA-CONICET), Universidad Nacional de Río Cuarto, Argentina; ² Geoscience Center, Georg-August University, Göttingen, Germany.

*nmaffini@exa.unrc.edu.ar

Keywords: fluid inclusion, ore deposits, hydrothermalism

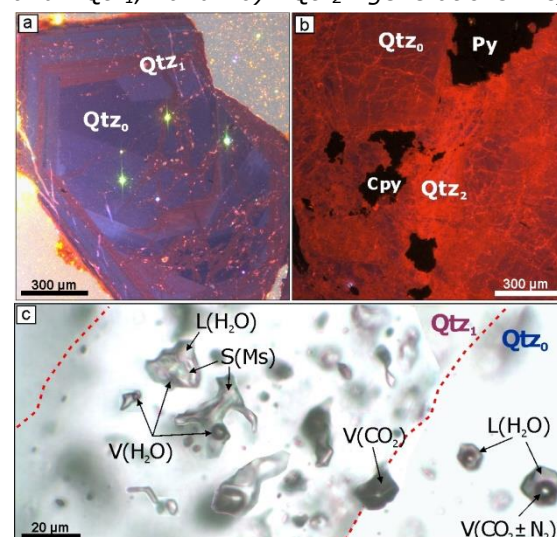
Polymetallic quartz veins (Pb-Zn-Cu-Ag ±Au) outcrop in the southern Sierras Pampeanas de Córdoba, Argentina. They are structurally controlled by NNW-striking brittle-ductile transtensional shear zones. Two main episodes of mineralization can be recognized: a first barren episode of milky quartz (Qtz₀ and Qtz₁), and a second ore-rich episode of grayish quartz (Qtz₂), sulfides (pyrite, galena, sphalerite, chalcopyrite and accessory tetrahedrite), Ag-Au tellurides and hematite. Illite from alteration zones reveals K/Ar ages of 329-315 Ma.

The primary quartz (Qtz₀) shows blue cathodoluminescence (CL), which correlates with high Al contents (up to 3000 ppm) as revealed by EPMA data. Qtz₀ is altered and partly replaced by Qtz₁ with brown-reddish CL (Fig. 1a) and lower Al (<60 ppm). An extreme brittle fissuring is produced by the injection of Qtz₂ with bright red CL and up to 145 ppm of Al. Other trace elements (Fe, Ti and Mn) did not show correlation with CL.

Primary aqueous-carbonic and aqueous fluid inclusions (FIs) were found in relict Qtz₀ (Fig. 1c). They show water vol. fracs. of 0.7-0.9, salinities of 5-10% NaCl and homogenization temperatures (Th) between 250-290 °C (aqueous-carbonic) and 150-260 °C (aqueous). Qtz₁ contains abundant large pseudo-secondary FIs (Fig. 1c), which comprise aqueous, aqueous-carbonic, and pure-CO₂ compositions with highly variable water vol. fracs., salinities (0.2-10% NaCl) and Th (130-450 °C). The large spread of Th can be explained by re-equilibration mechanisms, evidenced by modification textures (shape distortions), necking down, partial water leakage, and

precipitation of daughter minerals (muscovite). Raman analysis shows a slight increase of N₂ in the modified inclusions. On the other hand aqueous inclusions in Qtz₂ show relatively constant water vol. fracs. of 0.8-0.9, salinities of 2-8% NaCl and Th between 120-235 °C.

Fig. 1: CL photomicrographs showing a) Qtz₀ and Qtz₁, and b) Qtz₂ generations. c)



Photomicrograph of primary FIs in Qtz₀ and pseudo-secondary FIs in Qtz₁. L=liquid, V=vapor, S=solid, Ms=Muscovite.

Isochore calculations, combined with regional data constraints, indicate that primary FIs in Qtz₀ trapped at 320-400 °C / 1.5-2 kbar, representing the fluid system before ore deposition. Pseudo-secondary FIs in Qtz₁ were trapped along crackling microstructures at almost the same P-T conditions. The fluids associated with the ores (Qtz₂) were more diluted and relatively cooler, and must have been trapped at 250-330 °C / 1.3-1.8 kbar.

Fluid Inclusions in Scheelite from the W, (Mo,Cu) Ore Deposit of Borralha, NW Portugal

Marques de Sá C.^{1,2*}, Noronha F.¹ Bobos I.¹

¹ Instituto das Ciências da Terra, Porto, Portugal, ² Universidade Federal de Sergipe, Brasil

*dingesster@gmail.com

Keywords: fluid inclusion, ore deposits, hydrothermalism

The W, (Mo,Cu) mineralization occurs in quartz-veins and breccia structures, where wolframite and scheelite are the main W minerals. Scheelite occurs in veins and in the Santa Helena breccia constituted by micaschist and granite fragments or blocks. The selected scheelite samples were collected from quartz-scheelite, Fe,Mn-chlorite and wolframite assemblages. The fluid inclusion (FI) study was dedicated exclusively to scheelite. The scheelite crystals are fractured, making it difficult to distinguish primary from secondary and pseudo-secondary FI according to Roedder (1984). FI occur arranged in trails, zonations or isolated. The FI appear to be biphasic or three phases could be distinguished (Fig. 1), mostly dark due to internal reflections. Three different types of fluids in the FI hosted in scheelite were distinguished: i) aqueous fluids generally with low to moderate salinity; ii) aqueous-carbonic fluids with CO₂ as predominant carbonic phase, which contain sometimes also some CH₄ and N₂; and iii) aqueous-carbonic fluids with CH₄ as predominant carbonic phase. Raman spectrometric analyses performed on some representative FI of the carbonic types (CO₂ or CH₄ dominant) show that they essentially differ in the CO₂/CH₄ ratio. N₂ is only present in CO₂ dominant aqueous-carbonic inclusions. Aqueous-carbonic FI with CO₂ predominant have T_{mi} ranging from -7.2 to 0 °C, T_{clat} from 0.2 to 11.5 °C, T_h from 200 to 380 °C, salinity from 2.13 to 5.45 wt.eq.NaCl and 80 to 100 mol% XCO₂. Data for aqueous FI are T_{mi} -5.7 to 0 °C, T_h 130 to 357 °C, salinity from 0.18 to 5.38 wt% NaCl_{equiv}. Aqueous-carbonic FI with predominant CH₄ have T_{mi} ranging from -6.3 to 0 °C, T_{clat} from 7 to 11 °C, T_h from 220 to 323

°C, salinity from 4.24 to 5.14 wt.eq.NaCl, and 100 mol% CH₄.

The fluids entrapped in the scheelite crystals show evidence of both boiling and mixing of fluids which resulted in the mineralization. The initial fluid is aqueous CO₂-CH₄-N₂ fluid of moderate salinity. Boiling (at ~350 °C) results in the separation of the CH₄ fluid and mixing (at ~200°C) contributes to the aqueous saline fluid. Magmatic fluids of both vapour and hypersaline liquid, are a primary source of components in hydrothermal ore deposits. Contents of CO₂ and CH₄ could also represent the result of tectono-metamorphic events related to the emplacement of the deposit and the chemical contribution of the inclosing metasedimentary rocks.



Fig. 1: Isolated primary fluid inclusion in scheelite. Objective 5x. In the back, other primary isolated FI and intra-granular trails of pseudo-secondary FI.

References:

Roedder, (1984): Fluid Inclusions. Rev. in Min., Min. Soc. Am., 12, 644.

Hydrothermal silicification and concomitant oil cracking in Kwanza's Pre-salt Aptian Carbonate Reservoirs (Offshore Angola).

Tritlla J.^{1*}, Sánchez V.², Loma R.³, Caja M. A.², Peña J. L.², Sanders C.³, Fernández O.⁴, Olaiz A.³, Herra A.³, Carrasco A.³, Levresse G.⁵

¹*Independent Consultant, Llançà (Spain);* ²*Repsol TechLab, Móstoles (Spain),* ³*Repsol Exploración, Madrid (Spain);* ⁴*Dept. of Geology, Univ. of Vienna (Austria);* ⁵*Centro de Geociencias- UNAM, Querétaro (México).*

*jtritlla@gmail.com

Keywords: hydrothermal plume, pyrobitumen, Pre-salt Angola

The Kwanza Basin in Angola presents a remarkable correlation between tectonic domains, outlined by the thickness of the lithospheric crust, the pre-salt lacustrine carbonate distribution and their diagenetic transformations (Fernández et al, 2020). Kwanza's alkaline lacustrine carbonates can be considered as fully analogous to Santos and Campos Aptian carbonates (Brazil). Diagenetic evolution, similar in both Angolan and Brazilian basins, is characterized by syn-sedimentary micro-karstification processes (grainification, pulverization) prior to early-diagenetic (vadose, phreatic) pervasive silicification events (Tritlla et al, 2018). Silica is present as fine-grained opal (now microquartz) fully replacing carbonate components, and opal-chalcedony-quartz passive sequences cementing corrosion-enhanced primary porosity (framework, interparticle, microkarst). Silica diagenesis is dominated by opal-A inversion to microquartz or secondary chalcedony, microtexture destruction accompanied by dramatic porosity changes, resulting in a texturally complex rock. No fluid inclusions have been preserved trapped in these early silica phases.

A late high-temperature hydrothermal event overprinted the previously silicified rock. This hydrothermal phase is solely represented by a coarse crystalline quartz generation. This contains a mixture of abundant primary and pseudo-secondary brine-bearing and hydrocarbon-bearing fluid inclusions, minute corroded calcite crystals and highly-crystalline pyrobitumen as solid inclusions. Oil cracking temperature is well constrained

at 219-227 °C (Ro hydrothermal Tpeak). Paleofluid PVT calculations by isochore crossings estimated trapping temperatures of 197-221 °C, fully coincident with calculated pyrobitumen Tpeaks. All this data supports an early oil migration, later telescoped by hot, high salinity ($\approx 25\text{wt\%}$ eq NaCl) hydrothermal plumes, thermally cracking this pre-existing petroleum to wet gas (51-53 API) and residual pyrobitumen. In situ full oil cracking originated very high gas-fluid overpressures (11400-12400 psi / 780-850 bars), associated rock hydraulic fracturing and, probably hydrothermal explosion(s) as these estimated pressures exceed the calculated burden, assuming an Albian age for the hydrothermal event, as compared with Campos Basin late hydrothermal activity (J.Tritlla, unpublished data).

Similar processes, in different degrees, have been recognized in other reservoirs on trend within the same tectonic domain, suggesting that this diagenetic evolution is typical of Kwanza's ultra-stretched domain.

References:

- Fernandez, O., Olaiz, A., Cascone, L., Hernandez, P., Pereira, A. D. F., Tritlla, J., Ingles, M., Aida, B., Pinto, I., Rocca, R., Sanders, C., Herra, A. & Tur, N. (2020).- *Marine and Petroleum Geology*, 116, 104330.
- Tritlla, J.; Esteban, M.; Loma, R.; Mattos, A.; Sánchez, V.; Boix, C.; Vieria Da Luca, P.H.; Carballo, J.; Levresse, G. (2018).- *Search and Discovery Article #90323*.

Microthermobarometric characteristic of fluid inclusions of the Upper Paleozoic series of the Akcbulak location of South Torgai sedimentary basin, Kazakhstan

Yensepbayev T.^{1*}, Syzdykov A.¹, Kuldei M.², Giesseman K.²

¹ *Satbayev University (KazNRTU), 22 Satbayev str., Almaty 050013, Kazakhstan*

² *LLP "JV" KGM ", Kyzylorda obl, village Tasboget, 101.*

**tensep@mail.ru*

Keywords: fluid inclusions, sedimentary basins, diagenesis

The fluid inclusions in calcite of two series of Devonian and Carboniferous (Famenien-Tournaisien series of carbonates rocks and Serpukhovien-Middle Carboniferous series of clastic rocks) of Akcbulak location of Ayskum deflection of South Torgai sedimentary basin were studied. By the microthermometry method melting and homogenization temperatures of fluids in diagenetic crystals of calcite, were determined. The development of crystals is associated mainly with cracks and less often with calcite lenses. The biphasic aqueous inclusions were observed in the samples of carbonates rocks (D3fm-C1t) and clastic rocks (C1s-C2). In general, two groups of liquid inclusions can be distinguished. One group of biphasic fluid inclusions has homogenization temperatures from 130 to 170 °C and melting temperatures from -1 to -5 °C. The second group of fluid inclusions has homogenization temperatures of 210 – 250 °C and quite wide range of melting temperatures (-4/-17°C). For these samples the salinity of 3-14% of weight equivalents of NaCl is most typical with the presumed circulation of fluid flows of different composition and mineralization.

Interpretation of results

The interpretation of results of measurements of the samples of 1st group of inclusions has allowed defining most typical values of pressure and temperature equal, accordingly, 350-550 atm and 150 – 210 °C with geothermal gradient about 24 °C/km. The reconstruction of the P/T pair for 2nd group of inclusions shows an increase in the paleotemperature values to 250-300 °C and paleopressure to 700-800 atm, which corresponds to a geothermal

gradient exceeding 40 °C/km. High pressures can explain the relative poverty of fluid inclusions - opening and volatilization during deformation of calcite.

Conclusion

The complex of the obtained data shows conditions of diagenesis of the basin characterized by temperature changes in accordance with the geodynamic situation of the region. We associate the formation of fluid inclusions of the first flow of fluid generations ~~with~~ (paleotemperatures of 150 – 210 °C) with the Middle Carboniferous (Moscovian), and the subsequent hotter flows of fluids (250 – 300 °C) with the Upper Carboniferous, possibly Permian times associated with the gradual closure of the Ural ocean (1st group of fluid inclusion) and subduction processes between Ural ocean and South Turgai microcontinent with formation of Valerian-Beltau volcanic arc (2nd group of fluid inclusion).

AUTHORS INDEX:

A

ABIDI R. – 58
ADLAKHA E. – 38
ADLAKHA E. – 48
AIUPPA A. – 9
APPOLD M. S. – 44
ARADI L. E. – 17
ASTUDILLO D. – 31
ASTUDILLO MANOSALVA D. – 29
AUXERRE M. – 3

B

BAKKER R.J. – 11, 20
BALI E. – 30
BALITSKAYA E. D. – 46, 51
BALITSKY V. – 46, 51
BANKS D. A. – 49
BARALE L. – 44, 59
BARNES J. D. – 30
BARRÉ G. – 54
BARRES O. – 46, 51
BERKESI M. – 4, 17, 23, 55
BERNASCONI S. M. – 59
BERTOK C. – 44, 59
BOBOS I. – 61
BODNA, R. J. – 9
BOIRON M-C. – 27
BUL'BAK T. – 52
BURISCH M. – 44
BUSCHER J. – 24, 31

C

CAJA M. A. – 62
CALASSOU S. – 54
CANNATELLI C. – 24, 29, 31
CAO Y. – 35
CARACCIOLO A. – 30
CARRASCO A. – 62

CASTELLI D. – 56
CASTRUCCIO A. – 29
CAUMON M.-C. – 8, 10
CHOU I. – 6
CHRISTOPHE R. – 58
CONIGLIO, J. E. – 60
CONNOLLY J. A. D. – 58
COQUEREL G. – 13
COULIBALY Y. – 27
CRANE P. – 14
CRETON B – 8
CZUPPON G. – 59

D

D'ATRI A. – 59
DAYA P. – 37
DE GRAAF S. – 32, 49
DEICHA C. – 15
DEICHA I. – 15
DEMARTIS M. – 60
DENG J. – 6
DESLANDES A. – 14
DUDA J-P. – 5

E

EICHHUBL P. – 42
ELIAS BAHNAN A. – 6, 50, 54

F

FALCK H. – 38, 48
FALL A. – 42
FAN J. – 6, 50
FANARA S. – 24
FAURE F. – 3
FAYEK M. – 22
FERNÁNDEZ O. – 62
FERRANDO S. – 56, 59
FRENZEL M. – 44
FREZZOTTI M. L. – 9, 56

G

GALE J. F. W. – 42
GASQUET D. – 58
GAUCHER E. C. – 54
GERBER C. – 14
GIBSHER N. – 54
GIESSEMAN K. – 63
GIORNO M. – 44
GODOY B. – 31
GOMEZ GARCIA G. – 38
GONZÁLEZ-ACEBRÓN L. – 19
GRISHINA S. – 25
GROPPO C. – 56
GUÐFINNSSON G. H. – 30
GUZMICS T. – 17, 23

H

HALLDÓRSSON S. A. – 30
HANILÇI N. – 45
HANLEY J. J. – 2, 22, 37, 38, 48
HARLAUX M. – 28
HARTLEY M. E. – 30
HATIRA N. – 58
HEPVIDINLI B. – 455
HERNÁNDEZ PRAT L. – 29, 31
HERRA A. – 62
HIBSCH C. – 58

I

INCERPI N. – 59

J

JEON H. – 30

K

KAHL M. – 30
KERR M. – 2
KHOMENKO M. – 52
KINNAIRD J. – 2
KONTAK D. J. – 7
KOTOV A. – 26

KOVÁCS I.J. – 4

KRAEMER D. – 33

KULDEI M. – 63

KUZMIN D. – 26

L

LACHET V. – 8

LANDRY K. – 48

LANGE T.P. – 4

LE V-H. – 10

LECUMBERRI-SANCHEZ P. – 38

LEQUIN D. – 3

LEVRESSE G. – 62

LI J. – 6

LOMA R. – 63

LOPEZ-ELORZA M. – 19

LU W. – 12

LU X. – 6, 50

LÜDERS V. – 5, 32, 49

M

MA X. – 50

MAFFEIS A. – 56

MAFFINI M. N. – 60

MAKSIMOVICH I. – 26

MALLANTS D. – 14

MANATSCHAL G. – 59

MANTOVANI A. – 59

MARC L. – 13

MARIGNAC C. – 58

MARQUES DE SÁ C. – 61

MARSHALL E. W. – 30

MARTEL E. – 49

MARTÍN-CHIVELET J. – 19

MARTIRE L. – 45, 59

MCDONALD I. – 2

McFALL K. – 2

MICHELS R. – 54

MIGDISOVA N.A. – 40

MIßBACH. H. – 5

Authors Index

MOLNÁR G. – 4

MONECKE T. – 37

MORATA D. – 24, 31

MORORÓ E. A. A. – 23

MUÑOZ-GARCÍA M. B. – 19

MUNTEAN J. – 28

N

NEYEDLEY K. – 22, 37

NICOT J.-P. – 43

NIEDERMANN S. – 32

NIEDERMANN S. – 39, 49

NIZAMETDINOV I. – 26

NORONHA F. – 61

O

OLAIZ A. – 62

ORIOLO S. – 49

OUATTARA Z. – 27

OYHANTÇABAL P. – 47

ÖZTÜRK H. – 45

P

PACK A. – 5

PADRÓN-NAVARTA J. A. – 55

PALCSU L. – 59

PÁLOS Z. – 4

PEKKER P. – 4

PEÑA J. L. – 62

PENTELEY S. V. – 51

PETROVA M. – 52

PIANA F. – 59

PIERCEY S. – 38

PIRONON J. – 6, 47, 50, 51, 54, 58

PLOTNIKOVA I. N. – 48, 51

PÓSFAL M. – 4

R

RALLAKIS D. – 54

RANA S. – 53

RANDI A. – 8, 46, 51

RASMUSSEN K.L. – 38

RDDAD L. – 33

REITNER J. – 5

REMIGI S. – 9

RICHARD A. – 18

RIZZO A. L. – 9

RONGXI L. – 36

RUSH L. V. – 7

S

SAADALLAH K. – 8

SAMANIEGO P. – 29

SÁNCHEZ, V. – 62

SANDERS C. – 62

SANDOVAL-VELASQUEZ A. L. – 9

SANSELM, M. – 13

SANTAGUIDA F. – 7

SAZONOV A. – 52

SCHIAVI F. – 29

SCHNEIDER J.-M. – 13

SETKOVA T. – 46

SHAPARENKO E. – 52

SHAPLEY S. – 28

SHARMA R. – 53

SHARPE R. – 22

SHISHKINA T.A. – 41

SLIM-SHIMI N. – 58

SMIRNOV S. Z. – 25, 26

SMITH-SCHMITZ S. E. – 43

SOLEYMANI M. – 39

SOMARIN A. K. – 58

SOSA G. M. – 45, 47, 60

SOŚNICKA M. – 33, 49

SPOONER N. – 14

SPRÁNITZ T. – 17, 55

STERPENICH J. – 8

STOLTNOW M. – 32

SUCKOW A. – 14

SYZDYKOV A. – 63

Authors Index

SZABÓ Cs. – 4, 55

T

TAJEDDIN H. A. – 39

TAPIA-RODRÍGUEZ F. – 24

TARANTOLA A. – 10

TATTITC, B. – 2

TEREKHOVA A. – 48

THIEL V. – 5

TOMILENKO A. – 52

TRITLLA J. – 62

V

VAN DEN KERKHOF A. – 5, 45, 47, 60

W

WAGNER A. – 38

WANG W. – 12

WEMMER K. – 47, 60

WHITE S .E. – 7

WHITEHOUSE M. J. – 30

WILSKE C. – 14

X

XIAOLI W. – 36

Y

YAKOVLEV I. – 25

YENSEPBAYEV T. – 63

YUDOVSKAYA M. I. – 2

Z

ZHANG Z. – 35

Participant list

Abdulkadir	Abdulkadir	abdulkadir.abdulkadir.18@ucl.ac.uk	UCL
Riadh	Abidi	abidi1riadh@yahoo.com	Faculté des Sciences de Tunis
Ashley	Abraham	aabrah63@uwo.ca	Western University
Fernando	Althoff	fernando.althoff@ufsc.br	Geology Department
Elena	Amplieva	Amplieva-Alena@yandex.ru	IGEM RAS
Mahesh	Anand	mahesh.anand@open.ac.uk	The Open University
Natalia	Ankusheva	ankusheva@mail.ru	South-Urals Federal Research Center of Mineralogy and Geoecology, Urals Branch, Russian Academy of Sciences
Irvine	Annesley	irvine.annesley@univ-lorraine.fr	University of Lorraine
Bahrican	Ar	bahricanar@gmail.com	Karadeniz Technical University
László E.	Aradi	aradi.laszloelod@ttk.elte.hu	Lithosphere Fluid Research Laboratory, Eötvös University, Budapest
Daniel	Astudillo Manosalva	daniel.astudillo@ufl.edu	University of Florida
Marion	Auxerre	marion.auxerre@univ-lorraine.fr	CRPG
Aboulyakdane	Bakelli	Aboulykdane@gmail.com	University of Sciences and Technology Houari Boumediene USTHB
Ronald	Bakker	bakker@unileoben.ac.at	Resource Mineralogy, Department of Applied Geosciences and Geophysics
Eniko	Bali	eniko@hi.is	Institute of Earth Sciences, University of Iceland
Elizaveta	Balitskaya	Elizaveta.balitskaya@gmail.com	Institute of Experimental Mineralogy RAS
Vladimir	Balitsky	balvlad@iem.ac.ru	Institute of Experimental Mineralogy Ras

Participant list

Luca	Barale	luca.barale@igg.cnr.it	National Research Council of Italy, INstitute of Geosciences and Earth Resources
Hacı Alim	Baran	alimbaran@gmail.com	Batman University
Márta	Berkesi	marta.berkesi@gmail.com	Eötvös Loránd University, Lithosphere Fluid Research Lab
Thomas	Blaise	thomas.blaise@universite-paris-saclay.fr	Université Paris-Saclay
Iuliu	Bobos	ibobos@fc.up.pt	University of Porto, ICTerre-Porto, Portugal
Gülcan	Bozkaya	gulcan.bozkaya@gmail.com	Pamukkale University
Miguel Angel	Caja Rodriguez	miguelangel.caja@repsol.com	Repsol
Alberto	Caracciolo	alberto@hi.is	University of Iceland - Institute of Earth Sciences
Gabriele	Carnevale	gabriele.carnevale@unipa.it	University of Palermo
Patrick	Carr	carpatr@gmail.com	GeoRessources
Marie-Camille	Caumon	marie-camille.caumon@univ-lorraine.fr	Université de Lorraine
Chen	Chen	chenchen@mail.gyig.ac.cn	Institute of Geochemistry, Chinese Academy of Sciences
Ying	Chen	cy2014@idsse.ac.cn	Institute of Deep-sea Science and Engineering, Chinese Academy of Sciences
Nanfei	Cheng	chengnf@idsse.ac.cn	Institute of Deep-sea Science and Engineering, Chinese Academy of Sciences
Maria	Cherdantseva	mariya.cherdantseva@research.uwa.edu.au	The University of Western Australia
Antonio	Ciccolella	antonio.ciccolella93@gmail.com	Università degli Studi di Bari
Gérard	Coquerel	gerard.coquerel@univ-rouen.fr	Université de Rouen
Pelin	Coşanay	pelincsny@gmail.com	Ankara University

Participant list

Istvan	Csige	csige@science.unideb.hu	Institute for Nuclear Research
Tomasz	Ćwiertnia	tomasz.cwiertnia@agh.edu.pl	AGH University of Science and Technology
Priyal	Daya	priyal.daya@smu.ca	Saint Mary's University
Cyril	Deicha	cd@nwf.li	European Physical Society section Liechtenstein
Manuel	Demartis	mdemartis@exa.unrc.edu.ar	Universidad Nacional de Río Cuarto - CONICET
Aileen	Doran	aileen.doran@icrag-centre.org	UCD/iCrag
Idir	EL konty	idir.elkonty@gmail.com	cadi ayyad university Marrakech
Alexy	Elias Bahnan	alexey.elias-bahnan@univ-lorraine.fr	CNRS, Georessources Lab
Iván Mateo	Espinel Pachón	imespinelp@unal.edu.co	University of Geneva
András	Fall	andras.fall@beg.utexas.edu	The University of Texas at Austin
Junjia	Fan	junjia.fan@univ-lorraine.fr	RIPED
Klára	Felker-Kóthay	klara.kothay@gmail.com	Eötvös Loránd University
Yonggang	Feng	ygfeng@chd.edu.cn	Chang'an University
Simona	Ferrando	simona.ferrando@unito.it	Univerisity of Torino
Silvio	Ferrero	sferrero@uni-potsdam.de	Universität Potsdam
Rosa Anna	Fregola	rosaanna.fregola@uniba.it	Università degli studi di Bari Aldo Moro
Maria Luce	Frezzotti	maria.frezzotti@unimib.it	Dipartimento Scienze dell'Ambiente e della Terra, Università Milano Bicocca
Edith	Fuentes	edithfuentesg@gmail.com	UNAM
Abdulrazaq	Garba	razaqgarba@yahoo.com	NGSA
Kumar	Gaurav	gauravgeo78@gmail.com	Indian Institute of Technology Bombay
Johannes	Giebel	r.j.giebel@tu-berlin.de	Technische Universität Berlin

Participant list

Michele Andrea	Giorno	micheleandrea.giorno@unito.it	Università degli Studi di Torino
Sylvio	Gomes	sylvio.gomes@gmail.com	UFBA
Gabriel	Gomez Garcia	gabriel.gomez.garcia@smu.ca	Saint Mary's University
Laura	González Acebrón	lgcebron@geo.ucm.es	Universidad Complutense
Eloy	González-Esvertit	eloige@gmail.com	Universitat de Barcelona
Lucy	Gradwell	lucy.gradwell@open.ac.uk	The Open University
Svetlana	Grishina	grishina@igm.nsc.ru	Sobolev Institute of Geology and Mineralogy Siberian Branch of the Russian Academy of Sciences, Novosibirsk
Alexandra	Guedes	aguedes@fc.up.pt	University of Porto/Faculty of Sciences/ICT
Tibor	Guzmics	tibor.guzmics@gmail.com	Lithosphere Fluid Research Lab, Eötvös University Budapest
Steffen	Hagemann	steffen.hagemann@uwa.edu.au	Centre for Exploration Targeting, School of Earth sciences, University of Western Australia
Noémi	Halász	halasznoemi94@gmail.com	Department of Mineralogy, Geochemistry and Petrology. Faculty of Science and Informatics. University of Szeged
Nurullah	Hanilçi	nurullah@istanbul.edu.tr	Istanbul University-Cerrahpasa
Jacob	Hanley	jacob.hanley@smu.ca	Saint Mary's University, Department of Geology
Coralie	Heinis Dias	coralie.dias@uemg.br	Universidade do Estado de Minas Gerais
Petra	Herms	petra.herms@ifg.uni-kiel.de	Institute for Geoscience, University Kiel

Participant list

Loreto	Hernández Prat	loreto.hernandez@ug.uchile.cl	Universidad de Chile
Aicha	Hissou	chhissou@gmail.com	MNG
Ismail	Hossain	ismail_gm@ru.ac.bd	Department of Geology and Mining, University of Rajshahi
Ingrid	Hoyer	ingridshoyer@gmail.com	University of Brasilia
mohamed	idbaroud	idbaroud@gmail.com	University Cadi Ayyad
Abdelmajid	Jarni	abdelmajid.jarni@ced.uca.ma	Semlalia Faculty of Science - Cadi Ayyad University
Ziqi	Jiang	jiangziqi@mail.gyig.ac.cn	Institute of Geochemistry, Chinese Academy of Sciences
abdessamad	jinari	ab.jinari@gmail.com	Cadi Ayyad University, Faculty of Science
Erika	Kereskényi	kereskenyerika@yahoo.com	Herman Ottó Museum
Peter	Kodera	peter.kodera@gmail.com	Comenius University, Faculty of Natural Sciences, Department of Mineralogy, Petrology and Economic Geology
Sandor	Kormos	sandor.kormos@geo.u-szeged.hu	Department of Mineralogy, Geochemistry and Petrology, University of Szeged
Stepan	Krashennikov	spkrash09@gmail.com	Institute of Mineralogy Leibniz University Hannover
Anju	Kumari	best2anju29@gmail.com	Indian Institute of Technology, Bombay (IIT-B)
Thomas Pieter	Lange	lange.thomas@hotmail.com	Lithosphere Fluid Research Lab, Eötvös Loránd University
Thomas	Lange	thompiman@student.elte.hu	ELTE LRG
Van-Hoan	Le	van-hoan.le@univ-lorraine.fr	GeoRessources laboratory, University of Lorraine

Participant list

Louise	Lenoir	louise.lenoir@universite-paris-saclay.fr	GEOPS
Jianguo	Li	lijianguo@mail.gyig.ac.cn	Institute of Geochemistry, Chinese Academy of Sciences
Rongxi	Li	rongxi99@163.com	Chang'an University
Robert	Linnen	rlinnen@uwo.ca	University of Western Ontario
Zairong	Liu	presentzai@gmail.com	Deep-sea Science and Engineering, Chinese Academy of Sciences
Francesco Maria	Lo Forte	francescomaria.loforte@unipa.it	Università degli Studi di Palermo
Maialen	Lopez Elorza	maialen.lopez.elorza@gmail.com	Complutense University
Anikó	Lovász	lovasz.a0@gmail.com	Eötvös Loránd University
Wanjun	Lu	wjlu@cug.edu.cn	China University of Geosciences
Volker	Lüders	volue@gfz-potsdam.de	GFZ German Research Centre for Geosciences
Georgina	Lukoczki	gina.lukoczki@uky.edu	University of Kentucky
Andrea	Maffei	andrea.maffei@unito.it	Università degli Studi di Torino
Maria Natalia	Maffini	nmaffini@exa.unrc.edu.ar	Instituto de Ciencias de la Tierra, Biodiversidad y Ambiente - CONICET - Universidad Nacional de Río Cuarto
Miguel	Maia	mcmaiageo@gmail.com	Institute of Earth Sciences
Laureline	Marc	laureline.marc@univ-rouen.fr	Université de Rouen
Carlos	Marques de Sá	dingesster@gmail.com	ICT
Robert	Marschik	marschik@lmu.de	LMU Munich
Katie	McFall	mcfallk@cardiff.ac.uk	Cardiff University
Margarita	Melfou	Margaritamelfou@gmail.com	

Participant list

Reed	Mershon	reed.mershon@gmail.com	Hebrew University of Jerusalem
Amina	Messaoudi	messaoudi.amina.20@gmail.com	
Julie	Michaud	j.michaud@mineralogie.uni-hannover.de	Institute of Mineralogy, Hannover
Raymond	Michemls	raymond.michels@univ-lorraine.fr	GeoRessources/Université de Lorraine/CNRS
Kyaw	Min Khaing	kyawminkhaing.kmk@gmail.com	Maubin University
Nadia	Mohammadi	Nadia.mohammadi@unb.ca	Carleton University
Kata	Molnar	molnar.kata@atomki.hu	Institute for Nuclear Research
Daniel	Moncada	dmoncada@ing.uchile.cl	University of Chile
Emanuel	Mororó	mororo.emanuel@gmail.com	Eötvös Loránd University
yousra	Morsli	yousramorsli@gmail.com	Hassan 2 university of Casablanca
Josef	Mullis	josef.mullis@unibas.ch	Department of Environmental Sciences, University
Jon	Naden	Jna@bgs.ac.uk	British Geological Survey
Oded	Navon	oded.navon@mail.huji.ac.il	The Hebrew University
Bianca	Németh	nemethbj@student.elte.hu	Eötvös Loránd University
Ildar	Nizametdinov	inizametdinov@igm.nsc.ru	V.S. Sobolev Institute of Geology and Mineralogy SB RAS
Olusegun	Olisa	olusegun.Olisa@oouagoiwoye.edu.ng	Olabisi Onabanjo University
Amanda	Ostwald	ostwald@unlv.nevada.edu	University of Nevada, Las Vegas
Akira	Otsuki	akira.otsuki@univ-lorraine.fr	University of Lorraine
Zié	Ouattara	ziegbana@hotmail.fr	Université de Man
Fariba	Padyar	padyar@geologist.com	Geological Survey of Iran
Jacques	Pironon	jacques.pironon@univ-lorraine.fr	CNRS, Université de Lorraine, GeoRessources lab

Participant list

Fernando	Prado Araujo	fernando.pradoaraujo@kuleuven.be	KU Leuven - Earth and Environmental Sciences
Guilherme	Primo	guilherme.ale.primo@live.com	Unicamp - State University of Campinas
Lucilia Aparecida	Ramos de Oliveira	luciliar@gmail.com	CDTN
SHRUTI	RANA	shrtrn5@gmail.com	Wadia Institute of Himalayan Geology
Samantha	Remigi	s.remigi@campus.unimib.it	Università degli Studi di Milano-Bicocca
T. James	Reynolds	fluidinc@comcast.net	FLUID INC.
Antonin	Richard	antonin.richard@univ-lorraine.fr	Université de Lorraine
Lisa	Richter	Lisa.Richter@bgr.de	Federal Institute for Geosciences and Natural Resources (BGR), Hannover
Francisco Javier	Rios	javier@cdtn.br	CDTN / CNEN
Marcela	Rodrigues	up201510120@edu.fc.up.pt	Institute of Earth Sciences/ Faculty of Sciences, University of Porto
Inés	Rodríguez	irodriguez@uct.cl	Universidad Católica de Temuco
Remigio	Ruiz	remigioruiz@gmail.com	Y-TEC
Khouloud	Saadallah	Khouloud.saadallah@univ-lorraine.fr	Laboratory of Georessources-Vandœuvres les Nancy
Félix	Schubert	schubert@geo.u-szeged.hu	University of Szeged, Department of Mineralogy, Geochemistry and Petrology
Eszter	Sendula	seszter1@vt.edu	University of Pécs
Arkodeep	Sengupta	reach.arko.sg@gmail.com	Indian Institute of Technology Kharagpur
Linbo	Shang	shanglinbo@vip.gyig.ac.cn	Institute of Geochemistry, CAS
Elena	Shaparenko	shaparenkoe@gmail.com	VS Sobolev Institute of Geology and Mineralogy

Participant list

Sarah	Shapley	srshapley2@gmail.com	University of Nevada Reno
Olga	Shemelina	shem@igm.nsc.ru	Sobolev Institute of geology and mineralogy SB RAS
Tatiana	Shishkina	t.shishkina@geokhi.ru	Vernadsky GEOKHI RAS
Sarah	Smith-Schmitz	ses7f1@umsystem.edu	University of Missouri - Columbia
Krzysztof	Sokol	ks275@st-andrews.ac.uk	University of St Andrews
Majid	Soleymani	Soleymani.majid@ut.ac.ir	University of Tehran
Graciela	Sosa	gsosa@gwdg.de	Georg-August-Universität Göttingen
Marta	Sośnicka	marta.sosnicka@uni-jena.de	Institute of Geosciences, Friedrich Schiller University Jena
Tamás	Sprátnitz	spratom.elte@gmail.com	Lithosphere Fluid Research Lab, Department of Petrology and Geochemistry, Eötvös Loránd University, Budapest
Wang	Staccato	595682702@qq.com	IDSSE
Alice	Stephant	alice.stephant@inaf.it	Istituto Nazionale di Astrofisica
Malte	Stoltnow	mstolt@gfz-potsdam.de	GFZ German Research Centre for Geosciences
Anna	Terekhova	anna.terekhova.m@gmail.com	Saint Mary's University
Aung Myo	Thu	aungmyothugeol.mu@gmail.com	AGH University of Science and Technology
Jordi	Tritlla	jtritlla@gmail.com	
Subaru	Tsuruoka	subaru.tsuruoka@icrag-centre.org	Irish Centre for Research in Applied Geosciences (iCrag), University College Dublin
Alfons	van den Kerkhof	akerkho@gwdg.de	Georg-August University Göttingen
Amina	Wafik	wafik@uca.ac.ma	Faculty of sciences Semailia, Cadi

Participant list

			Ayyad University, Marrakech
Benjamin	Walter	b.walter@kit.edu	Karlsruhe Institute of Technology (KIT)
Ye	Wan	jswanye@163.com	Institute of Deep- Sea Science and Engineering
Xinsong	Wang	wangxinsong@mail.gyig.ac.cn	Institute of Geochemistry, Chinese Academy of Sciences
Wenjing	Wang	wenjingwang@cug.edu.cn	China University of Geosciences
Lee	White	lee.white@open.ac.u	The Open University
Cornelia	Wilske	cornelia.wilske@adelaide.edu.au	University of Adelaide
Jiuhua	Xu	jiuhuaxu@ces.ustb.edu.cn	University of Science and Technology Beijing
yabin	yuan	yuanyabin126@126.com	Southern University of Science and Technology
Khadra	Zaid	zaid.khdra@gmail.com	Mohammed First Oujda
Khin	Zaw	khinzaw.nilar@gmail.com	CODES University of Tasmania, Hobart
Fei	Zhang	feiz0824@gmail.com	Camborne School of Mines, University of Exeter
Haiyan	Zhang	hyzhang@idsse.ac.cn	Institute of Deep- sea Science and Engineering, Chinese Academy of Sciences
Yunhe	Zhou	zhouyunhe@mail.gyig.ac.cn	Institute of Geochemistry, Chinese Academy of Sciences
Martina	Zucchi	martina.zucchi@uniba.it	University of Bari